DISSERTATION

GRASSLAND PLANT-SOIL-MICROBIAL RESPONSES TO CLIMATE EXTREMES AND LAND USE CHANGE

Submitted by

Jordan Alexander Siggers

Graduate Degree Program in Ecology

In partial fulfillment of the requirements

For the Degree of Doctor of Philosophy

Colorado State University

Fort Collins, Colorado

Summer 2026

Doctoral Committee:

Advisor: Melinda Smith

Caroline Havrilla
Christine Hawkes
Michael Wilkins

ABSTRACT

GRASSLAND PLANT-SOIL-MICROBIAL RESPONSES TO CLIMATE EXTREMES AND LAND USE CHANGE

Atmospheric warming is intensifying the global hydrological cycle, leading to increased occurrence of hydroclimatic extremes. Extreme droughts and deluges (persistent, torrential rain events) are already impacting ecosystems globally, with each leaving legacy effects of altered plant-soil interactions and ecosystem structure and function. The likelihood of co-occurring hydroclimatic extremes, such as droughts and deluges, increases with each degree of warming, yet little is known about how ecosystems will be affected when these events co-occur, particularly through altered interactions between plants and soil microbiomes. Similarly, climate solutions, such as renewable energy development, are altering abiotic determinants of ecosystem functionality (e.g., light and water availability). Solar photovoltaic energy (PV) is currently the cheapest, most scalable renewable energy option, though PV arrays occupy greater land area than alternative energy forms and may have unintended consequences for their host ecosystems. Thus, global change drivers are altering precipitation inputs and other abiotic factors in profound and unique ways, yet experimental assessments of their ecological impacts are limited and highly context dependent. Further, altered precipitation regimes and land use changes are likely to be especially consequential in grasslands, where water is the predominant limiting resource and PV deployment is most expansive. In this dissertation I investigated how these global change drivers impacted grassland ecosystems through altered plant function and soil microbial communities across the United States Great Plains. The first chapter examined the legacy effects of extreme

drought on soil microbial communities across representative grassland types of the US Great Plains. The second chapter shifted focus to the shortgrass steppe of northeastern Colorado, where I investigated the ecosystem impacts of compounded extreme drought and deluge. The final chapter assessed plant-soil-microbial responses to a PV array in a C_3 pasture in northeastern Colorado. Altogether, this work suggests that global change drivers will have immense contemporaneous and lasting impacts on grassland ecosystems, highlighting the pressing need to understand our ecosystems before they are irreversibly altered.

ACKNOWLEDGMENTS

This section could easily be longer than any chapter given the endless support that I have received through my graduate degree. I would like to start by thanking my advisor, Melinda Smith, who took a chance on me as a lowly undergraduate with limited research experience. I cannot express how grateful I am for her insight, willingness to support my tireless pursuits of new projects and experiences, and ability to reel me in when necessary. I would likely still be waiting tables if it were not for Mendy's faith in my abilities. I would also like to thank my committee members. Christine Hawkes was willing to join my committee from afar and has always been so supportive and kind, even in moments of absolute brain fog. Similarly, Caroline Havrilla has been an advocate for prioritizing my personal wellbeing and always encouraged me to think of my work through a different lens. Mike Wilkins did not hesitate to join my committee long into my graduate career, which signaled a confidence in me that I truly appreciate. On my unofficial committee, Ed Hall has served as a mentor in many capacities, prompting me to think about science and ecology outside of my wheelhouse. Thank you to Alan Knapp as well for being a consistent source of support, mentorship, and humility.

I would be remiss not to thank the folks that I have had the pleasure of collaborating with through my completely unrelated side projects, notably my good buddy, Lennel Camuy-Vélez, my DLiA mentor, Will Kuhn, and the rest of the NSF IRES Australia crew. At CSU, I could not have been luckier to have such awesome colleagues in the Smith and Knapp labs, including Chance Roberts, Kathy Condon, Maddie Amick, Maggie Ross, Lucus Donne, Nico Matallana-Mejia, Adriana Jacobi, Anna Hall, Scott Otto, Francis Chaves-Rodriguez, Tim Ohlert, Kate Wilkins, Olivia Hajek, Heide Keeble, Greg Tooley, and Jenna Gardner. Thank you especially to

Leena Vilonen for shepherding me into the world of microbiome science in a lab of grass nerds and supporting me in my role with the Global Soil Biodiversity Initiative. Of course, our incredible undergraduates and mentees, Gabe Cordova, Neva Morgan, Shelby Mead, Izabella Rhomberg, Greg Paff, Josh Taft, Dani Rosario, Ella Wehrlen, Grayce Wojniak, and Mia Colangelo, have made my life so much easier. Huge shout out to Lillian Gordon for spending a year as my personal assistant- at least now we know how a sledgehammer works!

I would also like to thank my family for helping me make it this far. Thank you to my mother, Cecilia, and father, Robert, for supporting me wholeheartedly my entire life. I know I can call you anytime and never make it to voicemail. I guess I must thank my brothers, Nicholas and Daniel, as well, though they probably will not read this far in. Couldn't have done it without any of you, and I know I can always rely on you!

I am grateful for the Graduate Degree Program in Ecology at CSU, which coaxed me to become a more sociable person and inspired my ever-growing love for ecology. Through graduate school, I met some of my dearest friends and colleagues, including Matt Sturchio, Kord Dicke, and Amir Alayoubi. As we approach the best-for-last section (totally kidding, Mom), I thank my best friends G Harrison, Lindi Fitz-Harrison, Ty Bentley, and my newest buddy, Rex Fitz-Harrison, for always being a steady source of support.

Lastly, the goodest boys, Afie and Spud, got me through every day and ensured that I would never become a cat person. And the biggest thank you to the most considerate and supportive individual I have had the privilege of knowing, my wife, Kayla, who has discovered the perfect ratio of nodding along versus asking questions when I ramble about my research.

TABLE OF CONTENTS

CHAPTER 1: INTRODUCTION

Atmospheric CO_2 concentrations continue to rise as a direct result of anthropogenic fossil fuel emissions and land use change. In 2025, concentrations were at 425.7 ppm relative to 278 ppm in 1750 (Friedlingstein et al. 2025), contributing to a global surface temperature increase of 1.1°C above 1850-1900 temperatures (IPCC 2023). Such rapidly increasing temperatures are altering climate regimes and driving intensified precipitation patterns (IPCC 2023). Although uncertainty exists surrounding how overall precipitation amounts will shift in each region, these changes are already manifesting as more extreme droughts and deluges (Fischer & Knutti 2016, Prein et al. 2017, Swain et al. 2018, IPCC 2023, Feldman et al. 2024).

Climate extremes, by definition, alter ecosystems beyond the bounds of normal variability (Smith 2011). Indeed, extreme drought stunts biogeochemical cycling, leading to the collapse of primary productivity and a shift from carbon sink to source in many water-limited ecosystems (Hoover & Rogers 2016, Xu et al. 2019, Hoover et al. 2022, Smith et al. 2024). Though the immediate impacts of extreme drought are detrimental, there is growing concern that the lasting (legacy) effects persisting into the post-drought period may govern unforeseen responses to future climate extremes (Schwalm et al. 2017, Vilonen, Ross et al. 2022, Müller and Bahn 2022). For example, plants may experience xylem cavitation or reduced meristem density under extreme drought, inhibiting their ability to utilize water when it becomes available again (Anderegg et al. 2015). At a finer scale, soil microbial communities may undergo major compositional shifts, which alters their functional capacity and response to subsequent drought events (Canarini et al. 2021, Enderle et al. 2025, Ginnan et al. 2025, Hannula and Veen 2025, Oram et al. 2025). Indeed, soil microbial legacy effects influence future plant performance from

the individual to community scale (de Vries et al. 2023, Ginnan et al. 2025, Oram et al. 2025). Soil microbial legacy effects may endure long into the post-drought period regardless of whether nominal precipitation has returned to the system (Allison & Martiny 2008, Cordero et al. 2023), or they may not persist at all (Vilonen, Blair et al. 2022, Vilonen et al. 2023). Whether drought induces soil microbial legacy effects may depend on an ecosystem's climatic history, along with drought intensity, severity, and duration (Evans et al. 2022, Broderick et al. 2025, Oram et al. 2025). Understanding the contemporary and legacy effects of extreme drought is vital to predicting ecosystem functionality under future climate regimes. Concerningly, the likelihood of extreme drought co-occurring with other climate extremes (i.e., compound climate extremes) is rising due to anthropogenic forcing, obscuring our already-limited understanding of the ecological outcomes of extreme drought (IPCC 2023).

Compound climate extremes occur in many forms, including terrestrial heatwaves and extreme drought, high winds and deluges, and marine heatwaves and ocean acidification (AghaKouchak et al. 2020, Zscheischler et al. 2020). Often, these extremes interact to magnify the impacts of each extreme alone, driving immense ecosystem consequences (Zscheischler et al. 2018). For example, a 2015 storm in Italy created a storm surge coinciding with heavy precipitation, which overwhelmed drainage basins and caused millions of euros in damages (Bevacqua et al. 2017, Zscheischler et al. 2020). Similarly, a 2018 heatwave in the Western Alps interacted with anomalous precipitation to cause massive landslides and avalanches (Stoffel & Corona 2018). The projected increase in compound climate extremes is particularly troublesome in regions that are already vulnerable to climate change, such as ecosystems that experience persistent water limitation.

Dryland ecosystems (i.e., regions with an aridity index value < 0.65, Maestre et al. 2021), which cover roughly 40% of the global terrestrial surface (Schimel 2010), are highly responsive to precipitation inputs (Austin et al. 2004). Indeed, extreme drought and deluge events, individually, have well-documented impacts on these ecosystems, even within a single growing season; Extreme drought drives substantial reductions in productivity and biogeochemical cycling, while deluge events drive contrasting responses (Knapp et al. 2015, Post & Knapp 2020, Post & Knapp 2021, Hajek & Knapp 2024). In a semi-arid grassland, a deluge event aided in ecosystem recovery from a single growing season drought (Hoover et al. 2022). Although the impacts of single year droughts are substantial, the growing probability of extreme, multi-year droughts underscores immense threats to ecosystem functionality (Chen et al. 2025, Hoover & Smith 2025, Ohlert et al. 2025). Hence, there is an urgent need to understand how ecosystems will respond to extreme, multi-year droughts, deluge events, and their co-occurrence (Zscheischler et al. 2018, AghaKouchak et al. 2020). Understanding and mitigating the impacts of such climate extremes will facilitate sustained ecosystem functionality for future generations.

A key solution to reducing fossil fuel emissions, limiting further atmospheric warming, and mitigating the occurrence of climate extremes is the deployment of alternative energy production sources. Of the available options, solar photovoltaic (PV) energy production is the cheapest, most scalable avenue for the near future (Lee et al. 2023). However, the immense land use requirements have raised concerns about the ecological impacts of PV facilities (Armstrong et al. 2014). PV panels redistribute sunlight and precipitation, creating spatial and temporal heterogeneity in important resources, such as light and water, that may be especially impactful in semi-arid ecosystems (Knapp & Sturchio 2024). In the semi-arid grasslands of Colorado, PV arrays have proven to impact plant productivity (Sturchio et al. 2022), plant physiology (Sturchio

et al. 2024), and other measures of carbon cycling (Toy et al. 2025) that are intrinsically linked to belowground processes (Wardle et al. 2004). However, the belowground impacts of PV-induced environmental heterogeneity are relatively unknown, with very few studies investigating PV impacts on soil microbial communities (Lambert et al. 2021, Moscatelli et al. 2022, Carvalho et al. 2025). Overlooking the belowground drivers of biogeochemical cycling and plant functionality inhibits a holistic understanding of how renewable energy generation may alter ecosystems globally.

In this dissertation I will address how climate extremes and PV development impact grasslands of the North American Great Plains through field experiments. In Chapter 2, I investigated soil microbial legacy effects of extreme drought across the Great Plains precipitation gradient. In Chapter 3, I assessed the below- and aboveground ecosystem impacts of compound extreme drought and deluge in the shortgrass steppe of Colorado. In Chapter 4, I quantified belowground responses to PV-induced environmental heterogeneity in a central Colorado pasture. Through these studies, I seek to provide an improved understanding of how global change will impact our planet so that we may prepare for and adapt to an unforeseen future.

LITERATURE CITED

AghaKouchak, A., F. Chiang, L. S. Huning, C. A. Love, I. Mallakpour, O. Mazdiyasni, ... and M. Sadegh. 2020. "Climate Extremes and Compound Hazards in a Warming World." *Annual Review of Earth and Planetary Sciences* 48: 519–548. https://doi.org/10.1146/annurev-earth-071719-055226.

Allison, S. D., and J. B. Martiny. 2008. "Resistance, Resilience, and Redundancy in Microbial Communities." *Proceedings of the National Academy of Sciences* 105, no. 1: 11512–11519. https://doi.org/10.1073/pnas.0801925105.

Anderegg, W. R., C. Schwalm, F. Biondi, J. J. Camarero, G. Koch, M. Litvak, ... and A. Wolf. 2015. "Pervasive Drought Legacies in Forest Ecosystems and Their Implications for Carbon Cycle Models." *Science* 349, no. 6247: 528–532. https://doi.org/10.1126/science.aab1833.

Armstrong, A., S. Waldron, J. Whitaker, and N. J. Ostle. 2014. "Wind Farm and Solar Park Effects on Plant-Soil Carbon Cycling: Uncertain Impacts of Changes in Ground-Level Microclimate." *Global Change Biology* 20, no. 6: 1699–1706. https://doi.org/10.1111/gcb.12437.

Austin, A. T., L. Yahdjian, J. M. Stark, J. Belnap, A. Porporato, U. Norton, ... and S. M. Schaeffer. 2004. "Water Pulses and Biogeochemical Cycles in Arid and Semiarid Ecosystems." *Oecologia* 141: 221–235. https://doi.org/10.1007/s00442-004-1519-1.

Bevacqua, E., D. Maraun, I. Hobæk Haff, M. Widmann, and M. Vrac. 2017. "Multivariate Statistical Modelling of Compound Events via Pair-Copula Constructions: Analysis of Floods in Ravenna (Italy)." *Hydrology and Earth System Sciences* 21: 2701–2723. https://doi.org/10.5194/hess-21-2701-2017.

Broderick, C. M., G. M. N. Benucci, L. R. Bachega, G. D. Miller, S. E. Evans, and C. V. Hawkes. 2025. "Long-Term Climate Establishes Functional Legacies by Altering Microbial Traits." *The ISME Journal* 19, no. 1: wraf005. https://doi.org/10.1093/ismej/wrae005.

Canarini, A., H. Schmidt, L. Fuchslueger, V. Martin, C. W. Herbold, D. Zezula, ... and A. Richter. 2021. "Ecological Memory of Recurrent Drought Modifies Soil Processes via Changes in Soil Microbial Community." *Nature Communications* 12, no. 1: 5308. https://doi.org/10.1038/s41467-021-25675-4.

Carvalho, F., H. Montag, L. Bentley, et al. 2025. "Plant and Soil Responses to Ground-Mounted Solar Panels in Temperate Agricultural Systems." *Environmental Research Letters* 20, no. 2: 024003. https://doi.org/10.1088/1748-9326/ad977a.

Chen, L., P. Brun, P. Buri, S. Fatishi, A. Gessler, M. J. McCarthy, ... and D. N. Karger. 2025. "Global Increase in the Occurrence and Impact of Multiyear Droughts." *Science* 387: 278–284. https://doi.org/10.1126/science.adr2589.

Cordero, I., A. Leizeaga, L. C. Hicks, J. Rousk, and R. D. Bardgett. 2023. "High Intensity Perturbations Induce an Abrupt Shift in Soil Microbial State." *The ISME Journal* 17, no. 12: 2190–2199. https://doi.org/10.1038/s41396-023-01529-z.

De Vries, F., J. Lau, C. Hawkes, and M. Semchenko. 2023. "Plant–Soil Feedback Under Drought: Does History Shape the Future?" *Trends in Ecology & Evolution* 38, no. 8: 708–718. https://doi.org/10.1016/j.tree.2023.02.004.

Enderle, E., L. Hinojosa, V. Lombard, F. Hou, and F. T. de Vries. 2025. "Drought Legacy Effects on Plant Growth and Plant–Soil Feedback Are Mediated by Soil Microbial Communities Independently of Root Exudates and Root Litter." *Journal of Ecology* 113, no. 11: 3293–3312. https://doi.org/10.1111/1365-2745.14389.

Evans, S. E., S. D. Allison, and C. V. Hawkes. 2022. "Microbes, Memory and Moisture: Predicting Microbial Moisture Responses and Their Impact on Carbon Cycling." *Functional Ecology* 36, no. 6: 1430–1441. https://doi.org/10.1111/1365-2435.14041.

Feldman, A. F., X. Feng, A. J. Felton, A. G. Konings, A. K. Knapp, J. A. Biederman, and B. Poulter. 2024. "Plant Responses to Changing Rainfall Frequency and Intensity." *Nature Reviews Earth & Environment* 5: 276–294. https://doi.org/10.1038/s43017-024-00521-8.

Fischer, E. M., and R. Knutti. 2016. "Observed Heavy Precipitation Increase Confirms Theory and Early Models." *Nature Climate Change* 6: 986–991. https://doi.org/10.1038/nclimate3110.

Friedlingstein, P., M. O'Sullivan, M. W. Jones, R. M. Andrew, D. C. Bakker, J. Hauck, ... and G. P. Peters. 2025. "Global Carbon Budget 2025." *Earth System Science Data Discussions* 2025: 1–139. https://doi.org/10.5194/essd-2024-526.

Ginnan, N. A., V. Custódio, D. Gopaulchan, N. Ford, I. Salas-González, D. H. Jones, ... and G. Castrillo. 2025. "Precipitation Legacy Effects on Soil Microbiota Facilitate Adaptive Drought Responses in Plants." *Nature Microbiology*: 1–22. https://doi.org/10.1038/s41564-024-01907-w.

Hannula, S. E., and G. F. Veen. 2025. "Drought Has Short-Term Effects on Soil Fungal Communities Leading to Long-Term Effects on Soil Functions." *Soil Biology and Biochemistry* 209: 109893. https://doi.org/10.1016/j.soilbio.2024.109893.

Hoover, D. L., and B. M. Rogers. 2016. "Not All Droughts Are Created Equal: The Impacts of Interannual Drought Pattern and Magnitude on Grassland Carbon Cycling." *Global Change Biology* 22: 1809–1820. https://doi.org/10.1111/gcb.13161.

Hoover, D. L., O. L. Hajek, M. D. Smith, K. Wilkins, I. J. Slette, and A. K. Knapp. 2022. "Compound Hydroclimatic Extremes in a Semi-Arid Grassland: Drought, Deluge, and the Carbon Cycle." *Global Change Biology* 28: 2611–2621. https://doi.org/10.1111/gcb.16081.

Hoover, D. L., and W. K. Smith. 2025. "The Growing Threat of Multiyear Droughts." *Science* 387: 246–247. https://doi.org/10.1126/science.adu0471.

IPCC. 2023. "Summary for Policymakers." In: *Climate Change 2023: Synthesis Report. Contribution of Working Groups I, II and III to the Sixth Assessment Report of the Intergovernmental Panel on Climate Change* [Core Writing Team, H. Lee and J. Romero (eds.)]. IPCC, Geneva, Switzerland: 1–34. https://doi.org/10.59327/IPCC/AR6-9789291691647.001.

Knapp, A. K., C. J. W. Carroll, E. M. Denton, K. J. La Pierre, S. L. Collins, and M. D. Smith. 2015. "Differential Sensitivity to Regional-Scale Drought in Six Central US Grasslands." *Oecologia* 177: 949–957. https://doi.org/10.1007/s00442-015-3219-3.

Knapp, A. K., and M. A. Sturchio. 2024. "Ecovoltaics in an Increasingly Water-Limited World: An Ecological Perspective." *One Earth* 7, no. 10: 1705–1712. https://doi.org/10.1016/j.oneear.2024.09.001.

Lambert, Q., A. Bischoff, S. Cueff, A. Cluchier, and R. Gros. 2021. "Effects of Solar Park Construction and Solar Panels on Soil Quality, Microclimate, CO2 Effluxes, and Vegetation Under a Mediterranean Climate." *Land Degradation & Development* 32, no. 18: 5190–5202. https://doi.org/10.1002/ldr.4101.

Maestre, F. T., B. M. Bonito, M. Berdugo, L. Concostrina-Zubiri, M. Delgado-Baquerizo, D. J. Eldridge, E. Guirado, N. Gross, S. Kefi, Y. Le Bagousse-Pinguet, and R. Ochoa-Hueso. 2021. "Biogeography of global drylands." *New Phytologist* 231, no. 2: 540-558. https://doi.org/10.1111/nph.17395.

Moscatelli, M. C., R. Marabottini, L. Massaccesi, and S. Marinari. 2022. "Soil Properties Changes After Seven Years of Ground Mounted Photovoltaic Panels in Central Italy Coastal Area." *Geoderma Regional* 29, e00500. https://doi.org/10.1016/j.geodrs.2022.e00500.

Müller, L. M., and M. Bahn. 2022. "Drought Legacies and Ecosystem Responses to Subsequent Drought." *Global Change Biology* 28, no. 17: 5086–5103. https://doi.org/10.1111/gcb.16270.

Ohlert, T., M. D. Smith, S. L. Collins, A. K. Knapp, J. S. Dukes, O. Sala, ... and T. J. Terry. 2025. "Drought Intensity and Duration Interact to Magnify Losses in Primary Productivity." *Science* 390: 284–289. https://doi.org/10.1126/science.ads1254.

Oram, N. J., N. Praeg, R. D. Bardgett, F. Brennan, T. Caruso, P. Illmer, ... and F. T. de Vries. 2025. "Drought Intensity Shapes Soil Legacy Effects on Grassland Plant and Soil Microbial Communities and Their Responses to Future Drought." *Global Change Biology* 31, no. 9: e70495. https://doi.org/10.1111/gcb.70495.

Post, A. K., and A. K. Knapp. 2020. "The Importance of Extreme Rainfall Events and Their Timing in a Semi-Arid Grassland." *Journal of Ecology* 108: 2431–2443. https://doi.org/10.1111/1365-2745.13411.

Post, A. K., and A. K. Knapp. 2021. "How Big Is Big Enough? Surprising Responses of a Semiarid Grassland to Increasing Deluge Size." *Global Change Biology* 27: 1157–1169. https://doi.org/10.1111/gcb.15442.

Prein, A. F., R. M. Rasmussen, K. Ikeda, C. Liu, M. P. Clark, and G. J. Holland. 2017. "The Future Intensification of Hourly Precipitation Extremes." *Nature Climate Change* 7: 48–52. https://doi.org/10.1038/nclimate3168.

Schimel, D. S. 2010. "Drylands in the Earth System." *Science* 327: 418–419. https://doi.org/10.1126/science.1184946.

Schwalm, C. R., W. R. Anderegg, A. M. Michalak, J. B. Fisher, F. Biondi, G. Koch, ... and H. Tian. 2017. "Global Patterns of Drought Recovery." *Nature* 548, no. 7666: 202–205. https://doi.org/10.1038/nature23021.

Smith, M. D. 2011. "The Ecological Role of Climate Extremes: Current Understanding and Future Prospects." *Journal of Ecology* 99: 651–655. https://doi.org/10.1111/j.1365-2745.2011.01833.x.

Smith, M. D., K. D. Wilkins, M. C. Holdrege, P. Wilfahrt, S. L. Collins, A. K. Knapp, and W. Sun. 2024. "Extreme Drought Impacts Have Been Underestimated in Grasslands and Shrublands Globally." *Proceedings of the National Academy of Sciences* 121: e2309881120. https://doi.org/10.1073/pnas.2309881120.

Stoffel, M., and C. Corona. 2018. "Future Winters Glimpsed in the Alps." *Nature Geoscience* 11: 458–460. https://doi.org/10.1038/s41561-018-0164-z.

Sturchio, M. A., J. E. Macknick, G. A. Barron-Gafford, et al. 2022. "Grassland Productivity Responds Unexpectedly to Dynamic Light and Soil Water Environments Induced by Photovoltaic Arrays." *Ecosphere* 13, no. 12: e4334. https://doi.org/10.1002/ecs2.4334.

Sturchio, M. A., S. A. Kannenberg, T. A. Pinkowitz, and A. K. Knapp. 2024. "Solar Arrays Create Novel Environments that Uniquely Alter Plant Responses." *Plants, People, Planet* 6, no. 6: 1522–1533. https://doi.org/10.1002/ppp3.10543.

Swain, D. L., B. Langenbrunner, J. D. Neelin, and A. Hall. 2018. “Increasing Precipitation Volatility in Twenty-First-Century California.” *Nature Climate Change* 8: 427–433. https://doi.org/10.1038/s41558-018-0140-y.

Toy, C., N. Heider-Kuhn, and M. Schipanski. 2025. “Impact of Solar Energy Infrastructure and Ecovoltaic Management on Semi-Arid Grassland Carbon Cycling.” *Environmental Research Letters* 20, no. 7: 105005. https://doi.org/10.1088/1748-9326/ad74f5.

Vilonen, L., M. Ross, and M. D. Smith. 2022a. “What Happens After Drought Ends: Synthesizing Terms and Definitions.” *New Phytologist* 235, no. 2: 420–431. https://doi.org/10.1111/nph.18137.

Vilonen, L. L., J. Blair, P. Trivedi, L. Zeglin, and M. D. Smith. 2022b. “Limited Legacy Effects of Extreme Multiyear Drought on Carbon and Nitrogen Cycling in a Mesic Grassland.” *Elem Sci Anth* 10, no. 1: 000093. https://doi.org/10.1525/elementa.2021.00093.

Vilonen, L. L., S. Hoosein, M. D. Smith, and P. Trivedi. 2023. “Legacy Effects of Intensified Drought on the Soil Microbiome in a Mesic Grassland.” *Ecosphere* 14, no. 6: e4545. https://doi.org/10.1002/ecs2.4545.

Wardle, D. A., R. D. Bardgett, J. N. Klironomos, H. Setala, W. H. van der Putten, and D. H. Wall. 2004. “Ecological Linkages Between Aboveground and Belowground Biota.” *Science* 304, 1629-1633. https://doi.org/10.1126/science.1094875

Xu, C., N. G. McDowell, F. R. Fisher, L. Wei, S. Sevanto, B. O. Christofferson, ... and R. S. Middleton. 2019. “Increasing Impacts of Extreme Droughts on Vegetation Productivity Under Climate Change.” *Nature Climate Change* 9: 948–953. https://doi.org/10.1038/s41558-019-0630-6.

Zscheischler, J., S. Westra, B. J. Van Den Hurk, S. I. Seneviratne, P. J. Ward, A. Pitman, and X. Zhang. 2018. “Future Climate Risk from Compound Events.” *Nature Climate Change* 8: 469–477. https://doi.org/10.1038/s41558-018-0156-3.

Zscheischler, J., O. Martius, S. Westra, E. Bevacqua, C. Raymond, R. M. Horton, ... and E. Vignotto. 2020. “A Typology of Compound Weather and Climate Events.” *Nature Reviews Earth & Environment* 1: 333–347. https://doi.org/10.1038/s43017-020-0060-z.

CHAPTER 2: DROUGHT LEGACY EFFECTS OF ALTERED RHIZOSPHERE MICROBIAL COMMUNITIES ACROSS A GRASSLAND PRECIPITATION GRADIENT

2.1 Summary

Soil microbial responses to climate extremes will determine ecosystem functionality under climate change, yet the persistence of these responses remains a critical uncertainty. As drought is projected to increase in frequency and severity globally, understanding the lasting impacts, or 'legacy effects', of these extremes is essential for predicting ecosystem responses to climate change. Due to their differential drought sensitivity, grasslands are ideal systems for investigating the legacy effects of drought on soil microbial communities. We leveraged an experimental drought network spanning the North American Great Plains (the Extreme Drought in Grasslands Experiment – EDGE) to evaluate the legacy effects of differing drought intensities on soil prokaryotic and fungal communities. Experimental drought was imposed for four years as either: 1) Chronic drought, whereby each growing season precipitation event was reduced by 66%, or 2) Intense drought, whereby all growing season precipitation was excluded until a ~45% reduction in mean annual precipitation was reached. Soil sampling was conducted four years post-drought to investigate drought legacy effects on prokaryotic and fungal communities in bulk and rhizosphere soil niches. Bulk soil communities showed no drought legacies at any study site. However, prokaryotic and fungal rhizosphere communities showed legacies of altered community structure under the Chronic, but not Intense, drought treatment at each site. No legacies were present across diversity measures, suggesting legacies were determined by shifts in taxa abundance. Enriched taxa in previously-droughted treatments were site-dependent and did not correspond to taxa that are often enriched under contemporary drought, such as Actinobacteria. Rather, enriched taxa were dominated by relatively rare taxa, including

Crenarchaeota and cryptic phyla. Drought legacy effects were most persistent at the driest study site, the shortgrass steppe. Overall, our results highlight the importance of drought severity and soil niche in driving soil microbial legacy effects, which are difficult to generalize across systems.

2.2 Introduction

Atmospheric warming is rapidly shifting precipitation regimes, leading to increased drought frequency, severity, and duration (Cook et al. 2018, Naumann et al. 2018, Chen et al. 2025, Swain et al. 2025). Consequently, the detrimental impacts of drought, defined as "abnormal periods of low water availability of sufficient duration to potentially alter ecosystem structure and function" (Knapp et al. 2024), are becoming more widespread globally and are frequently manifest as severe reductions in primary productivity (Ohlert et al. 2025), plant diversity (Liu et al. 2021), and nutrient cycling (Song et al. 2019). These impacts are often immediately evident in grasslands, where water is the primary limiting resource, leaving them particularly vulnerable to changes in precipitation patterns (Knapp & Smith 2001, Huxman et al. 2004). Grasslands span ~23% of Earth's terrestrial surface (MacDougall et al. 2026), and store one third of terrestrial carbon stocks (Bai and Cotrufo 2022). Thus, understanding grassland drought responses is vital to predicting and mitigating the effects of global climate change.

Aboveground grassland drought responses have been studied intensively, with observational and experimental studies elucidating the impacts of increasing drought occurrence (e.g., Knapp et al. 2015, Carroll et al. 2021, Smith et al. 2024, Ohlert et al. 2025). Indeed, grasslands are relatively resistant (Craine et al. 2013) and resilient (Xu et al. 2021) to short-term drought, though extreme, multi-year drought may exceed the capacity of grassland ecosystems to resist drought, leading to collapses of aboveground productivity (Xu et al. 2021, Ohlert et al.

2025) and major shifts in plant community composition (Felton & Smith 2017, Griffin-Nolan et al. 2019, Knapp et al. 2020). However, soil microbiome responses do not always parallel the extent of plant community responses (de Vries, Griffiths et al. 2018, Schimel 2018), prompting a need to understand spatiotemporal dynamics of both above- and belowground drought responses.

As key determinants of ecosystem functionality, soil microbiomes play a crucial role in driving soil biogeochemical cycling, decomposition, plant growth, and carbon storage (Wagg et al. 2014, Trivedi et al. 2020, Hartmann and Six 2023). Soil microbiomes may be severely impacted by reduced soil water availability, leading to reduced soil functionality (Schrama and Bardgett 2016, Schimel 2018, Lozano et al. 2021), altered microbiome composition (Ochoa-Hueso et al. 2018, Malik and Bouskill 2022, Bazany et al. 2025), and changes in plant-soil feedback dynamics (De Long et al. 2019, Xi et al. 2022, de Vries et al. 2023). Yet, the immense taxonomic and functional diversity of soil microbes make it difficult to detect the immediate and lasting impacts of drought on soil microbiomes (Allison & Martiny 2008, Evans et al. 2022). Inconsistent responses are further confounded by differences in drought severity. For example, short-term, less intense drought may induce major shifts in soil microbiome structure and function in some settings (Naylor et al. 2017, Ochoa-Hueso et al. 2018, Bazany et al. 2022) but not others (Allison & Martiny 2008, Hueso et al. 2011, Allison 2023, Hussain et al. 2026). However, extreme droughts or those extending over multiple years more consistently alter microbiomes, often ‘priming’ them for future droughts (Preece et al. 2019, Canarini et al. 2021, Philipp et al. 2025).

Following the initial impacts of drought, substantial changes in soil microbiome structure and function may persist into the post-drought period (Preece & Peñuelas 2016, Kaisermann et al. 2017, Meisner et al. 2018, Canarini et al. 2021, Leizeaga et al. 2021, Müller and Bahn 2022,

Vilonen et al. 2023, Enderle et al. 2025, Hannula & Veen 2025, Oram et al. 2025). These lasting changes deemed 'legacy effects' may be realized as lingering shifts in soil microbial community structure (Leizeaga et al. 2021, Vilonen et al. 2022 Broderick et al. 2025) and/or decreased soil multifunctionality (Meisner et al. 2018, Canarini et al. 2021, Hannula & Veen 2025) that may subsequently impact future plant growth (Cordero et al. 2023, Enderle et al. 2025, Ginnan et al. 2025, Oram et al. 2025). The enrichment of drought tolerant soil microbial traits (Evans and Wallenstein 2014, Malik et al. 2020, Leizeaga et al. 2021, Evans et al. 2022) under water limitation has been attributed to improved future drought resistance, though these traits may not be favored under nominal conditions post-drought. Such shifts in soil microbiome structure and function may not return to a pre-drought state upon rewetting, potentially altering the long-term contribution of soil microbiomes to ecosystem function (Allison & Martiny 2008, Cordero et al. 2023). Yet, drought does not always prompt persistent legacy effects, as soil microbiome structure and functionality have also been shown to recover immediately following drought cessation (Vilonen, Blair et al. 2022, Vilonen et al. 2023). Differential drought legacy effects on soil microbiomes have been partially attributed to an ecosystem's climate history (Evans et al. 2022, Broderick et al. 2025), along with drought severity (Oram et al. 2025). Drought legacy effects may also differ between bulk and rhizosphere (i.e., "soil compartment influenced by plant roots", Bakker et al. 2013) soils due to contrasting drivers of microbiome structure and function across these niches. Bulk soil is generally carbon-limited, whereby microbes rely on plant litter inputs and available organic matter. The rhizosphere is a more carbon-rich environment, where microbes are subject to plant root exudation, sloughed root cells, and plant-driven changes in microenvironments (Ling et al. 2022). Hence, each soil niche hosts unique microbiomes under

ambient conditions (Trivedi et al. 2020), which may be differentially affected by extreme drought.

Leveraging a field experiment - the Extreme Drought in Grasslands Experiment (EDGE) - we investigated drought legacy effects on soil microbiome structure across a precipitation gradient in the United State Central Plains that encompassed four grassland types. Each grassland experienced four years of 1) Chronic drought (CHR, each growing season rainfall event reduced by 66%), 2) Intense drought (INT, complete rainfall exclusion until 45% of mean annual precipitation (MAP) was excluded), and 3) Control (CON, ambient conditions). Following the treatment period, each grassland experienced ambient conditions for four years prior to our determination of soil prokaryotic and fungal community structure. We assessed 1) if unique drought intensities resulted in legacies of altered soil prokaryotic and fungal community structure at each grassland site, 2) if legacy effects differed across soil niches (bulk vs. rhizosphere soil), and 3) if legacy effects were evident across microbial network components. We hypothesized prokaryotic communities that previously experienced drought would remain differentially structured from prokaryotic communities that experienced ambient conditions due to enrichment of drought-responsive taxa (e.g., Actinobacteria, Chloroflexi, Naylor & Coleman-Derr 2017), while we did not anticipate any legacies of altered fungal communities (Ochoa-Hueso et al. 2018). We expected legacy effects to be least evident in the tallgrass prairie, as few bulk soil microbial compositional and functional legacies persisted one- and two-years post-drought (Vilonen, Blair et al. 2022, Vilonen et al. 2023). We expected rhizosphere legacies to be more persistent than bulk soil legacies given drought commonly induces rhizosphere microbiome restructuring, while the bulk soil may remain unaffected (Naylor et al. 2017, Santos-Medellín et al. 2017, Hannula & Veen 2025). Lastly, we anticipated reductions in network complexity, with

fewer edges and increased modularity in communities that previously experienced drought (de Vries et al. 2018, Oram et al. 2025).

2.3 Methods

2.3.1 Site Description

This study was conducted in 2021 at four Central US grasslands representing the primary grassland types of the Central Plains (Fig. 2.1). The sites span a mean annual precipitation (MAP) gradient of ~500 mm, increasing from west to east (335 – 857 mm, calculated from 1990-2020; Condon et al. 2025). The shortgrass steppe (SGS) of the Central Plains Experimental Range in Nunn, Colorado receives the least MAP (335.1 mm) and is dominated by the C_4 graminoids, *Bouteloua gracilis* and *Bouteloua dactyloides*. The C_4 *Bouteloua gracilis* and C_3 *Pascopyrum smithii* co-dominate the northern mixed grass prairie (HPG, 385.1 mm MAP) of the High Plains Grassland Research Center in Cheyenne, Wyoming. The southern mixed grass prairie (HYS, 614.6 mm MAP) of the Hays Agricultural Research Station in Hays, Kansas is C_4-dominated by *Bouteloua curtipendula* and *Schizachyrium scoparium*, along with the C_3 *P. smithii*. The annually burned tallgrass prairie (KNZ, 856.7 mm MAP) of the Konza Prairie Biological Station is also C_4-dominated by *Andropogon gerardii* and *Sorghastrum nutans*.

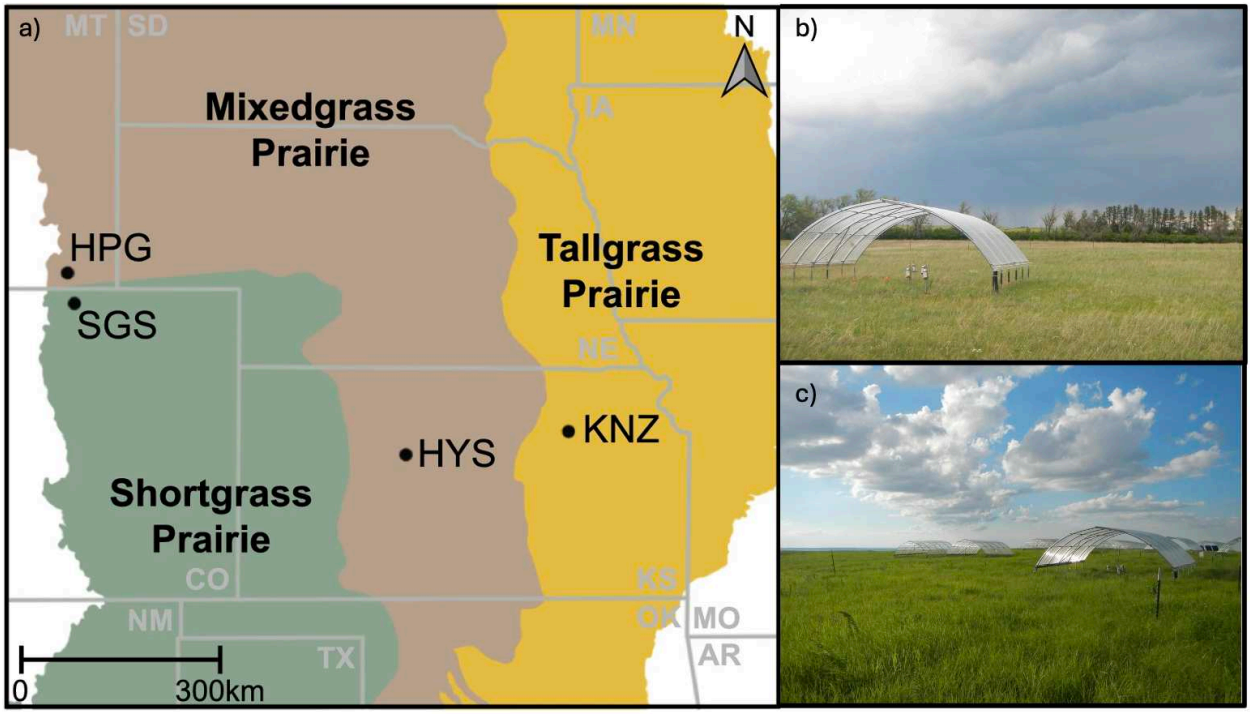

Site	Grassland Type	MAP (mm)	MAT (°C)	Sampled Species
SGS	Shortgrass	335.1	8.3	*Elymus elymoides*
HPG	C_3 Mixed	385.1	7.6	*Koeleria macrantha*
HYS	C_4 Mixed	614.6	12.4	*Bouteloua curtipendula*
KNZ	Tallgrass	856.8	12.5	*Andropogon gerardii*

Figure 2.1: **a**) Distribution of EDGE experimental sites across the North American Central Plains (adapted from Carroll et al. 2021 and Condon et al. 2025). **b**) Image of an EDGE rainout shelter in the C_3-dominated mixed-grass prairie of the High Plains Grassland Research Center (HPG) of Cheyenne, Wyoming. **c**) Image of an EDGE rainout shelter in the tallgrass prairie of Konza Prairie Biological Station (KNZ) of Manhattan, Kansas (photo credit Robert Griffin-Nolan). **Below**) Site-level mean annual precipitation (MAP) and mean annual temperature (MAT) based on long-term averages from 1990-2020 (adapted from Condon et al. 2025), along with the focal plant species sampled for rhizosphere soils in the present study.

2.3.2 EDGE Experimental Design

This study leveraged the Extreme Drought in Grasslands Experiment (EDGE), a large-scale rainfall exclusion experiment. Rainfall exclusion shelters (6 x 6 m of corrugated polycarbonate strips) were installed to impose drought from 2014 to 2017. All plots were trenched and hydrologically isolated to a depth of 1 m. The Chronic (CHR) drought treatment reduced each growing season rainfall event by 66% from April to September (n = 10/site). The Intense (INT) drought treatment completely excluded each growing season rainfall event from May to July (n = 10/site). The Control (CON) plots received the same hydrological isolation, but no shelters were constructed, thus receiving all ambient rainfall (n = 10/site). Both treatments resulted in a ~45-50% reduction in average annual rainfall (Carroll et al. 2021, Vilonen et al. 2023). See Carroll et al. (2021) for further details on rainfall exclusion. All shelters were removed at the end of the 2017 growing season and received ambient rainfall through our sampling campaign.

2.3.3 Soil Sampling

In 2021, bulk and rhizosphere soil samples were collected during the first week of October. This timing represents the end of the growing season in these ecosystems, when plants have begun to senesce. Although this timing did not capture peak biomass, it did allow for investigation of persistent shifts in microbial community structure. Highly abundant plant species that were present in each experimental plot were chosen as focal species for rhizosphere samples: *Elymus elymoides* at SGS, *Koeleria macrantha* at HPG, *Bouteloua curtipendula* at HYS, and *Andropogon gerardii* at KNZ. These species were in high abundance during and after the EDGE experiment. At each site, a subset of 6 plots per treatment were randomly chosen for sampling (n = 18 total plots per site). For each bulk soil sample, three random soil core samples were

homogenized (15 cm depth) from each plot, and a single subsample was used as a biological replicate. For each rhizosphere soil sample, two focal plants were excavated from each plot and rhizosphere soil was collected from connected roots, providing two unique biological samples. All soils were immediately placed in a cooler and returned to CSU, where they were sieved to 2 mm and frozen at -20° C until DNA extraction. DNA extractions took place within a month of sample collection.

2.3.4 DNA Extraction and Amplicon Sequencing

Soil microbial DNA was extracted using the DNEasy PowerSoil Pro Kit (Qiagen, Hilden, Germany) according to manufacturer's specifications. All DNA extractions were conducted at Colorado State University, and samples were assessed for quality and quantity with a Qubit 4 Fluorometer and NanoDrop Lite Spectrophotometer (ThermoFisher Scientific, MA, USA). Samples were extracted again if the 260/280 absorbance ratio was below 1.7, indicating low DNA quality. All samples were stored at -20°C until library preparation and sequencing were conducted at the Center for Microbial Exploration at the University of Colorado-Boulder (Boulder, Colorado). DNA was amplified using a SimpliAmp Thermocycler with Platinum II Hot Start Master Mix (ThermoFisher Scientific, MA, USA). Paired-end amplicon sequencing of the 16S V4 (515F/806R primers: Apprill et al. 2015; Parada et al. 2015) and ITS (ITS1-F/ITS2 primers; Smith & Peay 2014, Bellemain et al. 2010) regions was conducted on the Illumina MiSeq (Illumina Inc., CA, USA) using 2 x 250 bp chemistry at 500 cycles. Extraction and no-template controls were included in each run.

2.3.5 Bioinformatics

Raw sequences were received in FASTQ format and demultiplexed using QIIME2 Amplicon 2024.5 software (Bolyen et al. 2019). Sequences were demultiplexed, merged, and

denoised using the DADA2 plug-in (Bokulich et al. 2013, Callahan et al. 2016). Low-quality sequences (Q < 30, truncLen = (240, 230) for 16S) and primers (trimleft = (19,20) for 16S and trimleft = (20, 22) for ITS) were removed. Sequences with ambiguous bases, chimeric sequences, and short sequences (<100 bp) were removed using default settings. Amplicon sequence variants (ASVs) were generated using DADA2, and taxonomy was assigned against the SILVA (Yilmaz et al. 2014) database for 16S sequences and the UNITE (Nilsson et al. 2019) database for ITS sequences. Any sequences matching host chloroplast or mitochondria were removed. Following DADA2, 48,797 16S ASVs and 51,855 ITS ASVs were present. Feature tables and taxonomic assignments were exported for further analysis in R software (R Core Team 2023).

2.3.6 Statistical Analysis and Network Analysis

Samples were analyzed separately for prokaryotic (16S) and fungal (ITS) communities. ASVs under 30 total reads were removed from analyses to minimize contaminant and sequencing errors, as well as limit the noise introduced and improve the ability to detect key drivers of ecological patterns (Cao et al. 2021). Removing ASVs under 30 total reads resulted in 10,388 16S ASVs and 17,639 ITS ASVs moving forward. Samples were rarefied at 9,200 reads for both 16S rRNA and ITS rRNA. These values were chosen following the creation of rarefaction curves to retain the maximum number of samples and allow comparison of samples with differing sequence depths. Rarefied tables were only used for alpha diversity calculations, and unrarefied tables were used for further downstream analyses given the compositional nature of the data (Gloor et al. 2017). The ‘phyloseq’, ‘vegan’, and ‘mctoolsr’ packages were used to analyze microbial communities (McMurdie and Holmes 2013, Oksanen et al. 2013, Leff 2017). All statistical analyses were conducted on bulk soil and rhizosphere communities separately, as

we expected these niches to be ecologically distinct and thus display disparate legacy effects. 16S bulk soil samples had 1,219,934 total reads, and 16S rhizosphere soil samples had 2,315,336 total reads. ITS bulk soil samples had 1,384,364 total reads, and ITS rhizosphere soil samples had 2,556,115 total reads.

2.3.6.1 Alpha and Beta Diversity

Both 16S and ITS datasets were analyzed symmetrically to test the same hypotheses across kingdoms. To investigate alpha diversity, richness and Shannon diversity were first calculated using the diversity function in the vegan package. Richness and Shannon diversity were then compared across sites and treatments using generalized linear models (GLMs), followed by post hoc comparisons of estimated marginal means (EMMs). To test for differences in prokaryotic and fungal community structure, permutational multivariate analysis of variance (PERMANOVA) models were constructed using the adonis2 function in the vegan package. Aitchison distance (with a pseudo-count of one) was calculated for all beta diversity analyses (Gloor et al. 2017). Site, treatment, and their interaction were used as fixed factors, with block as a stratum to constrain permutations, and Type III Sum of Squares were used to evaluate the marginal effects of treatment and site. Although two distinct rhizosphere samples were collected from each plot, we controlled for pseudoreplication by restricting permutations to the plot level using the *permute* package (Simpson 2026). Specifically, whole plots were treated as the experimental units and permuted freely only within their respective spatial blocks, ensuring that the nested error structure was accounted for. For each test, we assessed the assumption of multivariate homogeneity of variance using the BetaDisper function in the *vegan* package (Oksanen et al. 2013). Planned comparisons were made to test for significant treatment differences at each site using the *pairwiseadonis* package (Arbizu 2020). Given significant site

by treatment interactions, site-level PERMANOVA models were also created with treatment as a fixed factor to test for the overall effect of treatment on community structure at each site. Notably, the site-by-treatment interaction was only significant for the 16S dataset ($p = 0.049$, Table 1), but we conducted site-level PERMANOVAs for both datasets to maintain analytical symmetry and to explore kingdom-specific sensitivities to our experimental treatments at each site. Beta diversity was then visualized using Constrained Analysis of Principal Coordinates (CAP) using the capscale function in the *vegan* package, followed by plotting in *ggplot2* (Wickham 2016). CAP allowed us to specifically isolate the variation attributable to our experimental treatments.

2.3.6.2 Taxonomic Analysis

Dominant taxa at each site were calculated using the summarize_taxonomy and taxa_summary_by_sample_type functions in mctoolsr. These were calculated at the phylum level for prokaryotes and order level for fungi. Taxa shared across sites were determined at the ASV resolution using core_members function in phyloseq. To test for the effect of treatment on rhizosphere prokaryotic phyla and fungal orders, Analysis of Compositions of Microbiomes with Bias Correction 2 (ANCOM-BC2, Lin & Peddada, 2020) was conducted on feature tables at the site level. These taxonomic levels were chosen given 1) the phylogenetic conservatism present in prokaryotic phylum level and limited taxonomic assignment confidence beyond the phylum level and 2) the lack of phylogenetic conservatism present at the fungal phylum level and functional divergence present at the order level. Given significant differences in community structure were prominent across CON and CHR treatments (see *Results*), we focused our taxonomic comparisons on these treatments. The phyla/orders had to be present in at least 10% of samples,

the maximum number of iterations was 100, and the level of significance was 0.05. Taxonomic differences were visualized on a log-fold-change basis.

2.3.6.3 Network Analysis

Prokaryotic and fungal co-occurrence networks were separately constructed from ASV feature tables. Networks were only created for the rhizosphere CON and CHR treatments given our emphasis on differences between these treatments. ASVs present in less than 20% of samples, with fewer than 30 total reads, or exhibiting zero variance were removed to minimize the influence of rare or erroneous taxa. Instead of traditional pairwise correlations (e.g., Spearman correlations), network topology was inferred using the Meinshausen and Bühlmann (MB) neighborhood estimation method (*sensu* Kurtz et al. 2015, Oram et al. 2025). This approach utilizes Lasso-regularized regression to identify conditional dependencies between taxa, effectively filtering out indirect associations that often confound correlation-based metrics. A stability-based selection procedure (StARS) was implemented to determine the optimal sparsity level, ensuring that only robust and reproducible edges were retained. Duplicate and self-loop edges were removed prior to final network construction. Topological features, including total edges, nodes, and modularity were calculated to characterize community architecture. Modularity was determined using the Louvain algorithm via the *igraph* package to identify densely connected sub-communities (Csárdi et al. 2026). All networks were visualized using the *ggraph* package with a Fruchterman-Reingold layout (Pederson 2025).

2.4 Results

2.4.1 Alpha Diversity

Bulk soil prokaryotic richness and Shannon diversity differed across sites (Fig. A1.1, Tables A1.1, A1.2, $p < 0.001$), but was not affected by treatment or the interaction between site

and treatment (Fig. A1.2, Tables A1.1, A1.2). Bulk soil prokaryotic richness and Shannon diversity were highest at HYS (517 ASVs; 5.69) and lowest at KNZ (381 ASVs; 5.21). Rhizosphere soil prokaryotic richness and Shannon diversity were unaffected overall by site, treatment, or the interaction (Tables A1.1, A1.2).

Bulk soil fungal richness and Shannon diversity differed across sites (Fig. A1.1, Tables A1.1, A1.2, $p < 0.001$), but was unaffected by treatment or the interaction between site and treatment. Bulk soil fungal richness was similarly highest at HYS (280 ASVs) and lowest at KNZ (158 ASVs), and Shannon diversity was highest at HPG (4.35) and lowest at KNZ (3.16). Rhizosphere fungal richness (Fig. A1.1, $p < 0.001$) and Shannon diversity ($p = 0.004$) was only affected by site. Rhizosphere fungal richness was highest at HPG (261 ASVs) and lowest at SGS (176 ASVs), and Shannon diversity was highest at HYS (4.40) and lowest at KNZ (3.95).

2.4.2 Beta Diversity

Bulk soil prokaryotic and fungal communities differed significantly across sites ($p < 0.001$, Figs. A1.4, A1.5), with no significant treatment differences nor interactions (Table 2.1). At the site level, planned treatment comparisons were insignificant. Rhizosphere soil prokaryotic and fungal communities also differed significantly across sites (Figs. A1.4, A1.5, $p < 0.001$), along with a significant site by treatment interaction for rhizosphere prokaryotic communities (p = 0.049) but not fungal communities (Table 2.1).

Given our experimental design and questions centered around treatment differences at the site level, we proceeded with site-level planned treatment analyses (*see Methods*). At the site level, planned comparisons indicated significant differences in rhizosphere prokaryotic communities across unique treatment combinations (Fig. 2.2, Table 2.2). At SGS, rhizosphere prokaryotic communities differed between CON-CHR ($p = 0.034$), but not between CON-INT or

CHR-INT (Table 2.2). At HPG, rhizosphere prokaryotic communities differed ($p < 0.001$) between CON-CHR ($p = 0.026$) and CON-INT ($p = 0.017$) but not CHR-INT (Table 2.2). The differences between CON-INT were likely driven by greater beta-dispersion of INT relative to CON or CHR communities (BetaDisper, $p = 0.059$, Table A1.3). At HYS, rhizosphere prokaryotic communities differed ($p = 0.013$) between CON-CHR ($p = 0.023$) but not CON-INT or CHR-INT (Table A1.2). At KNZ, rhizosphere prokaryotic communities marginally differed ($p = 0.056$) overall but did not differ under planned treatment comparisons (Fig. 2.2, Table 2.2). Overall, CON-CHR comparisons showed the most consistent site-level treatment differences, aside from KNZ (Fig. 2.2, Table 2.2).

At the site level, planned comparisons also indicated significant differences in rhizosphere fungal communities across unique treatment combinations (Fig. 2.2, Table 2.2). At SGS rhizosphere fungal communities differed between CON-CHR ($p = 0.042$), CON-INT ($p = 0.01$), and CHR-INT ($p = 0.035$, Table 2.2). At HPG, rhizosphere fungal communities differed between CON-INT ($p = 0.037$) but not CON-CHR or CHR-INT (Table 2.2). At HYS, rhizosphere fungal communities differed ($p = 0.001$) between CON-CHR ($p = 0.044$) but not CON-INT or CHR-INT (Table 2.2). At KNZ, rhizosphere fungal communities differed ($p = 0.004$) between CON-CHR ($p = 0.003$) but not CON-INT or CHR-INT (Table 2.2). No beta-dispersion tests indicated overdispersion of a treatment group at any site (Table A1.3). Overall, CON-CHR comparisons similarly showed the most consistent site-level treatment differences, apart from HPG (Fig. 2.2, Table 2.2).

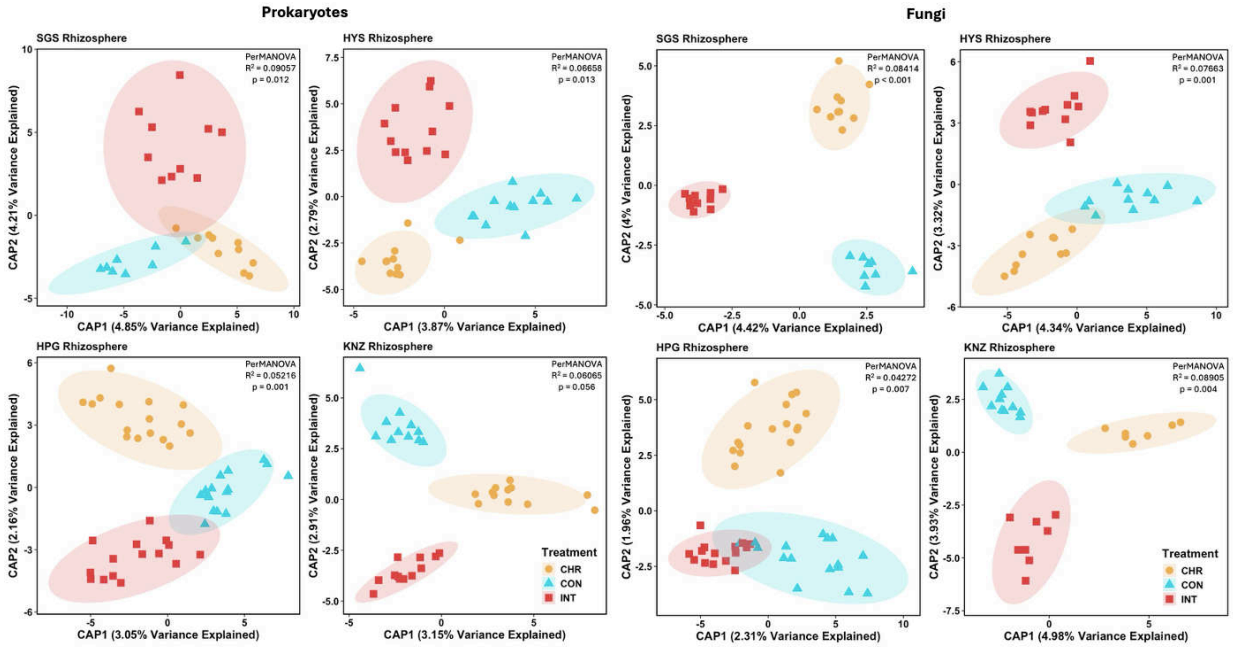

Figure 2.2: Constrained analysis of principal coordinates (CAPs) ordinations demonstrating the impact of previous drought treatments on (left) soil rhizosphere prokaryotic and (right) fungal communities. Permutational multivariate analysis of variance (PERMANOVA) model results of site level analyses are shown in upper corner of each panel. CAPs were conducted following detection of the significant site-level treatment effects via PERMANOVA ($p<0.05$).

Table 2.1: PERMANOVA results indicating the role of site, treatment, and their interactions in driving the microbial community composition of prokaryotes and fungi in the bulk soil and rhizosphere. Significant differences ($p < 0.05$) are bolded.

		Prokaryotes			**Fungi**		
Niche	**Driver**	Pseudo-F	R^2	*p*	Pseudo-F	R^2	*p*
Bulk	Site	9.4629	0.3043	0.001	5.6973	0.2162	**0.001**
	Treatment	1.0206	0.0219	0.393	1.0323	0.0261	0.306
	Site:Treatment	0.9728	0.0626	0.557	0.9857	0.0748	0.525
Rhizosphere	Site	17.3634	0.2679	0.001	9.6751	0.1820	**0.001**
	Treatment	1.1314	0.0116	0.189	1.0835	0.0136	0.243
	Site:Treatment	1.1865	0.0366	0.049	1.0440	0.0393	0.233

Table 2.2: Planned comparison results indicating the role of treatment in driving rhizosphere prokaryotic and fungal community structure within sites. Significant planned comparisons ($p < 0.05$) are bolded. Note, the significant difference between CON-INT at HPG was likely driven by greater beta-dispersion of INT relative to CON and CHR (Table A1.3).

		Prokaryotes			**Fungi**		
Site	**Comparison**	Pseudo-F	R^2	*p*	Pseudo-F	R^2	*p*
SGS	CON-CHR	1.357	0.0782	**0.034**	1.106	0.0646	**0.042**
	CON-INT	1.223	0.0710	0.092	1.190	0.0692	**0.010**
	CHR-INT	1.169	0.0610	0.093	1.150	0.0600	**0.035**
HPG	CON-CHR	1.307	0.0417	**0.026**	0.925	0.0290	0.410
	CON-INT	1.377	0.0453	**0.017**	1.102	0.0366	**0.037**
	CHR-INT	0.963	0.0321	0.546	0.995	0.0321	0.345
HYS	CON-CHR	1.273	0.0571	**0.023**	1.307	0.0643	**0.044**
	CON-INT	1.146	0.0495	0.128	1.196	0.0564	0.084
	CHR-INT	1.000	0.0455	0.441	1.103	0.0549	0.129
KNZ	CON-CHR	1.043	0.0473	0.327	1.253	0.0726	**0.003**
	CON-INT	1.012	0.0460	0.370	1.013	0.0562	0.388
	CHR-INT	1.044	0.0453	0.318	1.110	0.0787	0.137

2.4.3 Prokaryotic Taxonomic Differences

Phyla relative abundances are indicated as percentages within parentheses (Fig. A1.6). Acidobacteriota were the dominant bacterial phylum across bulk and rhizosphere samples at SGS (19%), HPG (23.3%), and HYS (31.1%), while Verrucomicrobiota dominated KNZ samples (26.1%, Fig. A1.6). Actinobacteriota were also highly abundant at SGS (14.1%), HPG (13.7%), HYS (10.5%), and KNZ (10.1%, Fig. A1.6). At SGS, the bacterial candidate phyla, WPS-2 (0.9%) and RCP2-54 (0.02%), along with Methylomirabilota (0.09%), Aenigmoarchaeota (0.003%), and Entotheonellaeota (0.15%) were significantly enriched under CHR, while Fibrobacterota (0.01%), Acidobacteriota (19%), Gemmatimonadota (0.9%), Thermoplasmatota (0.07%), Elusimicrobiota (0.04%), and the bacterial candidate phylum, WS2 (0.01%), were significantly enriched under CON (Fig. 2.3). At HPG, the bacterial candidate phylum, Hydrogenedentes (0.01%), and the archaeal Thermoplasmatota (0.02%) were enriched under CHR, while Latescribacterota (0.01%) and WS2 (0.04%) were enriched under CON (Fig. 2.3).

At HYS, Bdellovibrionota (0.2%), Crenarchaeota (8.4%), Entotheonellaeota (1.7%), Elusimicrobiota (0.05%), and WS2 (0.01%) were enriched under CHR, and Abditibacteriota (0.02%) and Thermoplasmatota (0.01%) were enriched under CON (Fig. 2.3). At KNZ, the bacterial candidate phyla, MBNT15 (0.01%), WPS-2 (0.01%), and WS2 (0.01%) were enriched under CHR, while Nanoarchaeota (0.01%) and Hydrogenedentes (0.01%) were enriched under CON (Fig. 2.3).

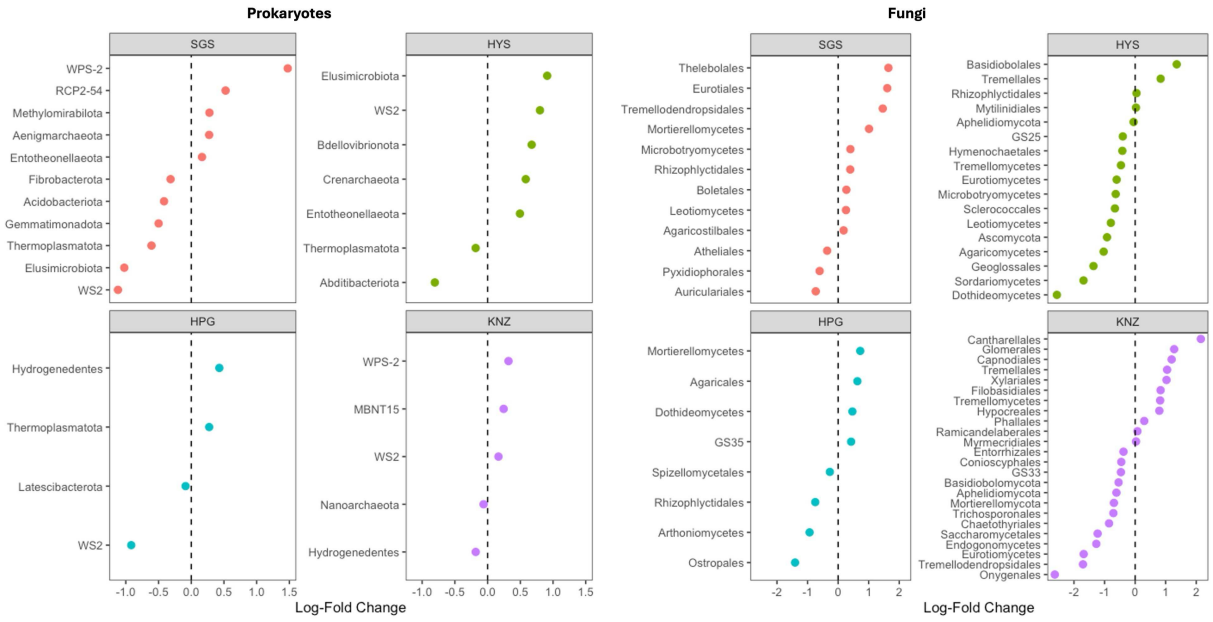

Figure 2.3: Differentially abundant soil rhizosphere (left) prokaryotic phyla and (right) fungal orders determined by ANCOM-BC2 analysis. Fungal taxa unannotated at the order level are annotated to the finest taxonomic resolution. Points on the left side of the dashed vertical line represent taxa enriched in the CON treatment, and points on the right side of the dashed vertical line represent taxa enriched in the CHR treatment. X-axes represent log-fold changes.

2.4.4. Fungal Taxonomic Differences

Order relative abundances are indicated as percentages within parentheses (Fig. A1.7). Pleosporales dominated SGS soils (23.6%), Agaricales dominated HPG (14.7%) and KNZ (32.1%), and Mortierellales dominated HYS (16%) soils (Fig. A1.7). At SGS, the fungal orders Thelebolales (0.3%), Eurotiales (0.3%), and Tremellodendropsidales (0.2%) were most enriched

under CHR, while Auriculariales (0.07%), Pyxidiophorales (0.01%), and Atheliales (<0.01%) were most enriched under CON (Fig. 2.3). At HPG, Agaricales (14.7%) and an undetermined order within the Mortierellomycetes (0.02%) were most enriched under CHR, and Ostropales (0.2%) and Rhizophlyctidales (0.01%) were most enriched under CON (Fig. 2.3). At HYS, Basidiobolales (0.06%), Tremellales (0.2%) and Mytilinidiales (0.01%) were most enriched under CHR, and undetermined orders within the Dothideomycetes (1.6%) and Sordariomycetes (0.7%) were most enriched under CON (Fig. 2.3). At KNZ, Cantharellales (0.6%), Glomerales (0.3%), and Capnodiales (0.09%) were most enriched under CHR, while Onygenales (0.3%), Tremellodendropsidales (0.1%), and an undetermined order within the Eurotiomycetes (1.0%) were most enriched under CON (Fig. 2.3).

2.4.5 Network Analysis

Prokaryotic and fungal networks were sporadically structured across sites and treatments, with no consistent legacy response to the CHR treatment relative to the CON treatment (Figs. 2.4, A1.10, Table 2.3). Evidence of legacy effects on network structure was only evident at SGS, where both the prokaryotic and fungal networks displayed decreased nodes, edges, and modularity in the CHR treatment relative to the CON treatment (Figs. 2.4, A1.10, Table 2.3). Overall, network node values mirrored the trends in prokaryotic and fungal diversity (Figs. 2.4, A1.10, Table 2.3).

Across all prokaryotic networks, the SGS CON treatment displayed the highest modularity (0.846, Fig. 2.4, Table 2.3), while the HPG CON treatment displayed the lowest modularity (0.389, Fig. 2.4, Table 2.3). Prokaryotic network nodes fell between 504 in the KNZ CON treatment and 696 in the SGS CON treatment. Prokaryotic network edges fell between 965 in the KNZ CON treatment and 2413 in the HPG CHR treatment.

Fungal network topology differed from prokaryotes, whereby nodes and edges were relatively lower overall, likely due to much lower fungal diversity (Fig. A1.10, Table 2.3). Fungal network modularity was highest in the HYS CON treatment (0.757) and lowest in the HPG CHR treatment (0.496). Fungal network nodes were between 167 in the SGS CHR treatment and 381 in the HPG CHR treatment, while edges were between 349 in the SGS CON treatment and 1970 in the HPG CHR treatment (Fig. A1.10, Table 2.3).

Table 2.3: Topological features of rhizosphere soil microbial co-occurrence networks by site, treatment, and taxonomic group.

		Prokaryotes			**Fungi**		
Site	**Treatment**	Nodes	Edges	Modularity	Nodes	Edges	Modularity
SGS	CON	696	1604	0.846	228	349	0.705
	CHR	622	1331	0.644	167	387	0.501
HPG	CON	601	2340	0.389	366	1805	0.504
	CHR	633	2413	0.407	381	1970	0.496
HYS	CON	604	1303	0.585	315	845	0.757
	CHR	545	1075	0.613	233	501	0.564
KNZ	CON	504	965	0.641	182	364	0.540
	CHR	578	1499	0.545	218	371	0.734

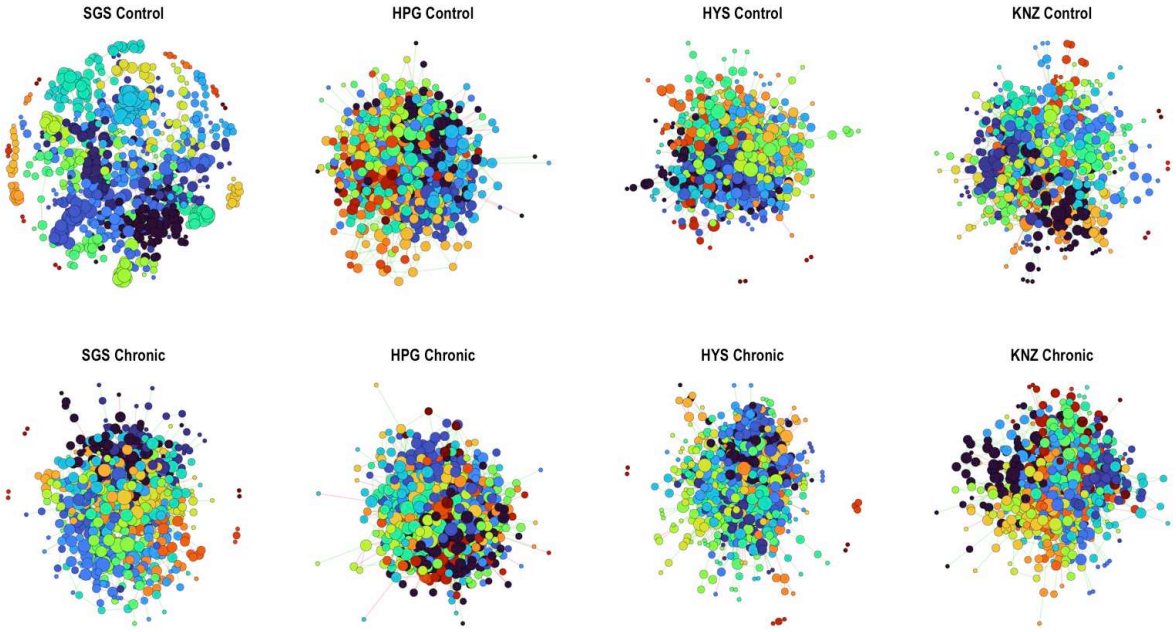

Figure 2.4: Soil rhizosphere prokaryotic co-occurrence networks for Control (CON) and Chronic drought (CHR) treatments at each study site. Individual nodes (circles) represent prokaryotic ASVs. Edges (lines) indicate positive (green) or negative (red) associations among ASVs. Node colors indicate distinct modules, representing clusters of tightly associated nodes.

2.5 Discussion

We sought to understand if extreme drought, imposed as either chronic or intense rainfall exclusion, induced legacy effects of altered soil microbial community structure in unique grassland ecosystems across a precipitation gradient. Previous studies within this experimental network determined that chronic drought catalyzed major changes in prokaryotic community structure and minor changes in fungal community structure across all sites during drought (Ochoa-Hueso et al. 2018), followed by limited evidence of bulk soil legacies in the tallgrass prairie site during the first two years post-drought (Vilonen, Blair et al. 2022, Vilonen et al. 2023). Hence, we anticipated few legacy effects to persist four years post-drought, with any legacy effects primarily evident in prokaryotic communities. Here, we provide *in situ* evidence that extreme drought elicited differential legacy effects of altered rhizosphere prokaryotic and

fungal community structure at each of the experimental sites. Chronic drought prompted more persistent legacy effects than intense drought, suggesting drought intensity is a prominent determinant of soil microbial legacy effects (Oram et al. 2025). Legacies were governed by subordinate and rare taxa that differed at each site, contrasting with common patterns of contemporaneous drought responses and limiting generalization across ecosystems (Ginnan et al. 2025).

2.5.1 Soil Microbial Legacy Effects Depend on Niche

Given bulk and rhizosphere microbial communities respond uniquely to drought via differences in plant-soil interactions (e.g., rhizodeposits and exudation profiles; Canarini and Dijkstra 2015, Williams and de Vries 2020), we investigated each niche separately. Bulk soil prokaryotic and fungal community structures were highly resilient to drought and showed no indication of legacy effects. This partially supports our hypothesis of limited legacy effects, particularly given the lack of bulk soil legacies found in previous studies within (Vilonen, Blair et al. 2022, Vilonen et al. 2023) and outside (Hannula & Veen 2025) of our study system. The notable differences between bulk soil and rhizosphere legacies may be explained by unique mechanisms operating in each niche before, during, and post-drought. For example, biotic filtering of rhizosphere communities may have governed differences between the initial pool of microbes in the bulk and rhizosphere soils (Trivedi et al. 2020, Hannula et al. 2021), whereby drought could reduce plant fitness, alter exudation patterns, and impact root architecture, thus driving legacy effects of altered rhizosphere communities indirectly via plant-soil interactions (Fuchslueger et al. 2014, de Vries et al. 2023, Hannula and Veen 2025). Notably, Hannula and Veen (2025) also found stronger drought legacy effects on rhizosphere fungal communities relative to bulk soil fungal communities in a mesocosm study. Recently, Ginnan et al. (2025) also

found precipitation legacy effects of altered rhizosphere microbial communities, which differed substantially depending on plant species. Direct impacts of drought on both bulk (Evans et al. 2014, Naylor et al. 2017, de Vries et al. 2018, Ochoa-Hueso et al. 2018, Preece et al. 2019, Philipp et al. 2025) and rhizosphere (Lagueux et al. 2020, Fan et al. 2023) soil microbes have been demonstrated, though we provide further support that bulk soil communities recover more rapidly. Hereafter, we solely discuss legacy effects of altered rhizosphere communities.

2.5.2 Rhizosphere Prokaryotic Legacies

Although all sites in this study are grasslands, each site harbored unique prokaryotic communities regardless of experimental treatments (Figs. A1.4). At each site, except for KNZ, chronic drought induced legacy effects of altered prokaryotic community structure, while intense drought only induced legacy effects at SGS (Fig. 2.2). Given prokaryotic diversity did not differ across treatments at the site-level (Fig. A1.2), compositional shifts mediated any differences between control and chronically-droughted communities. This supports previous studies suggesting drought does not necessarily alter soil microbial diversity, rather compositional shifts underscore treatment differences (Naylor et al. 2017).

Legacy effects of drought on prokaryotic communities were greatest at the most arid site, SGS, where aboveground productivity was significantly reduced (Carroll et al. 2021) and prokaryotic communities were substantially altered (Ochoa-Hueso et al. 2018) during the drought. At this semi-arid site, a previous study by Evans et al. (2014) found that after an 11-year drought, rewetting did not promote convergence of microbial community structure, thus providing indirect evidence of drought legacy effects. Given this site is characterized by limited, variable precipitation, soil microbial communities already experience persistent water limitation and are adapted to such conditions (Nielsen & Ball 2015, Evans et al. 2023). Extreme drought

likely reduced water availability beyond the nominal range of conditions, thus prompting major shifts in community composition (Ochoa-Hueso et al. 2018). Further, limited plant productivity and functionality under drought reduced carbon and nutrient inputs, further inhibiting microbial community recovery.

Chronic, but not intense, drought also impacted prokaryotic communities at both mixed-grass prairies, HPG and HYS. HPG is similarly productive to SGS, though it was relatively uninfluenced by the experimental drought treatments (Carroll et al. 2021) due to the C_3 dominance limiting the impacts of summer drought. However, rooting depth increased and BNPP decreased by the final drought year (Carroll et al. 2021), indicating drought-driven shifts in plant carbon allocation that could potentially influence long-term soil microbial community dynamics. At HYS, both above- and belowground productivity losses were pronounced during drought (Carroll et al. 2021), reducing substrate availability, though this does not fully explain legacy effects on rhizosphere community dynamics. Overall, the prevalence of legacy effects in chronic, but not intense, drought treatment plots could be explained by many interactive mechanisms; The intense drought imposed an acute, relatively short-term stress that may have allowed small soil pores to remain hydrated, induced microbial dormancy, and caused plants to limit photosynthesis and subsequent root exudation, all of which allow for a rapid return to baseline functionality upon rewetting (Preece & Peñuelas 2016, Schimel 2018, Williams & de Vries 2020). Alternatively, the chronic drought imposed a less intense, but longer-term stress that could have acted more as a selection pressure on plants and microbes. The gradual progression of chronic drought may have enabled plant and microbial physiological acclimation, shifting root exudation profiles to osmolytes and secondary metabolites, and encouraging microbial osmolyte synthesis and extracellular polymeric substance production (Schimel 2018). However, the specific

mechanisms underlying differential legacy effects under unique drought severities must be further explored.

Taxonomic differences between chronically-droughted and control plots were not determined by the dominant phyla, Acidobacteriota, Actinobacteriota, and Verrucomicrobiota, contrasting with the results of Ochoa-Hueso et al. (2018) and Vilonen et al. (2023). Often, Actinobacteria are enriched during drought (Naylor & Coleman-Derr 2018), however other prokaryotic taxa may be better suited to capitalize on post-drought rhizosphere dynamics as Actinobacteria matched control plot abundances. Notably, most of the enriched phyla composed less than 1% of the relative abundance at each site (Fig. A1.6), suggesting that subordinate and rare taxa play a major role in dictating grassland post-drought trajectories. The primary phyla enriched in chronically-droughted plots differed at each site (Fig. 2.3). At both SGS and KNZ, the candidate phylum, WPS-2 (now considered to be a member of Eremiobacterota; Sheremet et al. 2020), was the most enriched phylum in chronically-droughted plots. Though still cryptic, this phylum has been found in dry, nutrient-poor soils (Sheremet et al. 2020) and even post-wildfire soils in Colorado (Nelson et al. 2022), suggesting a potentially key role in post-disturbance successional dynamics. Two more candidate phyla, Hydrogenedentes and Elusimicrobiota, were most enriched in chronically-droughted plots at HPG and HYS, respectively (Fig. 2.3). To our knowledge, none of these enriched phyla have been previously connected to post-drought ecosystem dynamics, though few studies have investigated drought legacies this long into the post-drought period.

Unlike previous studies, we found that rhizosphere prokaryotic networks generally did not differ across treatments (Fig. 2.4, Table 2.2), suggesting either high structural resistance or resilience (given networks were not analyzed during the drought). However, at our most arid site,

SGS, chronic drought resulted in reduced nodes, edges, and modularity relative to the control treatment. This parallels the findings of de Vries et al. (2018), where drought decreased bacterial network complexity, which persisted into the post-drought period. Interestingly, networks from chronically-droughted plots at our most mesic site (KNZ) showed relatively more nodes and edges, supporting the findings from Vilonen et al. (2023). The lack of consistent legacy effects across grassland prokaryotic communities suggest that recovery dynamics depend, at least partially, upon drought severity, plant community structure, and climatic conditions at each site.

2.5.3 Rhizosphere Fungal Legacies

Fungal communities tend to be more drought resistant than prokaryotic communities (de Vries et al. 2018, Ochoa-Hueso et al. 2018, Lagueux et al. 2020). Thus, we anticipated few legacies of altered fungal community structure under either previous drought treatment. However, like prokaryotic communities, chronic drought imposed legacy effects of altered fungal communities at three out of four sites (SGS, HYS, and KNZ) due to compositional shifts (Fig. 2.2, Lagueux et al. 2020). The intense drought treatment only resulted in legacy effects of altered fungal community structure at HPG, though planned comparisons between control and intense drought communities explains the least amount of variance ($R^2 = 0.0366$) of any significant comparisons.

The strongest fungal legacy effects also persisted at SGS, likely mediated by similar mechanisms to prokaryotic communities. Persistent water limitation favors stress-tolerant, slow-growing fungi in semi-arid grasslands (Porras-Alfaro et al. 2011, Lopez et al. 2024); hence, these communities are unlikely to recover rapidly from extreme disturbances. This finding contrasts with Ochoa-Hueso et al. (2018), who found that soil fungi in more arid sites (including SGS) responded less to drought than those in more mesic sites. However, Ochoa-Hueso et al. (2018)

investigated the effects after two years of drought, rather than the full four-year drought treatments.

Chronic drought also induced fungal legacy effects at the two most mesic sites, KNZ and HYS (Fig. 2.2). Lagueux et al. (2020) found, within this experimental network, chronic drought re-ordered fungal communities within *A. gerardii* roots at KNZ and *B. curtipendula* roots at HYS, and these changes were similarly dictated by species reordering. Further, Vilonen et al. (2023) found few legacy effects of chronic drought on bulk soil fungal communities at KNZ, in the two years post-drought, though neither study explored rhizosphere responses. Collectively, these findings indicate that bulk soil fungal communities may recover rapidly from drought, while rhizosphere, and potentially root-associated, fungal communities take longer to recover.

No fungal orders were consistently enriched under previous chronic drought relative to control (Fig. 2.3). Rather, a unique suite of fungi was enriched at each site. At KNZ, the greatest number of fungal orders were enriched under chronic drought, dominated by primarily saprotrophic fungal orders. Surprisingly, Glomerales, the arbuscular mycorrhizal fungi (AMF), were the second most enriched order under chronic drought. The fungal primers used here tend to limit taxonomic resolution of AMF, biasing our results against detecting these taxa, so it is likely that these findings do not represent the full extent of AMF legacies (Öpik et al. 2010, Lekberg et al. 2018). Overall, the lack of consistency in fungal taxa enriched under previous chronic drought indicate that legacy effects may not be predictable based on understanding soil fungi enriched under contemporary drought, given post-drought soil fungal dynamics may be determined by substrate availability, plant community composition, and soil nutrient dynamics.

2.5.4 A Need to Further Understand Soil Legacy Effects

Global change is already amplifying severity of droughts globally (Gebrechorkos et al. 2025), magnifying the need to understand how ecosystems respond to and recover from drought. Increasing evidence indicates that drought legacy effects persist in some contexts (e.g., Kaisermann et al. 2017, Kannenberg and Schwalm 2020, Oram et al. 2025) but not others (e.g., Vilonen, Blair et al. 2022, Vilonen et al. 2023, Hannula et al. 2025) prompting a need to also understand when and where drought legacies impact ecosystem structure and function (Müller and Bahn 2022). Our findings suggest that extreme drought results in legacy effects of altered rhizosphere prokaryotic and fungal community structure across grasslands, though the magnitude of legacies were site dependent. Notably, rhizosphere legacies persisted late into the growing season, suggesting legacies may be evident beyond peak plant activity. We did not detect any bulk soil legacies, suggesting plant-mediated legacies may be more important than previously realized (de Vries et al. 2023). However, further investigation of plant community responses may lend insight into bulk soil microbial community dynamics.

Legacies were also dependent upon the severity of drought, adding another dimension to determining both contemporary and legacy effects (Oram et al. 2025). It is important to note that the variance in community structure explained by treatment was relatively low (~4-9%) compared to the variance explained by site (~18-30%), which suggests that other factors that differ across sites, such as soil pH, organic matter, or plant community composition, may have a predominant role in shaping microbial communities. Further, a single sampling event lends limited insight regarding the trajectories of soil microbial communities post-drought. Drought legacy effects may persist for years post-drought, but investigating the trajectory of community shifts would inform if these communities are recovering, or if there are persistent legacy effects and potentially altered community states (Cordero et al. 2023).

Nonetheless, although these data do not directly suggest altered soil functionality, lasting changes in microbial community structure are likely to influence long-term ecosystem functionality, especially under changing disturbance regimes. Hence, future work must also prioritize the drivers and mechanisms underlying soil legacy effects. Understanding post-drought ecosystem dynamics will require rigorous spatiotemporal investigations of both above- and belowground community structure and function.

LITERATURE CITED

Allison, S. D., and J. B. Martiny. 2008. "Resistance, Resilience, and Redundancy in Microbial Communities." *Proceedings of the National Academy of Sciences* 105, no. 1: 11512–11519. https://doi.org/10.1073/pnas.0801925105.

Allison, S. D. 2023. "Microbial Drought Resistance May Destabilize Soil Carbon." *Trends in Microbiology* 31, no. 8: 780–787. https://doi.org/10.1016/j.tim.2023.03.002.

Apprill, A., S. McNally, R. Parsons, and L. Weber. 2015. "Minor Revision to V5 Region SSU rRNA 806R Gene Primer Greatly Increases Detection of SAR11 Bacterioplankton." *Aquatic Microbial Ecology* 75, no. 2: 129–137. https://doi.org/10.3354/ame01753.

Arbizu, M. 2020. "pairwiseAdonis: Pairwise Multilevel Comparison Using Adonis." *R Package Version 0.4.1*. https://github.com/pmartinezarbizu/pairwiseAdonis.

Bai, Y., and M. F. Cotrufo. 2022. "Grassland Soil Carbon Sequestration: Current Understanding, Challenges, and Solutions." *Science* 377, no. 6606: 603–608. https://doi.org/10.1126/science.abo2380.

Bakker, P. A., R. L. Berendsen, R. F. Doornbos, P. C. Wintermans, and C. M. Pieterse. 2013. "The Rhizosphere Revisited: Root Microbiomics." *Frontiers in Plant Science* 4: 165. https://doi.org/10.3389/fpls.2013.00165.

Bazany, K. E., J. T. Wang, M. Delgado-Baquerizo, B. K. Singh, and P. Trivedi. 2022. "Water Deficit Affects Inter-Kingdom Microbial Connections in Plant Rhizosphere." *Environmental Microbiology* 24, no. 8: 3722–3734. https://doi.org/10.1111/1462-2920.15931.

Bazany, K., A. Dhar, K. Otto, Y. Jing, and P. Trivedi. 2025. "Water Deficit Stress Alters the Microbial Community Assembly, Structure, and Sources in Corn and Sugar Beet." *Environmental Microbiology* 27, no. 10: e70186. https://doi.org/10.1111/1462-2920.70186.

Bellemain, E., T. Carlsen, C. Brochmann, E. Coissac, P. Taberlet, and H. Kauserud. 2010. "ITS as an Environmental DNA Barcode for Fungi: An in Silico Approach Reveals Potential PCR Biases." *BMC Microbiology* 10, no. 1: 189. https://doi.org/10.1186/1471-2180-10-189.

Bokulich, N. A., S. Subramanian, J. J. Faith, et al. 2013. "Quality-Filtering Vastly Improves Diversity Estimates From Illumina Amplicon Sequencing." *Nature Methods* 10, no. 1: 57–59. https://doi.org/10.1038/nmeth.2276.

Bolyen, E., J. R. Rideout, M. R. Dillon, et al. 2019. "Reproducible, Interactive, Scalable and Extensible Microbiome Data Science Using QIIME 2." *Nature Biotechnology* 37, no. 8: 852–857. https://doi.org/10.1038/s41587-019-0209-9.

Broderick, C. M., G. M. N. Benucci, L. R. Bachega, G. D. Miller, S. E. Evans, and C. V. Hawkes. 2025. "Long-term Climate Establishes Functional Legacies by Altering Microbial Traits." *The ISME Journal* 19, no. 1: wraf005. https://doi.org/10.1093/ismej/wrae005.

Callahan, B. J., P. J. McMurdie, M. J. Rosen, A. W. Han, A. J. A. Johnson, and S. P. Holmes. 2016. "DADA2: High-Resolution Sample Inference From Illumina Amplicon Data." *Nature Methods* 13, no. 7: 581–583. https://doi.org/10.1038/nmeth.3869.

Canarini, A., and F. A. Dijkstra. 2015. "Dry-rewetting Cycles Regulate Wheat Carbon Rhizodeposition, Stabilization and Nitrogen Cycling." *Soil Biology and Biochemistry* 81: 195–203. https://doi.org/10.1016/j.soilbio.2014.11.014.

Canarini, A., H. Schmidt, L. Fuchslueger, V. Martin, C. W. Herbold, D. Zezula, et al. 2021. "Ecological Memory of Recurrent Drought Modifies Soil Processes via Changes in Soil Microbial Community." *Nature Communications* 12, no. 1: 5308. https://doi.org/10.1038/s41467-021-25675-4.

Cao, Q., X. Sun, K. Rajesh, et al. 2021. "Effects of Rare Microbiome Taxa Filtering on Statistical Analyses." *Frontiers in Microbiology* 11: 607325. https://doi.org/10.3389/fmicb.2020.607325.

Caporaso, J. G., C. L. Lauber, W. A. Walters, et al. 2012. "Ultra-High-Throughput Microbial Community Analysis on the Illumina HiSeq and MiSeq Platforms." *ISME Journal* 6, no. 8: 1621–1624. https://doi.org/10.1038/ismej.2012.8.

Carroll, C. J., I. J. Slette, R. J. Griffin-Nolan, L. E. Baur, A. M. Hoffman, E. M. Denton, et al. 2021. "Is a Drought a Drought in Grasslands? Productivity Responses to Different Types of Drought." *Oecologia* 197, no. 4: 1017–1026. https://doi.org/10.1007/s00442-021-04987-0.

Chen, L., P. Brun, P. Buri, S. Fatichi, A. Gessler, M. J. McCarthy, et al. 2025. "Global Increase in the Occurrence and Impact of Multiyear Droughts." *Science* 387, no. 6731: 278–284. https://doi.org/10.1126/science.adr2589.

Condon, K. V., C. J. Carroll, R. J. Griffin-Nolan, I. J. Slette, K. D. Wilkins, M. D. Smith, and A. K. Knapp. 2025. "Experimental Drought Consistently Underestimates Productivity Responses to Natural Drought in Four Central US Grasslands." *Oecologia* 207, no. 7: 104. https://doi.org/10.1007/s00442-025-05670-w.

Cook, B. I., J. S. Mankin, and K. J. Anchukaitis. 2018. "Climate Change and Drought: From Past to Future." *Current Climate Change Reports* 4, no. 2: 164–179. https://doi.org/10.1007/s40641-018-0093-2.

Cordero, I., A. Leizeaga, L. C. Hicks, J. Rousk, and R. D. Bardgett. 2023. "High Intensity Perturbations Induce an Abrupt Shift in Soil Microbial State." *The ISME Journal* 17, no. 12: 2190–2199. https://doi.org/10.1038/s41396-023-01529-z.

Craine, J. M., T. W. Ocheltree, J. B. Nippert, E. G. Towne, A. M. Skibbe, S. W. Kembel, and J. E. Fargione. 2013. "Global Diversity of Drought Tolerance and Grassland Climate-Change Resilience." *Nature Climate Change* 3, no. 1: 63–67. https://doi.org/10.1038/nclimate1634.

Csárdi, G., T. Nepusz, V. Traag, S. Horvát, F. Zanini, D. Noom, K. Müller, D. Schoch, and M. Salmon. 2026. "igraph: Network Analysis and Visualization in R." *R Package Version 2.2.2*. https://doi.org/10.5281/zenodo.7682609.

De Long, J. R., M. Semchenko, W. J. Pritchard, I. Cordero, E. L. Fry, B. G. Jackson, et al. 2019. "Drought Soil Legacy Overrides Maternal Effects on Plant Growth." *Functional Ecology* 33, no. 8: 1400–1410. https://doi.org/10.1111/1365-2435.13375.

De Vries, F., J. Lau, C. Hawkes, and M. Semchenko. 2023. "Plant–Soil Feedback Under Drought: Does History Shape the Future?" *Trends in Ecology & Evolution* 38, no. 8: 708–718. https://doi.org/10.1016/j.tree.2023.02.004.

De Vries, F. T., R. I. Griffiths, M. Bailey, H. Craig, M. Girlanda, H. S. Gweon, et al. 2018. "Soil Bacterial Networks Are Less Stable Under Drought Than Fungal Networks." *Nature Communications* 9, no. 1: 3033. https://doi.org/10.1038/s41467-018-05516-7.

Enderle, E., L. Hinojosa, V. Lombard, F. Hou, and F. T. de Vries. 2025. "Drought Legacy Effects on Plant Growth and Plant–Soil Feedback Are Mediated by Soil Microbial Communities Independently of Root Exudates and Root Litter." *Journal of Ecology* 113, no. 11: 3293–3312. https://doi.org/10.1111/1365-2745.14389.

Evans, S. E., S. D. Allison, and C. V. Hawkes. 2022. "Microbes, Memory and Moisture: Predicting Microbial Moisture Responses and Their Impact on Carbon Cycling." *Functional Ecology* 36, no. 6: 1430–1441. https://doi.org/10.1111/1365-2435.14041.

Evans, S. E., and M. D. Wallenstein. 2014. "Climate Change Alters Ecological Strategies of Soil Bacteria." *Ecology Letters* 17, no. 2: 155–164. https://doi.org/10.1111/ele.12206.

Fan, W., F. Tang, W. Wang, J. Dong, J. Xing, and F. Shi. 2023. "Drought-Induced Recruitment of Specific Root-Associated Bacteria Enhances Adaptation of Alfalfa to Drought Stress." *Frontiers in Microbiology* 14: 1114400. https://doi.org/10.3389/fmicb.2023.1114400.

Felton, A. J., and M. D. Smith. 2017. “Integrating Plant Ecological Responses to Climate Extremes From Individual to Ecosystem Levels.” *Philosophical Transactions of the Royal Society B: Biological Sciences* 372, no. 1723: 20160142. https://doi.org/10.1043/rstb.2016.0142.

Fuchslueger, L., M. Bahn, K. Fritz, R. Hasibeder, and A. Richter. 2014. “Experimental Drought Reduces the Transfer of Recently Fixed Plant Carbon to Soil Microbes and Alters the Bacterial Community Composition in a Mountain Meadow.” *New Phytologist* 201, no. 3: 916–927. https://doi.org/10.1111/nph.12569.

Gebrechorkos, S. H., J. Sheffield, S. M. Vicente-Serrano, C. Funk, D. G. Miralles, J. Peng, et al. 2025. “Warming Accelerates Global Drought Severity.” *Nature* 642, no. 8068: 628–635. https://doi.org/10.1038/s41586-025-08620-w.

Ginnan, N. A., V. Custódio, D. Gopaulchan, N. Ford, I. Salas-González, D. H. Jones, et al. 2025. “Precipitation Legacy Effects on Soil Microbiota Facilitate Adaptive Drought Responses in Plants.” *Nature Microbiology*: 1–22. https://doi.org/10.1038/s41564-024-01907-w.

Gloor, G. B., J. M. Macklaim, V. Pawlowsky-Glahn, and J. J. Egozcue. 2017. “Microbiome Datasets Are Compositional: And This Is Not Optional.” *Frontiers in Microbiology* 8: 2224. https://doi.org/10.3389/fmicb.2017.02224.

Griffin-Nolan, R. J., D. M. Blumenthal, S. L. Collins, T. E. Farkas, A. M. Hoffman, K. E. Mueller, T. W. Ocheltree, M. D. Smith, K. D. Whitney, and A. K. Knapp. 2019. “Shifts in Plant Functional Composition Following Long-Term Drought in Grasslands.” *Journal of Ecology* 107, no. 5: 2133–2148. https://doi.org/10.1111/1365-2745.13252.

Hannula, S. E., R. Heinen, M. Huberty, K. Steinauer, J. R. De Long, R. Jongen, and T. M. Bezemer. 2021. “Persistence of Plant-Mediated Microbial Soil Legacy Effects in Soil and Inside Roots.” *Nature Communications* 12, no. 1: 5686. https://doi.org/10.1038/s41467-021-25971-z.

Hannula, S. E., and G. F. Veen. 2025. “Drought Has Short-term Effects on Soil Fungal Communities Leading to Long-term Effects on Soil Functions.” *Soil Biology and Biochemistry* 209: 109893. https://doi.org/10.1016/j.soilbio.2024.109893.

Hartmann, M., and J. Six. 2023. “Soil Structure and Microbiome Functions in Agroecosystems.” *Nature Reviews Earth & Environment* 4, no. 1: 4–18. https://doi.org/10.1038/s43017-022-00366-z.

Hueso, S., T. Hernández, and C. García. 2011. “Resistance and Resilience of the Soil Microbial Biomass to Severe Drought in Semiarid Soils: The Importance of Organic Amendments.” *Applied Soil Ecology* 50: 27–36. https://doi.org/10.1016/j.apsoil.2011.07.014.

Hussain, U., M. C. Cambon, B. Crampton, S. Subramaniam, A. Kajamuhan, A. Ordoñez, J. Downie, J. Finch, M. Beckmann, N. Brown, and A. Elison. 2026. “Microbial

Communities in Semi-Mature Oak Trees Are Resilient to Drought, Nutrient Limitation, and Pathogen Challenge." *Cell Host & Microbe* 34, no. 2: 344–358. https://doi.org/10.1016/j.chom.2026.01.010.

Huxman, T. E., M. D. Smith, P. A. Fay, A. K. Knapp, M. R. Shaw, M. E. Loik, et al. 2004. "Convergence Across Biomes to a Common Rain-use Efficiency." *Nature* 429, no. 6992: 651–654. https://doi.org/10.1038/nature02561.

Kaisermann, A., F. T. de Vries, R. I. Griffiths, and R. D. Bardgett. 2017. "Legacy Effects of Drought on Plant–Soil Feedbacks and Plant–Plant Interactions." *New Phytologist* 215, no. 4: 1413–1424. https://doi.org/10.1111/nph.14661.

Kannenberg, S. A., C. R. Schwalm, and W. R. Anderegg. 2020. "Ghosts of the Past: How Drought Legacy Effects Shape Forest Functioning and Carbon Cycling." *Ecology Letters* 23, no. 5: 891–901. https://doi.org/10.1111/ele.13485.

Knapp, A. K., C. J. Carroll, E. M. Denton, K. J. La Pierre, S. L. Collins, and M. D. Smith. 2015. "Differential Sensitivity to Regional-scale Drought in Six Central US Grasslands." *Oecologia* 177, no. 4: 949–957. https://doi.org/10.1007/s00442-015-3219-3.

Knapp, A. K., A. Chen, R. J. Griffin-Nolan, L. E. Baur, C. J. Carroll, J. E. Gray, A. M. Hoffman, X. Li, A. K. Post, I. J. Slette, and S. L. Collins. 2020. "Resolving the Dust Bowl Paradox of Grassland Responses to Extreme Drought." *Proceedings of the National Academy of Sciences* 117, no. 36: 22249–22255. https://doi.org/10.1073/pnas.1922030117.

Knapp, A. K., K. V. Condon, C. C. Folks, M. A. Sturchio, R. J. Griffin-Nolan, S. A. Kannenberg, et al. 2024. "Field Experiments Have Enhanced Our Understanding of Drought Impacts on Terrestrial Ecosystems—But Where Do We Go From Here?" *Functional Ecology* 38: 76–97. https://doi.org/10.1111/1365-2435.14473.

Knapp, A. K., and M. D. Smith. 2001. "Variation Among Biomes in Temporal Dynamics of Aboveground Primary Production." *Science* 291, no. 5503: 481–484. https://doi.org/10.1126/science.291.5503.481.

Kurtz, Z. D., C. L. Müller, E. R. Miraldi, D. R. Littman, M. J. Blaser, and R. A. Bonneau. 2015. "Sparse and Compositionally Robust Inference of Microbial Ecological Networks." *PLoS Computational Biology* 11, no. 5: e1004226. https://doi.org/10.1371/journal.pcbi.1004226.

Lagueux, D., A. Jumpponen, A. Porras-Alfaro, J. Herrera, Y. A. Chung, L. E. Baur, et al. 2021. "Experimental Drought Re-Ordered Assemblages of Root-Associated Fungi Across North American Grasslands." *Journal of Ecology* 109, no. 2: 776–792. https://doi.org/10.1111/1365-2745.13504.

Leizeaga, A., L. C. Hicks, L. Manoharan, C. V. Hawkes, and J. Rousk. 2021. "Drought Legacy Affects Microbial Community Trait Distributions Related to Moisture Along a Savannah

Grassland Precipitation Gradient." *Journal of Ecology* 109, no. 9: 3195–3210. https://doi.org/10.1111/1365-2745.13733.

Lekberg, Y., M. Vasar, L. S. Bullington, S. K. Sepp, P. M. Antunes, R. Bunn, et al. 2018. "More Bang for the Buck? Can Arbuscular Mycorrhizal Fungal Communities Be Characterized Adequately Alongside Other Fungi Using General Fungal Primers?" *New Phytologist* 220, no. 4: 971–976. https://doi.org/10.1111/nph.15035.

Leff, J. W. 2017. "mctoolsr: Microbial Community Data Analysis Tools." *R Package Version 0.1.1.2*. https://github.com/leffj/mctoolsr.

Lin, H., and S. D. Peddada. 2020. "Analysis of Compositions of Microbiomes With Bias Correction." *Nature Communications* 11: 3514. https://doi.org/10.1038/s41467-020-17041-7.

Ling, N., T. Wang, and Y. Kuzyakov. 2022. "Rhizosphere Bacteriome Structure and Functions." *Nature Communications* 13, no. 1: 836. https://doi.org/10.1038/s41467-022-28448-9.

Liu, D., Zhang, C., Ogaya, R., Fernandez-Martinez, M., Pugh, T. A., and J. Peñuelas. 2021. "Increasing Climatic Sensitivity of Global Grassland Vegetation Biomass and Species Diversity Correlates with Water Availability." *New Phytologist* 230, no. 5: 1761–1771. https://doi.org/10.1111/nph.17268.

Lopez, A., M. Anthony, J. Catalan-Dibene, S. Ferrenberg, S. E. Jordan, B. Osborne, et al. 2024. "Dryland Fungi Are Spatially Heterogeneous and Resistant to Global Change Drivers." *Ecosphere* 15, no. 12: e70031. https://doi.org/10.1002/ecs2.70031.

Lozano, Y. M., C. A. Aguilar-Trigueros, G. Onandia, S. Maaß, T. Zhao, and M. C. Rillig. 2021. "Effects of Microplastics and Drought on Soil Ecosystem Functions and Multifunctionality." *Journal of Applied Ecology* 58, no. 5: 988–996. https://doi.org/10.1111/1365-2664.13839.

MacDougall, A. S., B. Vanzant, J. Sulik, S. Bagchi, D. Naidu, T. O. Muraina, et al. 2026. "The Global Extent of the Grassland Biome and Implications for the Terrestrial Carbon Sink." *Nature Ecology & Evolution*: 1–12. https://doi.org/10.1038/s41559-026-03120-x.

Malik, A. A., and N. J. Bouskill. 2022. "Drought Impacts on Microbial Trait Distribution and Feedback to Soil Carbon Cycling." *Functional Ecology* 36, no. 6: 1442–1456. https://doi.org/10.1111/1365-2435.14044.

Malik, A. A., J. B. Martiny, E. L. Brodie, A. C. Martiny, K. K. Treseder, and S. D. Allison. 2020. "Defining Trait-Based Microbial Strategies With Consequences for Soil Carbon Cycling Under Climate Change." *The ISME Journal* 14, no. 1: 1–9. https://doi.org/10.1038/s41396-019-0510-0.

McMurdie, P. J., and S. Holmes. 2013. "Phyloseq: An R Package for Reproducible Interactive Analysis and Graphics of Microbiome Census Data." *PLoS One* 8, no. 4: e61217. https://doi.org/10.1371/journal.pone.0061217.

Meisner, A., S. Jacquiod, B. L. Snoek, F. C. Ten Hooven, and W. H. van Der Putten. 2018. "Drought Legacy Effects on the Composition of Soil Fungal and Prokaryote Communities." *Frontiers in Microbiology* 9: 294. https://doi.org/10.3389/fmicb.2018.00294.

Müller, L. M., and M. Bahn. 2022. "Drought Legacies and Ecosystem Responses to Subsequent Drought." *Global Change Biology* 28, no. 17: 5086–5103. https://doi.org/10.1111/gcb.16270.

Naumann, G., L. Alfieri, K. Wyser, L. Mentaschi, R. A. Betts, H. Carrao, et al. 2018. "Global Changes in Drought Conditions Under Different Levels of Warming." *Geophysical Research Letters* 45, no. 7: 3285–3296. https://doi.org/10.1002/2017GL076521.

Naylor, D., and D. Coleman-Derr. 2018. "Drought Stress and Root-associated Bacterial Communities." *Frontiers in Plant Science* 8: 2223. https://doi.org/10.3389/fpls.2017.02223.

Naylor, D., S. DeGraaf, E. Purdom, and D. Coleman-Derr. 2017. "Drought and Host Selection Influence Bacterial Community Dynamics in the Grass Root Microbiome." *The ISME Journal* 11, no. 12: 2691–2704. https://doi.org/10.1038/ismej.2017.118.

Nelson, A. R., A. B. Narrowe, C. C. Rhoades, T. S. Fegel, R. A. Daly, H. K. Roth, et al. 2022. "Wildfire-Dependent Changes in Soil Microbiome Diversity and Function." *Nature Microbiology* 7, no. 9: 1419–1430. https://doi.org/10.1038/s41564-022-01203-y.

Nielsen, U. N., and B. A. Ball. 2015. "Impacts of Altered Precipitation Regimes on Soil Communities and Biogeochemistry in Arid and Semi-Arid Ecosystems." *Global Change Biology* 21, no. 4: 1407–1421. https://doi.org/10.1111/gcb.12758.

Nilsson, R. H., K. H. Larsson, A. F. S. Taylor, et al. 2019. "The UNITE Database for Molecular Identification of Fungi: Handling Dark Taxa and Parallel Taxonomic Classifications." *Nucleic Acids Research* 47, no. D1: D259–D264. https://doi.org/10.1093/nar/gky1022.

Ochoa-Hueso, R., S. L. Collins, M. Delgado-Baquerizo, K. Hamonts, W. T. Pockman, R. L. Sinsabaugh, et al. 2018. "Drought Consistently Alters the Composition of Soil Fungal and Bacterial Communities in Grasslands From Two Continents." *Global Change Biology* 24, no. 7: 2818–2827. https://doi.org/10.1111/gcb.14113.

Ohlert, T., M. D. Smith, S. L. Collins, A. K. Knapp, J. S. Dukes, O. Sala, et al. 2025. "Drought Intensity and Duration Interact to Magnify Losses in Primary Productivity." *Science* 390, no. 6770: 284–289. https://doi.org/10.1126/science.ads1254.

Oksanen, J., F. G. Blanchet, R. Kindt, et al. 2013. "Package 'Vegan'." *Community Ecology Package* 2, no. 9: 1–295. https://CRAN.R-project.org/package=vegan.

Öpik, M., A. Vanatoa, E. Vanatoa, M. Moora, J. Davison, J. M. Kalwij, et al. 2010. "The Online Database MaarjAM Reveals Global and Ecosystemic Distribution Patterns in Arbuscular Mycorrhizal Fungi (Glomeromycota)." *New Phytologist* 188, no. 1: 223–241. https://doi.org/10.1111/j.1469-8137.2010.03334.x.

Oram, N. J., N. Praeg, R. D. Bardgett, F. Brennan, T. Caruso, P. Illmer, et al. 2025. "Drought Intensity Shapes Soil Legacy Effects on Grassland Plant and Soil Microbial Communities and Their Responses to Future Drought." *Global Change Biology* 31, no. 9: e70495. https://doi.org/10.1111/gcb.70495.

Parada, A. E., D. M. Needham, and J. A. Fuhrman. 2015. "Every Base Matters: Assessing Small Subunit rRNA Primers for Marine Microbiomes With Mock Communities, Time Series and Global Field Samples." *Environmental Microbiology* 18, no. 5: 1403–1414. https://doi.org/10.1111/1462-2920.13023.

Pedersen, T. 2025. "ggraph: An Implementation of Grammar of Graphics for Graphs and Networks." *R Package Version 2.2.2.9000*. https://github.com/thomasp85/ggraph.

Philipp, L., E. Blagodatskaya, M. Tarkka, and T. Reitz. 2025. "Soil Microbial Communities Are More Disrupted by Extreme Drought Than by Gradual Climate Shifts Under Different Land-Use Intensities." *Frontiers in Microbiology* 16: 1649443. https://doi.org/10.3389/fmicb.2025.1649443.

Porras-Alfaro, A., J. Herrera, D. O. Natvig, K. Lipinski, and R. L. Sinsabaugh. 2011. "Diversity and Distribution of Soil Fungal Communities in a Semiarid Grassland." *Mycologia* 103, no. 1: 10–21. https://doi.org/10.3852/09-297.

Preece, C., and J. Peñuelas. 2016. "Rhizodeposition Under Drought and Consequences for Soil Communities and Ecosystem Resilience." *Plant and Soil* 409, no. 1: 1–17. https://doi.org/10.1007/s11104-016-3090-y.

Preece, C., E. Verbruggen, L. Liu, J. T. Weedon, and J. Peñuelas. 2019. "Effects of Past and Current Drought on the Composition and Diversity of Soil Microbial Communities." *Soil Biology and Biochemistry* 131: 28–39. https://doi.org/10.1016/j.soilbio.2018.12.022.

R Core Team. 2023. "R: A Language and Environment for Statistical Computing." *R Foundation for Statistical Computing*. https://www.R-project.org/.

Santos-Medellín, C., J. Edwards, Z. Liechty, B. Nguyen, and V. Sundaresan. 2017. "Drought Stress Results in a Compartment-Specific Restructuring of the Rice Root-Associated Microbiomes." *mBio* 8, no. 4: e00764-17. https://doi.org/10.1128/mBio.00764-17.

Schimel, J. P. 2018. “Life in Dry Soils: Effects of Drought on Soil Microbial Communities and Processes.” *Annual Review of Ecology, Evolution, and Systematics* 49, no. 1: 409–432. https://doi.org/10.1146/annurev-ecolsys-110617-062614.

Schrama, M., and R. D. Bardgett. 2016. “Grassland Invasibility Varies With Drought Effects on Soil Functioning.” *Journal of Ecology* 104, no. 5: 1250–1258. https://doi.org/10.1111/1365-2745.12604.

Sheremet, A., G. M. Jones, J. J. Jarett, R. M. Bowers, I. Bedard, C. Culham, et al. 2020. “Ecological and Genomic Analyses of Candidate Phylum WPS-2 Bacteria in an Unvegetated Soil.” *Environmental Microbiology* 22, no. 8: 3143–3157. https://doi.org/10.1111/1462-2920.15053.

Simpson, G. L. 2026. “permute: Functions for Generating Restricted Permutations of Data.” *R package version 0.9-10.* https://github.com/gavinsimpson/permute.

Smith, D. P., and K. G. Peay. 2014. “Sequence Depth, Not PCR Replication, Improves Ecological Inference From Next Generation DNA Sequencing.” *PLoS One* 9, no. 2: e90234. https://doi.org/10.1371/journal.pone.0090234.

Smith, M. D., K. D. Wilkins, M. C. Holdrege, P. Wilfahrt, S. L. Collins, A. K. Knapp, et al. 2024. “Extreme Drought Impacts Have Been Underestimated in Grasslands and Shrublands Globally.” *Proceedings of the National Academy of Sciences* 121, no. 4: e2309881120. https://doi.org/10.1073/pnas.2309881120.

Song, J., S. Wan, S. Piao, A. K. Knapp, A. T. Classen, S. Vicca, et al. 2019. “A Meta-Analysis of 1119 Manipulative Experiments on Terrestrial Carbon-Cycling Responses to Global Change.” *Nature Ecology & Evolution* 3, no. 9: 1309–1320. https://doi.org/10.1038/s41559-019-0958-3.

Swain, D. L., A. F. Prein, J. T. Abatzoglou, C. M. Albano, M. Brunner, N. S. Diffenbaugh, et al. 2025. “Hydroclimate Volatility on a Warming Earth.” *Nature Reviews Earth & Environment* 6: 35–50. https://doi.org/10.1038/s43017-024-00624-z.

Trivedi, P., J. E. Leach, S. G. Tringe, T. Sa, and B. K. Singh. 2020. “Plant–Microbiome Interactions: From Community Assembly to Plant Health.” *Nature Reviews Microbiology* 18, no. 11: 607–621. https://doi.org/10.1038/s41579-020-0412-1.

Vilonen, L. L., J. Blair, P. Trivedi, L. Zeglin, and M. D. Smith. 2022. “Limited Legacy Effects of Extreme Multiyear Drought on Carbon and Nitrogen Cycling in a Mesic Grassland.” *Elementa: Science of the Anthropocene* 10, no. 1: 000093. https://doi.org/10.1525/elementa.2021.00093.

Vilonen, L., M. Ross, and M. D. Smith. 2022. “What Happens After Drought Ends: Synthesizing Terms and Definitions.” *New Phytologist* 235, no. 2: 420–431. https://doi.org/10.1111/nph.18137.

Vilonen, L. L., S. Hoosein, M. D. Smith, and P. Trivedi. 2023. "Legacy Effects of Intensified Drought on the Soil Microbiome in a Mesic Grassland." *Ecosphere* 14, no. 6: e4545. https://doi.org/10.1002/ecs2.4545.

Wagg, C., S. F. Bender, F. Widmer, and M. G. Van Der Heijden. 2014. "Soil Biodiversity and Soil Community Composition Determine Ecosystem Multifunctionality." *Proceedings of the National Academy of Sciences* 111, no. 14: 5266–5270. https://doi.org/10.1073/pnas.1320054111.

Wickham, H. 2016. *ggplot2: Elegant Graphics for Data Analysis*. Springer-Verlag New York. ISBN 978-3-319-24277-4. https://ggplot2.tidyverse.org.

Williams, A., and F. T. de Vries. 2020. "Plant Root Exudation Under Drought: Implications for Ecosystem Functioning." *New Phytologist* 225, no. 5: 1899–1905. https://doi.org/10.1111/nph.16223.

Xi, N., D. Chen, M. Bahn, H. Wu, C. Chu, M. W. Cadotte, and J. M. Bloor. 2022. "Drought Soil Legacy Alters Drivers of Plant Diversity-Productivity Relationships in Oldfield Systems." *Science Advances* 8, no. 18: eabn3368. https://doi.org/10.1126/sciadv.abn3368.

Xu, C., Y. Ke, W. Zhou, W. Luo, W. Ma, L. Song, M. D. Smith, D. L. Hoover, K. R. Wilcox, W. Fu, and W. Zhang. 2021. "Resistance and Resilience of a Semi-Arid Grassland to Multi-Year Extreme Drought." *Ecological Indicators* 131: 108139. https://doi.org/10.1016/j.ecolind.2021.108139.

Yilmaz, P., L. W. Parfrey, P. Yarza, J. Gerken, E. Pruesse, C. Quast, et al. 2014. "The SILVA and 'All-Species Living Tree Project (LTP)' Taxonomic Frameworks." *Nucleic Acids Research* 42, no. D1: D643–D648. https://doi.org/10.1093/nar/gkt1209.

CHAPTER 3: COMPOUND HYDROCLIMATIC EXTREMES DRIVE BIOGEOCHEMICAL HOT MOMENTS, BUT NOT ECOSYSTEM RECOVERY, IN A SEMI-ARID GRASSLAND

3.1 Summary

Atmospheric warming is projected to fundamentally alter precipitation regimes, leading to more frequent extreme drought and heavy precipitation (or "deluge") events. Hydroclimatic whiplash, whereby ecosystems rapidly transition from exceptionally dry to wet conditions, is a key manifestation of predicted future precipitation regimes, increasing the likelihood of co-occurring drought and deluge events. The ecological impacts of compound drought and deluge are likely to be particularly consequential in semi-arid ecosystems, which are governed by persistent water limitation. Here, we investigated the interactive effects of an extreme, multi-year drought and deluge in a semi-arid C_4 grassland. To disentangle interactive versus individual impacts of each hydroclimatic extreme, we imposed four treatments: 1) Control (average precipitation), 2) Drought (66% precipitation reduction across two growing seasons), 3) Deluge (60 mm, 98th percentile event), and 4) Drought-Deluge (drought interrupted by a deluge in the second growing season). We expected the deluge to partially rescue aboveground plant productivity from drought, capitalizing on the accumulation of soil nitrogen and ability for the dominant grasses to respond to precipitation pulses. While the deluge did stimulate a biogeochemical "hot moment" of increased soil CO_2 efflux and nutrient cycling, aboveground productivity remained unresponsive. Rather, the lack of photosynthetically active plant tissue under extreme drought conditions inhibited carbon sequestration, causing the deluge to briefly elevate carbon losses. Consequently, a deluge interrupting an extreme, multi-year drought prompted the system to become a carbon source, suggesting that semi-arid ecosystem carbon sink dynamics will become increasingly vulnerable under shifting precipitation regimes.

3.2 Introduction

Rising atmospheric temperatures are driving increasingly stochastic precipitation regimes characterized by more frequent and severe precipitation anomalies (Huntington 2006, Knapp et al. 2008, Rahmstorf & Coumou 2011, Trenberth 2011, Prein et al. 2017, Swain et al. 2018, Feldman et al. 2024). Extreme drought and deluge events (i.e., "persistent, torrential rain events", Fischer & Knutti 2016) are projected to be key manifestations of such global hydrological intensification (Donat et al. 2016, Chen et al. 2025, Hoover & Smith 2025, Swain et al. 2025). Indeed, anthropogenically driven increases in these climate extremes have already been observed (IPCC 2023). Individually, each extreme has detrimental impacts on ecosystems, including substantial losses of productivity (Xu et al. 2019, Smith et al. 2024), collapse of trophic networks (Ledger et al. 2013, de Vries et al. 2018), and persistent shifts in biogeochemical cycles (Hoover & Rogers 2016, Schlesinger et al. 2016). Furthermore, of all the consequences of anthropogenic climate change, discrete climate extremes are projected to impose the most significant disruptions to ecosystem functionality (Smith 2011).

Concerningly, the co-occurrence of climate extremes (i.e., compound climate extremes, Zscheischler et al. 2018) has already become more common throughout the 21st century (Diffenbaugh et al. 2015, AghaKouchak et al. 2020, IPCC 2023). Compound climate extremes can interact to exacerbate the consequences of either extreme alone (Zscheischler et al. 2020). For example, marine heatwaves and ocean acidification synergistically drive mass die-offs of marine life and nutrient blooms (Burger et al. 2022), while extreme droughts and heatwaves can elicit vast mortality across trophic levels (e.g., Ciais et al. 2005). A series of temporally compounding climate extremes had significant consequences for Southern California when an extreme, multi-year drought was followed by a deluge, stimulating biomass production, which

served as abundant fuel for wildfires during the following dry season (AghaKouchak et al. 2014, 2020). Thus, compound climate extremes have already proven to be a costly outcome of anthropogenic climate change.

It is important to consider, however, that compound hydroclimatic extremes, specifically drought-deluge events, introduce a unique suite of contrasting ecosystem impacts that have the potential to create biogeochemical "hot moments" (i.e., periods of time that exhibit disproportionately high reaction rates relative to intervening time periods, McClain et al. (2003), Kuzyakov & Blagodatskya (2015)) that may contribute to ecosystem recovery, or a 'rescuing effect', during ongoing drought. Extreme drought drives substantial reductions in ecosystem functionality, including reduced aboveground net primary productivity (ANPP), net ecosystem exchange (NEE), plant cover, and soil microbial activity, causing the ecosystem to switch from a carbon sink to carbon source during the growing season (Corlett 2016, Hoover & Rogers 2016, Sellers et al. 2018, Smith et al. 2024). Furthermore, limited carbon inputs, reduced soil pore connectivity, and inhibited biogeochemical cycling facilitate the accumulation of soil nitrogen and extracellular enzymes that may drive rapid biogeochemical transformations upon rewetting (Homyak et al. 2017). If extreme drought persists across years, ecosystem impacts are likely to be amplified as short-term resistance mechanisms are superseded (Hoover & Smith 2025, Ohlert et al. 2025). Contrastingly, deluge events have proven to elevate soil moisture for up to one month and stimulate plant growth above- and belowground (Post & Knapp 2020, Hoover et al. 2022). Coincident pulses in soil respiration and nitrogen availability support the idea that a single extreme deluge event can enhance biogeochemical cycling. Hence, there is abundant potential for hydroclimatic extremes to interact and stimulate biogeochemical hot moments. These hot moments are expected to temporarily release ecosystems from key resource constraints, allowing

plants to take advantage of excess water and nitrogen, and aid in recovery (or 'rescue') of ecosystem functionality during drought (Hoover et al. 2022).

The relief from water limitation that a deluge affords during a compound hydroclimatic extreme is particularly important in dryland ecosystems, which are characterized by chronic water scarcity and highly variable precipitation (Austin et al. 2004, Huxman et al. 2004, Wang et al. 2022). Covering approximately 40% of the global terrestrial surface (Schimel 2010), carbon cycling of these vast landscapes is primarily governed by precipitation variability across both intra- and interannual scales, contributing substantially to interannual variability in the global terrestrial CO_2 sink (Poulter et al. 2014, Ahlström et al. 2015, Sitch et al. 2024). In semi-arid ecosystems, particularly, drought events have repeatedly proven to reduce ecosystem functionality (see Knapp et al. 2024, Smith et al. 2024), while deluges may have a range of outcomes from positive (e.g., enhanced plant growth, Post & Knapp 2020) to negative (e.g., reduced net ecosystem exchange (NEE), Hao et al. 2017). However, to our knowledge, only one study has investigated the interactive effects of drought and deluge events on a semi-arid grassland, where a deluge event aided in the recovery of ecosystem functionality from a flash drought (Hoover et al. 2022).

Given the anticipated proliferation of compound hydroclimatic extremes and multi-year droughts, we explored how a deluge event interrupting a multi-year drought would impact ecosystem carbon and nutrient cycling in a semi-arid shortgrass steppe grassland in eastern Colorado, USA. We initiated a factorial experiment over two growing seasons where we investigated the independent and interactive effects of extreme, multi-year drought and a mid-growing season deluge event in the second growing season. We hypothesized that 1) a deluge event interrupting an extreme drought would stimulate biogeochemical hot moments of soil

nutrient cycling and carbon efflux and 2) facilitate recovery of ecosystem function, potentially rescuing plant productivity and net ecosystem exchange under drought. We further hypothesized that 3) a mid-season deluge event, independently, would stimulate all measures of ecosystem carbon and nutrient cycling, leading to higher productivity relative to all other treatments.

3.3 Methods

3.3.1 Site Description

This study was conducted in 2024 and 2025 at the USDA-ARS Central Plains Experimental Range (CPER; 40°50'N, 104°43'W) located in northeastern Colorado, USA. The 6280-ha site is composed of native, semi-arid grassland representative of the western Great Plains shortgrass steppe biome. CPER receives 342 mm mean annual precipitation, most of which (~75%) falls during the growing season. Average growing season (April 15-September 30) precipitation was calculated using site-level, gap-filled precipitation data compiled by Condon et al. (2026) during 1990-2021. These data were a combination of site rain gauges, nearby weather stations, and nearby National Oceanic and Atmospheric Administration stations (Condon et al. 2026). Growing season precipitation totals during 2024-2025 were calculated using tipping-bucket rain gauges located adjacent to the experimental site. Elevation is 1645 m above sea level, and mean annual temperature is 8.6°C (Lauenroth & Sala 1992, Hoover et al. 2021). Perennial C_4 grasses (*Bouteloua gracilis* [Willd. ex Kunth] Lag ex Griffiths and *Bouteloua dactyloides* [Nutt.] J.T. Columbus) dominate plant communities, with perennial C_3 grasses (e.g., *Pascopyrum smithii* [Rydb] A. Love), cool-season annual grasses, forbs, shrubs, and cacti composing subdominant and rare species (Hoover et al. 2021). ANPP ranges from 57-100 g m^{-2} on average depending on topographic position (Hoover et al. 2021). The study site had relatively homogenous vegetation and little slope. Soils are classified in the Ascalon (Aridic Arguistolls)

and Renohill Series (Ustic Haplargids), and the texture is sandy clay loam (59 ± 4% sand, 20 ± 2% silt, 21 ± 3% clay), with slight textural variation across the site. The study site historically experienced heavy cattle grazing until 2023, when a fence was installed to prevent access to the study site.

3.3.2 Experimental Design

In May 2023, 10 blocks comprised of two paired 12 x 4 m plots were established (n = 20 total plots) in the study site (Fig. A2.1). Plots were separated by 3 m, and the blocks were arrayed at least 5 m apart in relatively homogeneous vegetation. Each plot contained two 2 x 4 m subplots (n = 40 total subplots) separated by a 3 m buffer (Fig. A2.1). Each 2 x 4 m subplot was trenched and lined with aluminum flashing (5 cm aboveground and 15 cm belowground) at least 0.25 m beyond plot boundaries to ensure hydrological isolation. The plots within each block were randomly assigned to either the drought or average rainfall (control) treatments, and each subplot within each plot was randomly assigned to either the deluge or non-deluge (control) treatment. This resulted in four treatment combinations of manipulated precipitation inputs: 1) Control- average precipitation, 2) Drought- a continuous 66% reduction of average precipitation, 3) Deluge- a 60 mm deluge added in early-July of the second growing season, and 4) Drought-Deluge- a continuous 66% reduction of average precipitation interrupted by a 60 mm deluge in July of the second growing season. The deluge amount was based on long-term precipitation records from the site, whereby a 60 mm deluge corresponds with a 98th percentile event size (Post & Knapp 2021, Hoover et al. 2022). The mid-growing season deluge timing was chosen, because this is when deluge events have occurred historically and key measures of ecosystem functionality (e.g., ANPP and soil respiration) have been most strongly influenced relative to other times during the growing season (Post & Knapp 2020).

Prior to the start of the growing season in 2024, passive rainfall reduction shelters (12 x 4 m round cold frames; GrowSpan, CT, USA) were erected over the drought treatment plot in each block. Previous studies indicate minimal indirect effects of rainout shelters on abiotic and biotic variables (Loik et al. 2019, Post & Knapp 2020, Hoover et al. 2022), including light, which we confirmed with a AccuPAR LP-80 ceptometer (Edaphic Scientific).

On May 5, 2024, the drought shelters were covered with roofs consisting of corrugated polycarbonate strips that covered 66% of the shelter. This design has been used previously to passively manipulate rainfall at the CPER (e.g., Carroll et al. 2021, Ohlert et al. 2025). Shelter roofs remained in place throughout the duration of the experiment, and thus rainfall was manipulated year-round. Due to below average growing season precipitation at the start of the 2024 growing season, water was added to all plots to keep precipitation inputs within the long-term average for the CPER (Table A2.1, Fig. A2.2). For the Control treatments, 15 mm was added on June 12, 14, 20, 24, and 27, with another 9 mm addition on July 25, 2024. For Drought plots, 5 mm was added on June 12, 14, 20, 24, and 27, with another 3 mm addition on July 25, 2024. In the second year of the study, ambient precipitation was near average (Table A2.1, Fig. A2.2), and therefore water additions were not needed. The 60 mm deluge event was added on July 9-10, 2025. All water additions and the deluge treatment were applied by hand with a watering wand attached to a pump. A digital flow meter (01N31GM 1” nylon water meter, Great Plains Industries, Inc.) was used to track calibrated water inputs. Water was applied at a rate that allowed soil infiltration and limited pooling on the soil surface.

3.3.3 Response Variables

Each of the subplots within each plot contained a 2 x 2 m sampling area in which measurements of all response variables were taken. This plot size has been shown to be sufficient

to represent measures of plant productivity and carbon cycling processes (e.g., Carroll et al. 2021, Hoover et al. 2022, Smith et al. 2024). The 2 x 2 m sampling area was divided into four 1 x 1 m subplots: one of which was designated to non-destructive sampling (greenness measures), a second for carbon flux measures, while the other two were designated for destructive sampling measurements (Fig. A2.1).

3.3.3.1 Soil Moisture

Volumetric water content (VWC), or soil moisture (SM), was measured at 15-minute intervals across a subset of plots (n = 5/treatment) throughout the study. Sensors (CS616 Water Content Reflectometers, Campbell Scientific, Logan, UT) were installed within one of the destructive measurement subplots within the 2 x 2 m sampling plot in a subset of drought and control plots (n = 10). Sensors measuring 0-15 cm were installed at a 45° angle. Data was stored on a CR1000 datalogger (Campbell Scientific, Logan, UT) and retrieved bi-weekly. SM values were averaged daily within plots for analysis.

3.3.3.2 Plant Phenology (Canopy Greenness)

Plot canopy greenness was quantified weekly (with more frequent measurements following Deluge application in 2025) with repeat digital photography (adapted from Hoover et al. 2022, Post & Knapp 2020, 2021). Measurements were taken between 11:00-14:00 MST to minimize shadows in the image. For each measurement, a camera was positioned directly at a 90° angle over a 0.5 x 0.5 m^2 frame in the designated 1 x 1 m subplot within each sampling plot. Images were cropped to just within the 0.25 m^2 frame before image analysis in R. The EBImage package (Pau et al. 2010) was used to calculate the average green chromatic coordinates (GCC) of pixels in each image. Each GCC value accounts for differences in image lighting by

calculating greenness relative to total brightness of each pixel (i.e., green/(red + blue + green); Filippa et al. 2016, Hoover et al. 2022).

3.3.3.3 Carbon Flux Measurements

Net ecosystem exchange (NEE) and ecosystem respiration (ER) measurements were collected on a subset of plots (n = 5/treatment combination) using a custom portable flux chamber (0.5 x 0.5 x 0.5 m) attached to a LI-6400 (LiCOR, Inc.) following methods adapted from Hoover et al. (2022) and Hopping et al. (2018). An aluminum base (0.5 x 0.5 m) was installed in the subset of 1 x 1 m subplots designated for these measurements, allowing the chamber to seal and limit external gas interference. Measurements were collected weekly during the 2025 growing season (with more frequent measurements following the Deluge event) between 8:00 and 13:00 MST to maximize assessment of peak plant activity. Measurements ceased on August 4, 2025. For each measurement, the chamber was vented for 7 s, then placed on the aluminum base as two internal fans circulated air. The first light measurement (representing NEE) was then collected for 2 minutes. The process was repeated to collect the second NEE measurement. The chamber was then vented again, covered with a blackout curtain to inhibit photosynthesis, and measured as before (representing ER). Data were pulled from the LI-6400, and the final 30 s of each measurement were averaged to generate a single value for each measurement. Gross primary productivity (GPP) was then calculated as GPP = NEE – ER.

3.3.3.4 Soil Respiration

Soil respiration was measured weekly throughout the study from 10:00 – 14:00 MST, with more frequent measurements following the Deluge event. Permanent PVC collars (10-cm diameter) were installed in each of the 1 x 1 subplots designated for these measurements to a depth of 2.4 cm, with 2 cm extending above the soil. Collars were cleared of vegetation

following initial installation and prior to each set of measurements. Soil CO_2 efflux was measured using a LI-6400 (LiCOR, Inc.) with a 6400-09 soil flux chamber attachment. Measurements ceased on September 1, 2025. Given soil moisture and temperature are primary controls over soil respiration (Orchard & Cook 1983), we concurrently measured soil moisture to a depth of 20 cm using a Campbell Hydrosense II time-domain reflectometry (TDR) probe (Campbell Scientific, Logan, UT) and soil temperature to 5 cm. These soil moisture values correlated strongly with the continuous measures of SM (see above) and were only used in statistical models of soil respiration. Soil respiration measurements also correlated strongly with ecosystem respiration measurements (above) but provide complementary, higher resolution measurements at the soil surface.

3.3.3.5 Soil Nutrient Availability

Plant root simulator (PRS) probes (Western Ag Innovations, Saskatoon, Saskatchewan, CA) were used to quantify plant available macronutrients (N, P, and K) and micronutrients (Al, B, Ca, Cd, Cu, Fe, Mg, Mn, Pb, S, and Zn). PRS probes simulate plant uptake of ions using paired 10 cm^2 cation and anion exchange resin membranes. Pairs of probes were buried in triplicate within a subset of the 1 x 1 m subplots designated for these measurements (n = 5/treatment) at four points throughout the study: early (June 4-July 4) 2024, late (July 26-August 27) 2024, pre-deluge (May 20-June 19) 2025, and post-deluge (July 7-July 28) 2025. Each pair of probes was retrieved and sent to WesternAg Innovations, where pairs from the same plot were eluted together.

3.3.3.6 Aboveground Net Primary Productivity

At the end of each growing season (August 18, 2024, and August 24, 2025), aboveground net primary productivity (ANPP) was measured in each of the 1 x 1 m subplots designated for

these measurements (n = 10/treatment combination). All biomass was harvested within two 20 x 50 cm^2 quadrats and sorted by functional group (C_3 grass, C_4 grass, forb, woody) in the field. Samples were dried at 60°C for two days, and weighed to the nearest 0.01 g. Prior to weighing, any previous year's biomass in the sample (appearing grey in color) was removed.

3.3.4 Statistical Analyses

To evaluate the effects of drought and subsequent deluge events on ecosystem responses, we employed linear mixed-effects models using a structure that reflected the nested, split-plot experimental design. Drought (Drought vs. Control) was treated as the main-plot factor, with the deluge event (Deluge vs. No Deluge) as the nested subplot factor. Further, plots were nested within blocks arranged across our experimental pasture. To account for the spatial hierarchy of our experimental design, plots nested within blocks were included as random intercepts. This ensured that the 2024 treatment history was tested against the appropriate plot-level error term, while the 2025 deluge effects and their interactions with time were tested against the within-plot error. Analyses presented in the primary manuscript focus on the ecosystem measurements taken during 2025, given this is when the deluge event occurred, while all analyses of ecosystem measurements taken during 2024 are presented in the supplemental information. Hence, analyses conducted for the 2025 growing season investigate all four treatments (Control, Drought, Deluge, and Drought-Deluge), even prior to the deluge event, to assess the ecosystem impacts of the deluge event and account for any potential pre-deluge differences. Analyses from 2024 are included in the supplemental information to provide context regarding drought impacts prior to 2025.

Measurements of soil moisture, plant phenology, and carbon fluxes were taken repeatedly from the same plots over both growing seasons. Hence, date was treated as a categorical fixed

factor to account for non-linear fluctuations. To address temporal autocorrelation due to more intensive sampling following the deluge event, a first-order autoregressive (AR1) correlation structure was included. Models were built using the 'nlme' package in R (Pinheiro et al. 2019). Model parameters were estimated using Restricted Maximum Likelihood (REML), and significance of fixed effects and their interactions were tested using Analysis of Variance (ANOVA) with Type III Sums of Squares. Denominator degrees of freedom were determined via the containment method due to the necessary inclusion of the autoregressive correlation structure. All post-hoc comparisons and estimated marginal means were calculated using the 'emmeans' package (Lenth & Piaskowski 2025), and p-values were adjusted with Tukey HSD.

Additional analyses were conducted to assess the impacts of the deluge treatment on ecosystem measures. Measurements taken pre-deluge (April 15-July 08, 2025) and post-deluge (July 11-October 15, 2025) were averaged at the subplot-level, then within treatments to account for within-subplot repeated measures. Linear models were then created with ecosystem responses as dependent variables, and Treatment and Period (pre- or post-deluge) as explanatory variables, with Block as a random effect. ANOVA with Type 3 Sums of Squares and Tukey HSD post-hoc pairwise comparisons were then conducted to assess the significance of fixed effects and their interactions. Denominator degrees of freedom were estimated using Satterthwaite approximation given these tests did not include an autoregressive correlation structure.

3.4 Results

3.4.1 Soil Moisture Response to Drought-Deluge

At study initiation in 2024, all treatments had similar soil moisture levels (35% volumetric water content [VWC], Fig. A2.3). Soil moisture gradually decreased across all treatments throughout the first growing season, with divergence of soil moisture between the

Control (34% VWC) and Drought (27% VWC) treatments by mid-May (Fig. A2.3). On average, the Control treatment had higher soil moisture (+5% VWC) than the Drought treatment across the first growing season (Fig. A2.3, Table A2.2, $p < 0.001$). During the dormant season, soil moisture gradually declined across both treatments, with the Control treatment maintaining higher soil moisture than the Drought treatment (Fig. A2.4, $p < 0.001$).

Prior to the deluge event in the second growing season, soil moisture remained elevated in the Control and Deluge treatments relative to the Drought and Drought-Deluge treatments (Fig. 3.1), and there were no soil moisture differences between the Control and Deluge or Drought and Drought-Deluge treatments, respectively. Following the deluge event, soil moisture rapidly diverged, with the Deluge and Drought-Deluge treatments both peaking on July 11, 2025 (Fig. 3.1). The Deluge treatment peaked at 48% VWC (Fig. 3.1) and remained elevated (+8%) relative to the Control treatment for the remainder of the growing season (Fig. 3.1). The Drought-Deluge treatment peaked at 39% VWC, then dried down to match the Control treatment at both depths by late August (Fig. 3.1). However, the Drought-Deluge treatment remained elevated (+11%) relative to the Drought treatment for the remainder of the growing season (Fig. 3.1). The Control and Drought treatments gradually decreased and did not differ throughout the remainder of the growing season (Fig. 3.1). On average, the Deluge treatment had the highest soil moisture during the second growing season (Fig. 3.1, 28% VWC), followed by Control (23% VWC), then Drought-Deluge (21% VWC) and Drought (16% VWC).

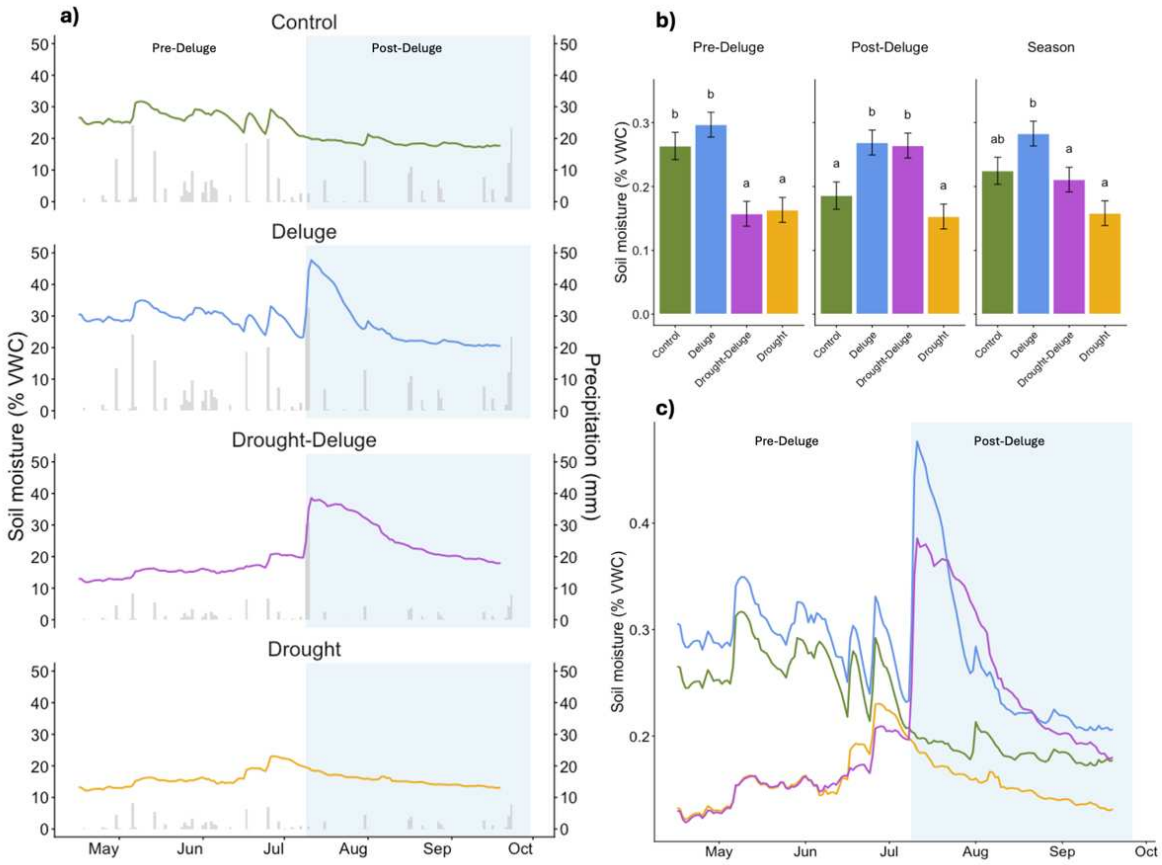

Figure 3.1: Soil moisture and precipitation inputs during the second growing season (April 15–September 30) of the experiment. a) Soil moisture through time with daily precipitation values. b) Average soil moisture for the pre-deluge period (April 15-July 9), post-deluge period (July 10-September 30), and full growing season for each treatment. Error bars indicate ± 1 SE, and letters indicate significant ($p < 0.05$) treatment differences. c) Soil moisture trends for treatment comparison. Pre-deluge differences in soil moisture across the Control and Deluge treatment, along with Drought and Drought-Deluge treatments, were unintended given they received the same precipitation inputs. However, soil and vegetation heterogeneity were likely responsible for these marginal differences. VWC = volumetric water content.

3.4.2 Plant Phenological Response to Drought-Deluge

Like soil moisture, all treatments had similar canopy greenness at initiation of the experiment (Fig. A2.5). In the first growing season, greenness did not diverge between the Control and Drought treatments until mid-June, and the Control treatment remained significantly

higher than the Drought treatment throughout the growing season (Table A2.2, $p < 0.001$), peaking twice in early July and mid-August due to naturally occurring rainfall events (Fig. A2.5).

In the second growing season, greenness of the Control and Deluge treatments gradually increased from mid-April to early July, while greenness of the Drought and Drought-Deluge treatments remained relatively static due to limited new plant growth (Fig. 3.2). There were no greenness differences between the Control and Deluge or Drought and Drought-Deluge treatments, respectively, prior to the deluge event. The deluge event stimulated a rapid green-up in the Deluge and Drought-Deluge treatments, while the Control treatment gradually decreased in greenness over time, and the Drought treatment remained consistently low in greenness (Fig. 3.2). The Deluge and Drought-Deluge treatments peaked on July 18 (8 days after the deluge event), with the Deluge treatment displaying the greatest greenness response (Fig. 3.2). The Drought-Deluge treatment matched the Control treatment in greenness for most of July, though this was underscored by plant growth in a subset of plots, leading to higher variability (3.2% CV) in greenness values when compared to the Control (1.68% CV) or Drought treatments (1.20% CV, Fig. 3.2). By early August, the Deluge treatment matched the Control treatment, and the Drought-Deluge treatment matched the Drought treatment, for the remainder of the growing season, while differences between the Control and Drought treatments were maintained (Fig. 3.2). When averaged across the growing season, the Deluge treatment had the greatest greenness response (0.356 ± 0.001 GCC), followed by the Control treatment (0.350 ± 0.001 GCC), then the Drought-Deluge (0.343 ± 0.001 GCC) and Drought (0.340 ± 0.001 GCC) treatments.

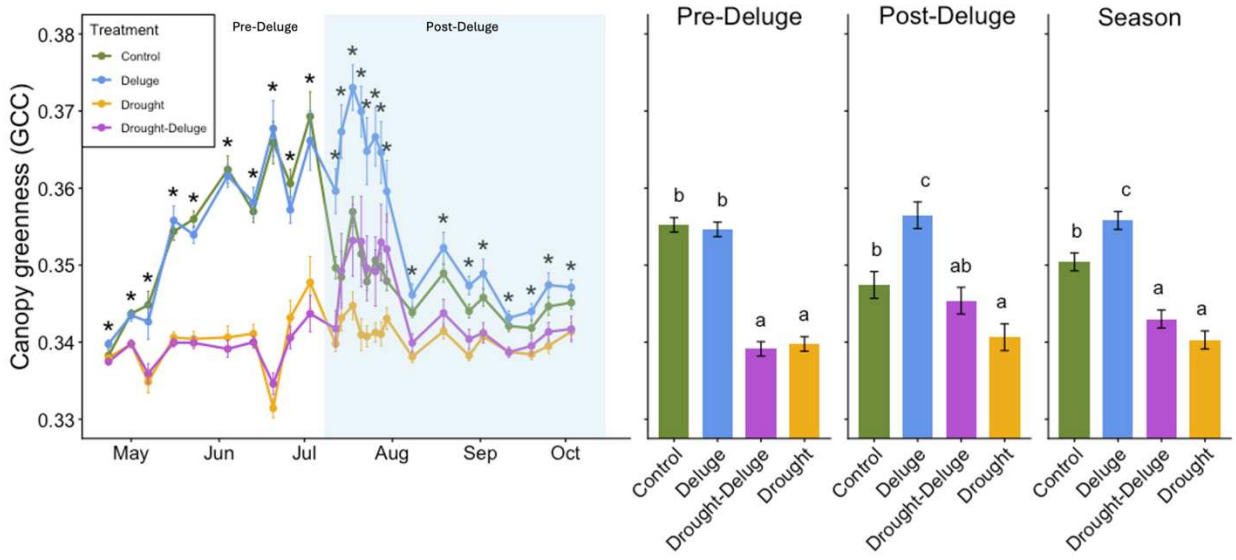

Figure 3.2: Canopy greenness, as measured with green chromatic coordinate index (GCC), during the second growing season. Left) Patterns of greenness through time. Right) Greenness averages pre-deluge (April 23-July 8), post-deluge (July 12-October 3), and for the entire growing season (April 23-October 3). Error bars indicate ± 1 SE, and asterisks/letters indicate significant ($p < 0.05$) treatment differences.

3.4.3 Carbon Flux Responses to Drought-Deluge

3.4.3.1 Ecosystem Respiration (ER), Gross Primary Production (GPP), and Net Ecosystem Exchange (NEE)

Measurements of GPP, ER and NEE were not made during the first growing season in 2024. However, prior to the deluge event in 2025, GPP, ER, and NEE were significantly reduced in the Drought and Drought-Deluge treatments relative to the Control and Deluge treatments (Fig. 3.3). On average, each flux in the Drought and Drought-Deluge treatments remained within a standard deviation of zero prior to the deluge event (Fig. 3.3). The Control and Deluge treatments were carbon sinks prior to the deluge event, with relatively high ER offset by even higher GPP. Notably, there were no differences between the Control and Deluge or Drought and Drought-Deluge treatments, respectively, prior to the deluge event (Fig. 3.3).

Following the deluge event, there was a rapid increase in ER, GPP, and NEE in the Deluge treatment, which persisted through the remainder of the growing season. Relative to the Control treatment, ER increased by 313%, GPP increased by 453%, and NEE increased by 806% during the post-deluge portion of the growing season (Fig. 3.3). Similarly, ER, GPP, and NEE increased in the Drought-Deluge treatment, though this was muted and only marginally differed from the Drought treatment for one month following the deluge (Fig. 3.3). Each flux in the Control treatment gradually declined through the growing season, and the Drought treatment remained consistently low. Thus, the Control, Drought, and Drought-Deluge treatments did not differ following the deluge event (Fig. 3.3). Over the entire growing season, the Deluge treatment exhibited the greatest ER, GPP, and NEE, followed by the Control treatment, then Drought-Deluge and Drought treatments (Table A2.3, Fig. 3.3).

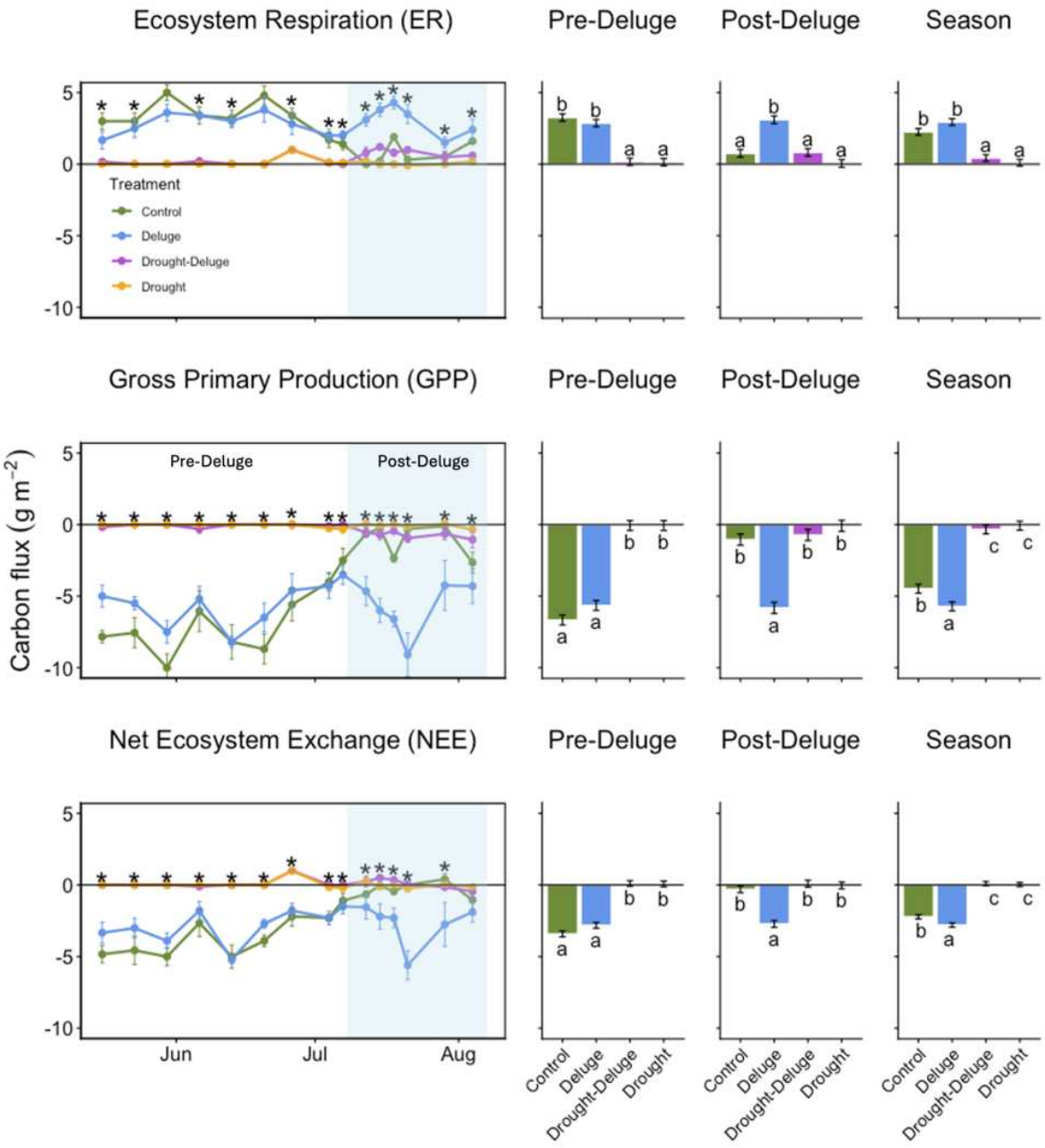

Figure 3.3: Effects of drought and deluge treatments on carbon fluxes, measured as ecosystem respiration (ER), gross primary production (GPP), net ecosystem exchange (NEE) during the second growing season of the experiment. Left) Patterns of carbon fluxes over time. Right) Average carbon fluxes for each treatment pre-deluge (May 16-July 7), and post-deluge (July 12-August 4) along with the entire growing season (May 16-August 4). Error bars indicate ± 1 SE, and asterisks/letters indicate significant ($p < 0.05$) treatment differences.

3.4.3.2 Soil Respiration

During the first growing season, soil respiration (CO_2 efflux) did not diverge between the Control and Drought treatments until mid-June (Fig. A2.6). The Control treatment remained elevated until mid-July, when the Control and Drought treatments converged and followed similar trajectories through the remainder of the growing season (Fig. A2.6). In mid-August, a large precipitation event (Fig. A2.3) stimulated increases in both treatments, but the effects of this event decreased more rapidly in the Drought treatment (Fig. A2.6). Overall, the Control treatment had higher soil respiration than the Drought treatment over the first growing season (Table A2.2, Fig. A2.6).

At the start of the second growing season, there were no differences in soil respiration across treatments (Fig. 3.4). Treatments immediately diverged, with the Control and Deluge treatments increasing until mid-June (Fig. 3.4). Notably, the Deluge and Control treatments differed at two timepoints prior to the deluge event (June 6 and July 4), though they did not significantly differ on average across this period. Soil respiration in the Drought and Drought-Deluge treatments did not begin increasing until mid-June, coinciding with multiple precipitation events (Figs. 3.1, 3.4). The Drought and Drought-Deluge treatments did not significantly differ at any time prior to the deluge (Table A2.3, Fig. 3.4).

Immediately following the deluge event, soil respiration was elevated in the Deluge and Drought-Deluge treatments (Fig. 3.4). The Deluge treatment continued to increase until peaking on July 18, while the Drought-Deluge treatment gradually decreased over time (Fig. 3.4). All treatments converged in mid-August, with only one more precipitation-driven pulse in respiration in the Deluge and Control treatments on August 18 (Fig. 3.4). Overall, the Deluge treatment exhibited a 175% increase in soil respiration relative to the Control treatment

following the deluge event (Fig. 3.4). Similarly, the Drought-Deluge treatment exhibited a 105% increase in soil respiration relative to the Drought treatment following the deluge event (Fig. 3.4). The Control and Drought treatments did not significantly differ following the deluge event (Fig. 3.4). Across the entire growing season, the Deluge treatment displayed the highest soil respiration, followed by the Control treatment, then the Drought-Deluge and Drought treatments (Fig. 3.4).

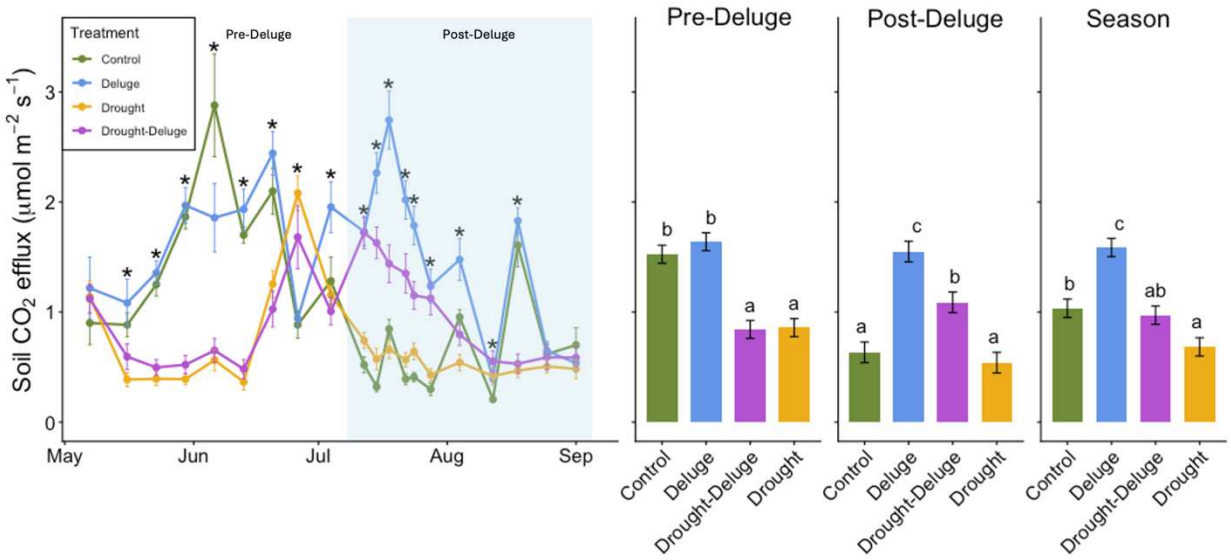

Figure 3.4: Left) Effects of drought and deluge treatments on soil respiration (soil CO_2 efflux) patterns during the growing season in the second year of the experiment. Right) Average soil respiration pre-deluge (May 7-July 4), post-deluge (July 12-September) and for the entire growing season (May 7-September 1) for each treatment. Error bars indicate ± 1 SE, and asterisks/letters indicate significant ($p < 0.05$) treatment differences.

3.4.4 Soil Nutrient Responses to Drought-Deluge

Soil nutrient availability was measured during both growing seasons to assess early and late season availability, along with the impacts of the deluge event across treatments. The probes capture a variety of micro- and macronutrients (see Methods), though we primarily focus on nitrogen (N) and phosphorus (P). Across all timepoints, ammonium-nitrogen (NH_4-N) availability was negligible and showed no treatment differences (Tables A2.2, A2.3, Figs. 3.5, A2.7). Nitrate-nitrogen (NO_3-N) availability was higher in the Control treatment relative to the Drought treatment during the first growing season (Table A2.2, Fig. A2.7). However, this flipped during the second growing season pre-deluge, when NO_3-N availability was highest in the Drought and Drought-Deluge treatments, followed by the Control and Deluge treatments (Fig. 3.5). Following the deluge event, NO_3-N availability increased significantly in the Drought-Deluge treatment, with no significant differences across the other three treatments (Fig. 3.5). Phosphate-P (P) was also higher in the Control treatment relative the Drought treatment during the entire first growing season (Table A2.2, Fig. A2.7). During the second growing season pre-deluge, no differences in P were evident across treatments, however the deluge event prompted a large and significant increase in both the Deluge and Drought-Deluge treatments (Fig. 3.5, Table A2.3).

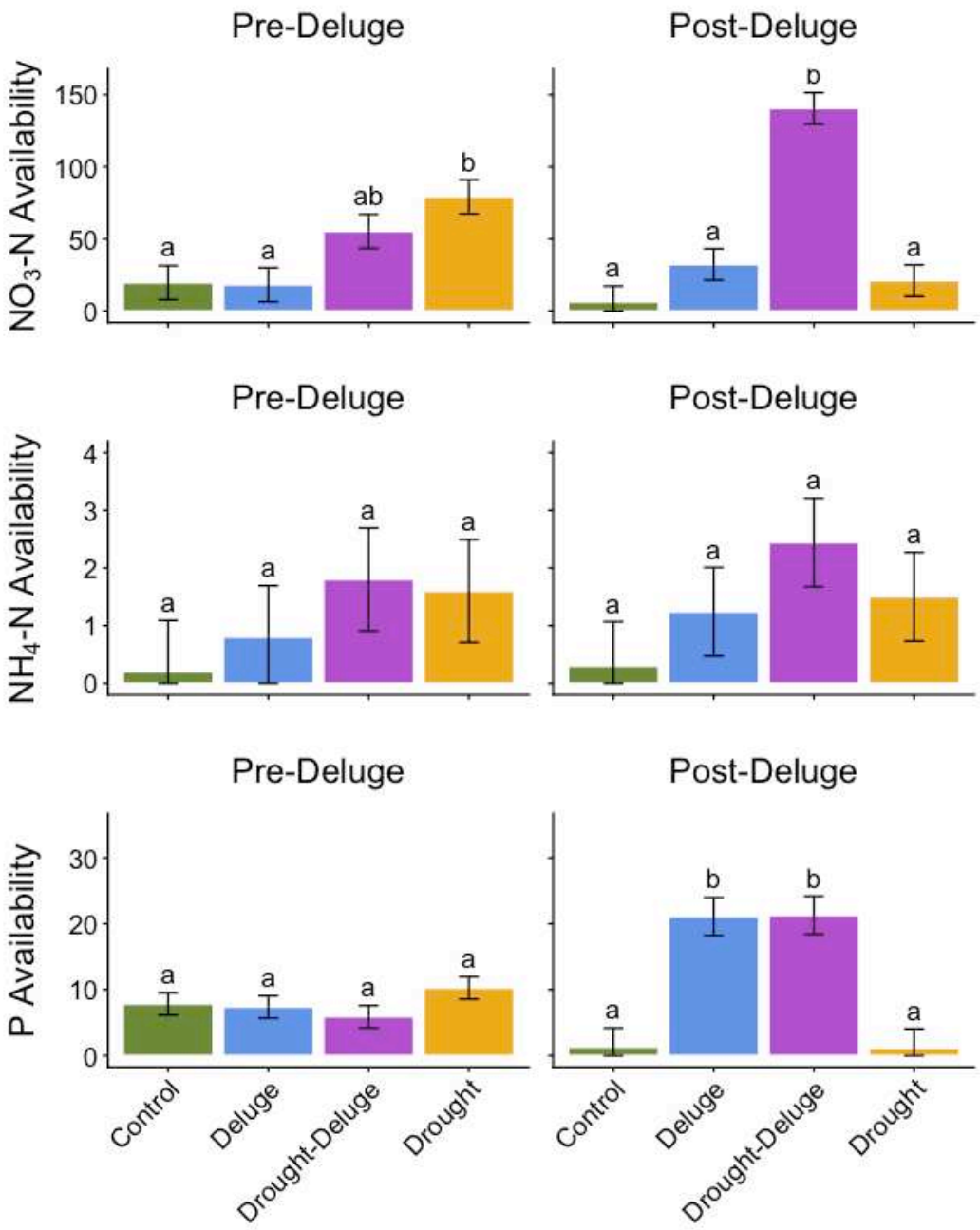

Figure 3.5: Soil nutrient availability for each treatment measured by plant root simulator probes (see Methods) during the second growing season. Probes were buried during the pre-deluge (May 20-June 19) and post-deluge (July 7-July 28) periods to capture deluge event-related changes in availability. Nutrients are measured in units of (μg/10cm^2/burial length). Error bars indicate ± 1 SE, and letters indicate significant ($p < 0.05$) treatment differences.

3.4.5 Aboveground Productivity (ANPP) Responses to Drought-Deluge

During the 2024 growing season, ANPP was significantly reduced under the Drought treatment (by 27%, Table A2.2, Fig. A2.8). During the 2025 growing season, ANPP was reduced even further under the Drought treatment (by 96%, Fig. 3.6). The deluge event (Deluge or Drought-Deluge treatments) did not result in a difference in ANPP when compared to either the Control or Drought treatments, respectively (Table A2.3, Fig. 3.6).

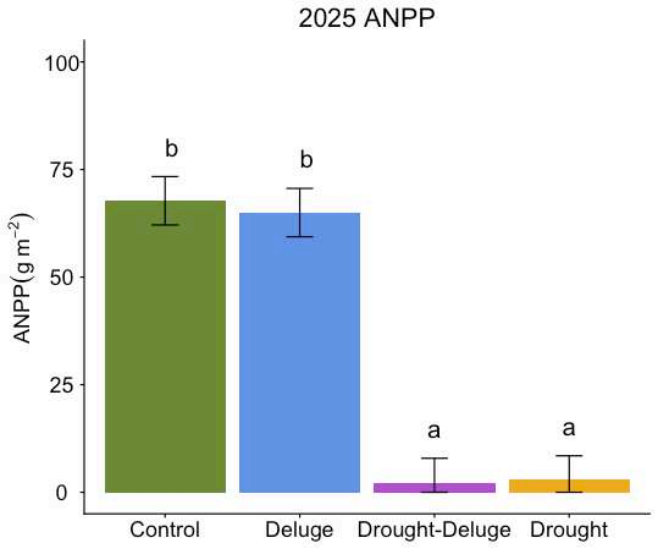

Figure 3.6: Effects of drought and deluge treatments on aboveground net primary productivity (ANPP) during the second growing season of the experiment. Error bars indicate ± 1 SE, and letters indicate significant ($p < 0.05$) treatment differences.

3.5 Discussion

We sought to determine how extreme, multi-year drought and deluge, independently and interactively, impacted ecosystem processes in a semi-arid grassland given the prominent role of these water-limited systems in dictating the global carbon cycle (Poulter et al. 2014, Ahlström et al. 2015, Sitch et al. 2024) and projected increase in the frequency of hydroclimatic extremes (Donat et al. 2016, Chen et al. 2025, Hoover & Smith 2025, Swain et al. 2025). The contrasting impacts of extreme drought and deluge on semi-arid ecosystems hinder prediction of their joint ecological consequences. Results from our study showed that extreme drought inhibited most

ecosystem measures, while the deluge event stimulated all ecosystem measures. When the deluge event interrupted extreme drought, soil moisture and carbon fluxes were temporarily elevated, and soil nutrient availability increased, creating biogeochemical hot moments. Surprisingly, these hot moments did not contribute to the rescue of plant productivity, causing the system to remain a carbon source for the remainder of the growing season.

3.5.1 Ecological Impacts of Extreme, Multi-year Drought

Extreme drought reduced all ecosystem measures relative to the Control treatment within the first growing season. As expected, soil moisture, greenness, and soil respiration all responded coincidently with decreased precipitation inputs (Figs. A2.3, A2.5, and A2.6). Due to historically low precipitation inputs during the first growing season, soil moisture gradually declined under drought until a relatively large precipitation pulse (7.3 mm) in mid-August drove a spike in soil respiration, reflecting a Birch effect exacerbated by antecedent drought conditions (Fig. A2.6, Birch 1958). By the end of the first growing season, drought significantly reduced aboveground productivity relative to the Control treatment (Fig. A2.8).

The impacts of the drought accumulated throughout the second growing season (Ohlert et al. 2025), as soil moisture remained limited, and plant cover (i.e., greenness as a proxy) was severely depleted (Figs. 3.1, 3.2). Indeed, plant growth was negligible under extreme drought conditions, with only subtle increases in greenness in late June following precipitation pulses (Fig. 3.2). Surprisingly, ANPP averaged only 2.9 g m^{-2} under the Drought treatment (relative to 67.7 g m^{-2} in the Control treatment) at the end of the second growing season, a stark departure from the long-term average range of ANPP values at this site (Hoover et al. 2021, 2022). Such detrimental effects of extreme drought were likely exacerbated by high ambient temperatures and atmospheric vapor pressure deficit over the two growing seasons. Further, a lack of

photosynthetically active plant tissue and limited soil water availability stunted all carbon flux measures and facilitated soil NO_3-N accumulation (Figs. 3.5, A2.7).

3.5.2 Ecological Impacts of Deluge

The deluge event occurred in the middle of the second growing season (July 9-10), when deluge events have the greatest effect on ecosystem processes relative to other periods in the growing season (Post & Knapp 2020). Although plant growth in the shortgrass steppe is primarily dependent upon early season rainfall (Derner & Hart 2007, Parton et al. 2012), studies also suggest that mid-season deluge events may be equally effective at promoting plant growth responses (Hermance et al. 2015, Post & Knapp 2020). Indeed, the middle of the growing season (July) experiences high ambient temperatures and limited precipitation inputs in this system (Lauenroth & Milchunas 1991, Pielke & Doesken 2008), causing plants to slow down metabolically between precipitation pulses (Sala & Lauenroth 1982, Schwinning & Sala 2004). The deluge event induced immediate pulses in soil moisture, with soil moisture peaking near 50% VWC in the Deluge treatment and persisting for the remainder of the growing season (Fig. 3.1). Surprisingly, and in contrast with Hoover et al. (2022), soil moisture did not dry down to match the Control treatment levels following the deluge event (Fig. 3.1). The retention of relatively shallow soil moisture could have been synergistically caused by joint mechanisms of root uptake at deeper soil layers, hydraulic redistribution to shallow soil layers, and capillary movement induced by high vapor pressure deficit. Following the deluge event, the site did not experience a precipitation event > 7 mm for three weeks, creating very hot and dry conditions that could have established a steep water potential gradient. Further, the co-dominant plant species at the study site, *B. gracilis* and *B. dactyloides*, maintain deep roots that allow them to

sustain hot, dry periods (Sala et al. 1982, Lauenroth & Milchunas 1992, Schwinning & Sala 2004).

Mirroring soil moisture fluctuations, the deluge event elevated carbon fluxes in the Deluge treatment for one month post-deluge (relative to the Control treatment, Fig. 3.3). During this period, carbon efflux and sequestration both increased, with net ecosystem exchange (NEE) indicating the system was a carbon sink (Fig. 3.3). Before the deluge, the Control and Deluge treatments were already a carbon sink, and both treatments gradually approached an equivocal balance (NEE) between efflux (ER) and sequestration (GPP) as the deluge event approached (Fig. 3.3). Hence, the deluge event stimulated plant activity as plants were becoming physiologically dormant, causing the Deluge treatment to remain a carbon sink for the entirety of the growing season. Semi-arid ecosystems are vulnerable to shifting carbon source-sink dynamics depending on precipitation seasonality and amount (Scott et al. 2015, Morgan et al. 2016), thus a well-timed deluge prompts extended carbon drawdown in this system. Compared to prior studies of deluge impacts in this system, the duration of the soil respiration pulse was similar to those previously observed (Post & Knapp 2020, 2021).

Notably, elevated greenness, increased stomatal conductance, and abundant nutrient availability did not translate to higher ANPP (Fig. 3.6), suggesting existing plant tissue was likely rehydrated, with a subsequent increase in chlorophyll production (Schwinning & Sala 2004). Further, the extended green-up could have facilitated carbon redistribution belowground to root production (Ogle & Reynolds 2004). The combination of nominal spring precipitation and plant productivity were plausibly responsible for the lack of ANPP response following the deluge event. In other words, existing plant tissue from earlier growth primed the system for a greenness response, but not a productivity response (Vermeire et al. 2009). Our results support

those of Byrne et al. (2013) and Condon et al. (2026), who found that summer precipitation addition did not increase ANPP at our experimental site. However, these findings contrast with multiple previous studies, where supplemental summer precipitation (i.e., multiple events or a deluge) significantly increased ANPP in *B. gracilis*-dominated systems (Heitschmidt & Vermeire 2006, Heisler-White et al. 2009, Post & Knapp 2020). Thus, antecedent conditions and deluge timing likely play a primary role in determining ecological outcomes following a deluge event (Post & Knapp 2020, Hajek & Knapp 2022).

3.5.3 Ecological Impacts of Compound Drought and Deluge

The second year of extreme drought substantially inhibited ecosystem functionality, with only negligible pulses in soil moisture and respiration prior to the deluge event. Further, extreme drought facilitated the accumulation of soil nitrogen and plant substrates (Figs. 3.5, A2.7; Reichmann et al. 2013, Homyak et al. 2017), priming the system for a biogeochemical pulse upon rewetting. We expected that the deluge event would stimulate all ecosystem measures and induce biogeochemical hot moments that would contribute to ecosystem recovery. Indeed, when the mid-season deluge event interrupted drought (i.e., the Drought-Deluge treatment), soil moisture, respiration, and nutrient availability all pulsed, generating a hot moment due to microbial processing of accumulated plant material, microbial cell lysis, and rehydration of plant roots (Birch 1958, Kuzyakov & Blagodatskya 2015, Homyak et al. 2017). Greenness and stomatal conductance also increased immediately, though this response was brief and limited relative to the Deluge treatment (Figs. 3.2, A2.9). A lack of photosynthetically active plant tissue stunted aboveground responses, and the overall trends were likely mediated by growth of invasive forbs (e.g., *Salsola tragus*) and green-up of cacti (*Opuntia polyacantha*) in few plots.

Like the Deluge treatment, these immediate responses did not translate to increased ANPP and promoted an overall loss of carbon from the system (Fig. 3.6).

These findings contrast with the expectations put forth by Schwinning & Sala (2004), whereby large pulse events disproportionately increase plant productivity relative to microbially-induced carbon losses. Further, these findings are surprising given the ability of the dominant plant species, *B. gracilis,* to take advantage of precipitation pulses (Sala & Lauenroth 1982, Schwinning & Sala 2004). The failure of the deluge event to stimulate a compensatory growth response suggests that the preceding extreme drought imposed a severe vegetation constraint on the system (Knapp and Smith 2001, Yahdjian and Sala 2006, Felton et al. 2019). By reducing productivity to near-zero levels, the drought likely depleted the meristematic bud bank and drove overall loss of plant functionality. Consequently, the regenerative capacity of the plant communities was insufficient to exploit the sudden resource pulse, as physiological recovery was likely promoted prior to biomass accumulation.

Hence, a single deluge event was insufficient to promote ecosystem recovery from extreme, multi-year drought. Unlike the findings of Hoover et al. (2022), where a deluge partially "rescued" the system from drought within the same growing season, the cumulative effects of multi-year drought overwhelmed the potential for recovery. Thus, drought duration and intensity are crucial determinants of ecosystem responses to deluge events, and when plant functionality is severely depleted, the deluge event may cause the system to become a carbon source for extended periods.

3.5.4 The Future Role of Compound Hydroclimatic Extremes in Semi-arid Ecosystems

Precipitation regimes dictate carbon source-sink dynamics in semi-arid systems. Hence, shifting precipitation patterns and amounts will alter the contribution of semi-arid systems to the

global carbon cycle interannually. Under drought, these systems become a net carbon source due to the continuation of microbial processes as plant functionality is reduced (Nagy et al. 2007, Scott et al. 2015, Ma et al. 2016, Hoover & Smith 2021, Smith et al. 2024). Generally, precipitation events (> 5 mm, Sala & Lauenroth 1982) promote both plant carbon uptake and soil respiration, with larger events expected to enhance plant carbon uptake more than soil respiration and induce a net carbon sink (Schwinning & Sala 2004, Bachman et al. 2010, Guo et al. 2016, Post & Knapp 2020). However, prior studies have not accounted for the detrimental impacts of extreme, multi-year drought on semi-arid systems creating antecedent conditions that promote overall carbon losses following a deluge event. This suggests that the impacts of compound hydroclimatic extremes on the carbon balance of semi-arid systems are highly dependent upon the dimensions (e.g., duration, intensity, severity, timing) of each extreme (AghaKouchak et al. 2020, Zscheischler et al. 2020).

It is important to note that the spatial scales of droughts and deluges differ substantially, as droughts tend to occur on much larger scales than deluge events (Sheffield et al. 2009, Hoover et al. 2022). Hence, a deluge event in the background of a regional drought will likely drive a highly localized spike in carbon cycling, with the balance between sequestration and efflux dependent upon antecedent conditions (Hoover et al. 2022). Further, we know little about how compound hydroclimatic extremes influence ecosystem recovery trajectories following the cessation of drought. For instance, soil physical structure may be irreversibly altered under extreme drought, with consequences for ecosystem hydrology and microbial functionality (Thotakuri et al. 2025).

Our results indicate that a deluge event during a drought stimulates biogeochemical hot moments, but the rapid pulse in water and nutrient availability does not necessarily precede

recovery of plant productivity. Rather, the deluge-induced hot moment results in a carbon efflux and extends the duration of net carbon loss from the system. Relative to compound hydroclimatic extremes within a single growing season (Hoover et al. 2022), a multi-year, extreme drought inhibits the potential for ecosystem recovery following a deluge event.

LITERATURE CITED

AghaKouchak, A., L. Cheng, O. Mazdiyasni, and A. Farahmand. 2014. "Global Warming and Changes in Risk of Concurrent Climate Extremes: Insights from the 2014 California Drought." *Geophysical Research Letters 41*: 8847–8852. https://doi.org/10.1002/2014GL062308.

AghaKouchak, A., F. Chiang, L. S. Huning, C. A. Love, I. Mallakpour, O. Mazdiyasni, H. Moftakhari, S. M. Paplexiou, E. Ragno, and M. Sadegh. 2020. "Climate Extremes and Compound Hazards in a Warming World." *Annual Review of Earth and Planetary Sciences 48*: 519–548. https://doi.org/10.1146/annurev-earth-071719-055226.

Ahlström, A., M. R. Raupach, G. Schurgers, B. Smith, A. Arneth, M. Jung, and N. Zeng. 2015. "The Dominant Role of Semi-Arid Ecosystems in the Trend and Variability of the Land CO2 Sink." *Science 348*, no. 6237: 895–899. https://doi.org/10.1126/science.aaa1668.

Austin, A. T., L. Yahdjian, J. M. Stark, J. Belnap, A. Porporato, U. Norton, D. Ravetta, and S. M. Schaeffer. 2004. "Water Pulses and Biogeochemical Cycles in Arid and Semiarid Ecosystems." *Oecologia 141*: 221–235. https://doi.org/10.1007/s00442-004-1519-1.

Bachman, S., J. L. Heisler-White, E. Pendall, D. G. Williams, J. A. Morgan, and J. Newcomb. 2010. "Elevated Carbon Dioxide Alters Impacts of Precipitation Pulses on Ecosystem Photosynthesis and Respiration in a Semi-Arid Grassland." *Oecologia 162*: 791–802. https://doi.org/10.1007/s00442-009-1491-3.

Birch, H. F. 1958. "The Effect of Soil Drying on Humus Decomposition and Nitrogen Availability." *Plant and Soil 10*: 9–31. https://doi.org/10.1007/BF01343734.

Burger, F. A., J. Terhaar, and T. L. Frölicher. 2022. "Compound Marine Heatwaves and Ocean Acidity Extremes." *Nature Communications 13*: 4722. https://doi.org/10.1038/s41467-022-32141-w.

Byrne, K. M., W. K. Lauenroth, and P. B. Adler. 2013. "Contrasting Effects of Precipitation Manipulations on Production in Two Sites Within the Central Grassland Region, USA." *Ecosystems 16*: 1039–1051. https://doi.org/10.1007/s10021-013-9666-z.

Carroll, C. J., I. J. Slette, R. J. Griffin-Nolan, L. E. Baur, A. M. Hoffman, E. M. Denton, J. E. Gray, A. K. Post, M. K. Johnston, Q. Yu, and S. L. Collins. 2021. "Is a Drought a Drought in Grasslands? Productivity Responses to Different Types of Drought." *Oecologia 197*: 1017–1026. https://doi.org/10.1007/s00442-021-05044-6.

Chen, L., P. Brun, P. Buri, S. Fatishi, A. Gessler, M. J. McCarthy, F. Pellicciotti, B. Stocker, and D. N. Karger. 2025. "Global Increase in the Occurrence and Impact of Multiyear Droughts." *Science 387*: 278–284. https://doi.org/10.1126/science.adp6601.

Ciais, P., M. Reichstein, N. Viovy, A. Granier, J. Ogée, V. Allard, M. Aubinet, C. Bernhofer, N. Buchmann, A. Carrara, F. Chevallier, N. De Noblet, A. D. Friend, P. Friedlingstein, T. Grünwald, B. Heinesch, P. Keronen, A. Knohl, G. Krinner, D. Loustau, G. Manca, G. Matteucci, F. Miglietta, J. M. Ourcival, D. Papale, K. Pilegaard, S. Rambal, G. Seufert, J. F. Soussana, M. J. Sanz, E. D. Schulze, T. Vesala, and R. Valentini. 2005. "Europe-Wide Reduction in Primary Productivity Caused by the Heat and Drought in 2003." *Nature 437*: 529–533. https://doi.org/10.1038/nature03972.

Corlett, R. T. 2016. "The Impacts of Droughts in Tropical Forests." *Trends in Plant Science 21*: 584–593. https://doi.org/10.1016/j.tplants.2016.02.003.

Derner, J. D., and R. H. Hart. 2007. "Grazing-Induced Modifications to Peak Standing Crop in Northern Mixed-Grass Prairie." *Rangeland Ecology and Management 60*: 270–276. https://doi.org/10.2111/1551-5028(2007)60.

De Vries, F. T., R. I. Griffiths, M. Bailey, H. Craig, M. Girlanda, H. S. Gweon, S. Hallin, A. Kaisermann, P. Mariotte, A. Mason-Williams, A. Meisner, N. Ostle, I. Prior, A. J. Stringer, B. C. Thomson, and R. D. Bardgett. 2018. "Soil Bacterial Networks Are Less Stable Under Drought Than Fungal Networks." *Nature Communications 9*: 3033. https://doi.org/10.1038/s41467-018-05516-0.

Diffenbaugh, N. S., D. L. Swain, and D. Touma. 2015. "Anthropogenic Warming Has Increased Drought Risk in California." *Proceedings of the National Academy of Sciences 112*: 3931–3936. https://doi.org/10.1073/pnas.1422385112.

Dodd, R. J., D. R. Chadwick, I. M. Harris, A. Hines, D. Hollis, T. Economou, D. Gwynn-Jones, J. Scullion, D. A. Robinson, and D. L. Jones. 2021. "Spatial Co-Localisation of Extreme Weather Events: A Clear and Present Danger." *Ecology Letters 24*: 60–72. https://doi.org/10.1111/ele.13620.

Donat, M. G., A. L. Lowry, L. V. Alexander, P. A. O'Gorman, and N. Maher. 2016. "More Extreme Precipitation in the World's Dry and Wet Regions." *Nature Climate Change 6*: 508–513. https://doi.org/10.1038/nclimate2941.

Feldman, A. F., X. Feng, A. J. Felton, A. G. Konings, A. K. Knapp, J. A. Biederman, and B. Poulter. 2024. "Plant Responses to Changing Rainfall Frequency and Intensity." *Nature Reviews Earth & Environment 5*: 276–294. https://doi.org/10.1038/s43017-024-00523-3.

Felton, A. J., S. Zavislan-Pullaro, and M. D. Smith. 2019. "Semiarid Ecosystem Sensitivity to Precipitation Extremes: Weak Evidence for Vegetation Constraints." *Ecology 100*: e02572. https://doi.org/10.1002/ecy.2572.

Filippa, G., E. Cremonese, M. Migliavacca, M. Galvagno, M. Forkel, L. Wingate, E. Tomelleri, and A. D. Richardson. 2016. "Phenopix: A R Package for Image-Based Vegetation Phenology." *Agricultural and Forest Meteorology 220*: 141–150. https://doi.org/10.1016/j.agrformet.2016.01.006.

Fischer, E. M., and R. Knutti. 2016. "Observed Heavy Precipitation Increase Confirms Theory and Early Models." *Nature Climate Change 6*: 986–991. https://doi.org/10.1038/nclimate3110.

Hajek, O. L., and A. K. Knapp. 2022. "Shifting Seasonal Patterns of Water Availability: Ecosystem Responses to an Unappreciated Dimension of Climate Change." *New Phytologist 233*: 119–125. https://doi.org/10.1111/nph.17772.

Hammerlynck, E. P., R. L. Scott, and J. J. Stone. 2012. "Soil Moisture and Ecosystem Function Response of Desert Grassland Varying in Vegetative Cover to a Saturating Precipitation Pulse." *Ecohydrology 5*: 297–305. https://doi.org/10.1002/eco.218.

Hao, Y. B., C. T. Zhou, W. J. Liu, L. F. Li, X. M. Kang, L. L. Jiang, X. Z. Huang, X. Y. Cui, and C. Y. Xu. 2017. "Aboveground Net Primary Productivity and Carbon Balance Remain Stable Under Extreme Precipitation Events in a Semiarid Steppe Ecosystem." *Agricultural and Forest Meteorology 240–241*: 1–9. https://doi.org/10.1016/j.agrformet.2017.03.006.

Harrison, S. P., L. L. LaForgia, and A. M. Latimer. 2018. "Climate-Driven Diversity Change in Annual Grasslands: Drought Plus Deluge Does Not Equal Normal." *Global Change Biology 24*: 1782–1792. https://doi.org/10.1111/gcb.14018.

Heisler-White, J. L., J. M. Blair, E. F. Kelly, K. Harmoney, and A. K. Knapp. 2009. "Contingent Productivity Responses to More Extreme Rainfall Regimes Across a Grassland Biome." *Global Change Biology 15*: 2894–2904. https://doi.org/10.1111/j.1365-2486.2009.01961.x.

Heitschmidt, R. K., and L. T. Vermeire. 2006. "Can Abundant Summer Precipitation Counter Losses in Herbage Production Caused by Spring Drought?" *Rangeland Ecology and Management 59*: 392–399. https://doi.org/10.2111/05-131R1.1.

Hermance, J. F., D. J. Augustine, and J. D. Derner. 2015. "Quantifying Characteristic Growth Dynamics in a Semi-Arid Grassland Ecosystem by Predicting Short-Term NDVI Phenology from Daily Rainfall: A Simple Four Parameter Coupled-Reservoir Model." *International Journal of Remote Sensing 36*: 5637–5663. https://doi.org/10.1080/01431161.2015.1103917.

Homyak, P. M., S. D. Allison, T. E. Huxman, M. L. Goulden, and K. K. Treseder. 2017. "Effects of Drought Manipulation on Soil Nitrogen Cycling: A Meta-Analysis." *Journal of Geophysical Research: Biogeosciences 122*: 3260–3272. https://doi.org/10.1002/2017JG004146.

Hoover, D. L., and B. M. Rogers. 2016. "Not All Droughts Are Created Equal: The Impacts of Interannual Drought Pattern and Magnitude on Grassland Carbon Cycling." *Global Change Biology 22*: 1809–1820. https://doi.org/10.1111/gcb.13161.

Hoover, D. L., W. K. Lauenroth, D. G. Milchunas, L. M. Porensky, D. J. Augustine, and J. D. Derner. 2021. "Sensitivity of Productivity to Precipitation Amount and Pattern Varies by Topographic Position in a Semiarid Grassland." *Ecosphere 12*: e03376. https://doi.org/10.1002/ecs2.3376.

Hoover, D. L., Hajek, O. L., Smith, M. D., Wilkins, K., Slette, I. J., and A. K. Knapp. 2022. "Compound Hydroclimatic Extremes in a Semi-arid Grassland: Drought, Deluge, and the Carbon Cycle." *Global Change Biology 28*: 2611-2621.

Hoover, D. L., and W. K. Smith. 2025. "The Growing Threat of Multiyear Droughts." *Science 387*: 246–247. https://doi.org/10.1126/science.adr9556.

Hopping, K. A., A. K. Knapp, T. Dorji, and J. A. Klein. 2018. "Warming and Land Use Change Concurrently Erode Ecosystem Services in Tibet." *Global Change Biology 24*: 5534–5548. https://doi.org/10.1111/gcb.14417.

Huntington, T. G. 2006. "Evidence for Intensification of the Global Water Cycle: Review and Synthesis." *Journal of Hydrology 319*: 83–95. https://doi.org/10.1016/j.jhydrol.2005.07.003.

Huxman, T. E., K. A. Snyder, D. Tissue, A. J. Leffler, K. Ogle, W. T. Pockman, D. R. Sandquist, D. L. Potts, and S. Schwinning. 2004. "Precipitation Pulses and Carbon Fluxes in Semiarid and Arid Ecosystems." *Oecologia 141*: 254–268. https://doi.org/10.1007/s00442-004-1590-7.

IPCC. 2023. "Summary for Policymakers." In: Climate Change 2023: Synthesis Report. Contribution of Working Groups I, II and III to the Sixth Assessment Report of the Intergovernmental Panel on Climate Change [Core Writing Team, H. Lee and J. Romero (eds.)]. IPCC, Geneva, Switzerland: 1–34. https://doi.org/10.59327/IPCC/AR6-9789291691647.001.

Knapp, A. K., and M. D. Smith. 2001. "Variation Among Biomes in Temporal Dynamics of Aboveground Primary Production." *Science 291*: 481–484. https://doi.org/10.1126/science.291.5503.481.

Knapp, A. K., C. Beier, D. D. Briske, A. T. Classen, Y. Luo, M. Reichstein, M. D. Smith, S. D. Smith, J. E. Bell, P. A. Fay, J. L. Heisler, S. W. Leavitt, R. Sherry, B. Smith, and E. Weng. 2008. "Consequences of More Extreme Precipitation Regimes for Terrestrial Ecosystems." *BioScience 58*: 811–821. https://doi.org/10.1641/B580908.

Knapp, A. K., K. V. Condon, C. C. Folks, M. A. Sturchio, R. J. Griffin-Nolan, S. A. Kannenberg, I. J. Slette, and M. D. Smith. 2024. "Field Experiments Have Enhanced Our Understanding of Drought Impacts on Terrestrial Ecosystems—But Where Do We Go from Here?" *Functional Ecology 38*: 76–97. https://doi.org/10.1111/1365-2435.14473.

Kuzyakov, Y., and E. Blagodatskaya. 2015. “Microbial Hotspots and Hot Moments in Soil: Concept & Review.” *Soil Biology and Biochemistry 83*: 184–199. https://doi.org/10.1016/j.soilbio.2015.01.025.

Lauenroth, W. K., and D. G. Milchunas. 1991. “Short-Grass Steppe.” In: Natural Grasslands: Introduction and Western Hemisphere [R. T. Coupland (ed.)]. Elsevier, Amsterdam: 183–226.

Lauenroth, W. K., and O. E. Sala. 1992. “Long-Term Forage Production of North American Shortgrass Steppe.” *Ecological Applications 2*: 397–403. https://doi.org/10.2307/1941874.

Ledger, M. E., L. E. Brown, F. K. Edwards, A. M. Milner, and G. Woodward. 2013. “Drought Alters the Structure and Functioning of Complex Food Webs.” *Nature Climate Change 3*: 223–227. https://doi.org/10.1038/nclimate1684.

Lenth, R., and J. Piaskowski. 2025. “emmeans: Estimated Marginal Means, aka Least-Squares Means.” R package version 2.0.1. https://rvlenth.github.io/emmeans/.

Li, L., Z. Zheng, J. A. Biederman, C. Xu, Z. Xu, R. Che, Y. Wang, X. Cui, and Y. Hao. 2019. “Ecological Responses to Heavy Rainfall Depend on Seasonal Timing and Multi-Year Recurrence.” *New Phytologist 223*: 647–660. https://doi.org/10.1111/nph.15832.

Loik, M. E., J. C. Lesage, T. M. Brown, and D. O. Hastings. 2019. “DroughtNet Rainfall Shelters Did Not Cause Nondrought Effects on Photosynthesis for California Central Coast Plants.” *Ecohydrology 12*: e2138. https://doi.org/10.1002/eco.2138.

Ma, X., A. Huete, J. Cleverly, D. Eamus, F. Chevallier, J. Joiner, B. Poulter, J. Zscheischler, L. Guanter, W. Meyer, Z. Xie, and G. Ponce-Campos. 2016. “Drought Rapidly Diminishes the Large Net CO2 Uptake in 2011 over Semi-Arid Australia.” *Scientific Reports 6*: 37747. https://doi.org/10.1038/srep37747.

McClain, M. E., E. W. Boyer, C. L. Dent, S. E. Gergel, N. B. Grimm, P. M. Groffman, S. C. Hart, J. W. Johnson, G. M. Louett, W. H. McDowell, N. Z. Shanzl, and G. Pinay. 2003. “Biogeochemical Hot Spots and Hot Moments at the Interface of Terrestrial and Aquatic Ecosystems.” *Ecosystems 6*: 301–312. https://doi.org/10.1007/s10021-003-0161-9.

Morgan, J. A., W. Parton, J. D. Derner, T. G. Gilmanov, and D. P. Smith. 2016. “Importance of Early Season Conditions and Grazing on Carbon Dioxide Fluxes in Colorado Shortgrass Steppe.” *Rangeland Ecology and Management 69*: 342–350. https://doi.org/10.1016/j.rama.2016.05.002.

Nagy, Z., K. Pintér, S. Z. Czóbel, J. Balogh, L. Horváth, S. Z. Fóti, Z. Barcza, Z. Csintalan, and Z. Tuba. 2007. “The Carbon Budget of Semi-Arid Grassland in a Wet and a Dry Year in Hungary.” *Agriculture, Ecosystems and Environment 121*: 21–29. https://doi.org/10.1016/j.agee.2006.12.003.

Ocheltree, T. W., J. B. Nippert, and P. V. V. Prasad. 2012. "Changes in Stomatal Conductance Along Grass Blades Reflect Changes in Leaf Structure." *Plant, Cell & Environment 35*: 1040–1049. https://doi.org/10.1111/j.1365-3040.2011.02470.x.

Ogle, K., and J. F. Reynolds. 2004. "Plant Responses to Precipitation in Desert Ecosystems: Integrating Functional Types, Pulses, Thresholds, and Delays." *Oecologia 141*: 282–294. https://doi.org/10.1007/s00442-004-1507-5.

Ohlert, T., M. D. Smith, S. L. Collins, A. K. Knapp, J. S. Dukes, O. Sala, J. B. Sankey,... and T. J. Terry. 2025. "Drought Intensity and Duration Interact to Magnify Losses in Primary Productivity." *Science 390*: 284–289. https://doi.org/10.1126/science.adq1234.

Orchard, V. A., and F. J. Cook. 1983. "Relationship Between Soil Respiration and Soil Moisture." *Soil Biology and Biochemistry 15*: 447–453. https://doi.org/10.1016/0038-0717(83)90010-X.

Parton, W., J. Morgan, D. Smith, S. Del Grosso, L. Prihodko, D. LeCain, R. Kelly, and S. Lutz. 2012. "Impact of Precipitation Dynamics on Net Ecosystem Productivity." *Global Change Biology 18*: 915–927. https://doi.org/10.1111/j.1365-2486.2011.02611.x.

Pau, G., F. Fuchs, O. Skylar, M. Boutros, and W. Huber. 2010. "EBImage—An R Package for Image Processing with Applications to Cellular Phenotypes." *Bioinformatics 26*: 979–981. https://doi.org/10.1093/bioinformatics/btq046.

Pendergrass, A. G., and R. Knutti. 2018. "The Uneven Nature of Daily Precipitation and its Change." *Geophysical Research Letters 45*: 11980–11988. https://doi.org/10.1029/2018GL080298.

Piao, S., X. Wang, K. Wang, X. Li, A. Bastos, J. G. Canadell, P. Ciais, P. Friedlingstein, C. Mountain, S. Sitch, Z. Yan, and Z. Zuo. 2019. "Interannual Variation of Terrestrial Carbon Cycle: Issues and Perspectives." *Global Change Biology 26*: 300–318. https://doi.org/10.1111/gcb.14884.

Pielke, R. A., and N. J. Doesken. 2008. "Climate of the Shortgrass Steppe." In: Ecology of the Shortgrass Steppe: A Long-Term Perspective [W. K. Lauenroth and I. C. Burke (eds.)]. Oxford University Press, New York: 14–29.

Pinheiro, J., D. Bates, S. DebRoy, D. Sarkar, and R Core Team. 2019. "nlme: Linear and Nonlinear Mixed Effects Models." R package version 3.1-141. https://CRAN.R-project.org/package=nlme.

Post, A. K., and A. K. Knapp. 2020. "The Importance of Extreme Rainfall Events and Their Timing in a Semi-Arid Grassland." *Journal of Ecology 108*: 2431–2443. https://doi.org/10.1111/1365-2745.13478.

Post, A. K., and A. K. Knapp. 2021. "How Big is Big Enough? Surprising Responses of a Semiarid Grassland to Increasing Deluge Size." *Global Change Biology 27*: 1157–1169. https://doi.org/10.1111/gcb.15487.

Poulter, B., D. Frank, P. Ciais, R. Myneni, N. Andela, J. Bi, G. Broquet, J. G. Canadell, F. Chevallier, Y. Y. Liu, S. W. Running, S. Sitch, and G. R. van der Werf. 2014. "Contribution of Semi-Arid Ecosystems to Interannual Variability of the Global Carbon Cycle." *Nature 509*: 600–603. https://doi.org/10.1038/nature13376.

Prein, A. F., R. M. Rasmussen, K. Ikeda, C. Liu, M. P. Clark, and G. J. Holland. 2017. "The Future Intensification of Hourly Precipitation Extremes." *Nature Climate Change 7*: 48–52. https://doi.org/10.1038/nclimate3168.

Rahmstorf, S., and D. Coumou. 2011. "Increase of Extreme Events in a Warming World." *Proceedings of the National Academy of Sciences 108*: 17905–17909. https://doi.org/10.1073/pnas.1101766108.

Reich, E., J. Guo, D. Peltier, E. Palmquist, K. Samuels-Crow, R. Boone, and K. Ogle. 2025. "Precipitation Pulse Dynamics Are Not Ubiquitous: A Global Meta-Analysis of Plant and Ecosystem Carbon- and Water-Related Pulse Responses." *Global Change Biology 31*: e70327. https://doi.org/10.1111/gcb.70327.

Reichmann, L. G., O. E. Sala, and D. P. Peters. 2013. "Water Controls on Nitrogen Transformations and Stocks in an Arid Ecosystem." *Ecosphere 4*: 1–17. https://doi.org/10.1890/ES12-00263.1.

Sala, O. E., and W. K. Lauenroth. 1982. "Small Rainfall Events: An Ecological Role in Semiarid Regions." *Oecologia 53*: 301–304. https://doi.org/10.1007/BF00389014.

Sala, O. E., W. K. Lauenroth, and W. J. Parton. 1982. "Plant Recovery Following Prolonged Drought in a Shortgrass Steppe." *Agricultural Meteorology 27*: 49–58. https://doi.org/10.1016/0002-1571(82)90019-3.

Schimel, D. S. 2010. "Drylands in the Earth System." *Science 327*: 418–419. https://doi.org/10.1126/science.1184946.

Schlesinger, W. H., M. C. Dietze, R. B. Jackson, R. P. Phillips, C. C. Rhoades, L. E. Rustad, and J. M. Vose. 2016. "Forest Biogeochemistry in Response to Drought." *Global Change Biology 22*: 2318–2328. https://doi.org/10.1111/gcb.13105.

Schwinning, S., and O. E. Sala. 2004. "Hierarchy of Responses to Resource Pulses in Arid and Semi-Arid Ecosystems." *Oecologia 141*: 211–220. https://doi.org/10.1007/s00442-004-1520-8.

Scott, R. L., J. A. Biederman, E. P. Hamerlynck, and G. A. Barron-Gafford. 2015. "The Carbon Balance Pivot Point of Southwestern U.S. Semiarid Ecosystems: Insights from the 21st

Century Drought." *Journal of Geophysical Research: Biogeosciences 120*: 2612–2624. https://doi.org/10.1002/2015JG003168.

Sellers, P. J., D. S. Schimel, B. Moore, III, J. Liu, and A. Eldering. 2018. "Observing Carbon Cycle–Climate Feedbacks from Space." *Proceedings of the National Academy of Sciences 115*: 7860–7868. https://doi.org/10.1073/pnas.1711271115.

Sheffield, J., K. M. Andreadis, E. F. Wood, and D. P. Lettenmaier. 2009. "Global and Continental Drought in the Second Half of the Twentieth Century: Severity-Area-Duration Analysis and Temporal Variability of Large-Scale Events." *Journal of Climate 22*: 1962–1981. https://doi.org/10.1175/2008JCLI2722.1.

Sitch, S., M. O'Sullivan, E. Robertson, P. Friedlingstein, C. Albergel, P. Anthoni, A. Arneth, V. K. Arora, A. Bastos, V. Bastrikov, N. Bellouin, and TRENDY Project Team. 2024. "Trends and Drivers of Terrestrial Sources and Sinks of Carbon Dioxide: An Overview of the TRENDY Project." *Global Biogeochemical Cycles 38*: e2024GB008102. https://doi.org/10.1029/2024GB008102.

Smith, M. D. 2011. "The Ecological Role of Climate Extremes: Current Understanding and Future Prospects." *Journal of Ecology 99*: 651–655. https://doi.org/10.1111/j.1365-2745.2011.01833.x.

Smith, M. D., K. D. Wilkins, M. C. Holdrege, P. Wilfahrt, S. L. Collins, A. K. Knapp, and W. Sun. 2024. "Extreme Drought Impacts Have Been Underestimated in Grasslands and Shrublands Globally." *Proceedings of the National Academy of Sciences 121*: e2309881120. https://doi.org/10.1073/pnas.2309881120.

Swain, D. L., B. Langenbrunner, J. D. Neelin, and A. Hall. 2018. "Increasing Precipitation Volatility in Twenty-First-Century California." *Nature Climate Change 8*: 427–433. https://doi.org/10.1038/s41558-018-0140-y.

Swain, D. L., A. F. Prein, J. T. Abatzoglou, C. M. Albano, M. Brunner, N. S. Diffenbaugh, D. Singh, C. B. Skinner, and D. Touma. 2025. "Hydroclimate Volatility on a Warming Earth." *Nature Reviews Earth & Environment 6*: 35–50. https://doi.org/10.1038/s43017-024-00624-z.

Thotakuri, G., M. Dor, M. Smith, A. Guber, and A. Kravchenko. 2025. "Soil Pore-Size Distributions and Selected Biochemical Properties in Short-Grass Steppe Under Long-Term Drought." *Journal of Environmental Management 391*: 126557. https://doi.org/10.1016/j.jenvman.2024.126557.

Trenberth, K. E. 2011. "Changes in Precipitation with Climate Change." *Climate Research 47*: 123–138. https://doi.org/10.3354/cr00953.

Vermeire, L. T., R. K. Heitschmidt, and M. J. Rinella. 2009. "Primary Productivity and Precipitation-Use Efficiency in Mixed-Grass Prairie: A Comparison of Northern and

Southern US Sites." *Rangeland Ecology and Management 62*: 230–239. https://doi.org/10.2111/08-142R1.1.

Wang, L., W. Jiao, N. MacBean, M. C. Rulli, S. Manzoni, G. Vico, and P. D'Odorico. 2022. "Dryland Productivity Under a Changing Climate." *Nature Climate Change 12*: 981–994. https://doi.org/10.1038/s41558-022-01485-y.

Wang, S. Y. S., J. H. Yoon, E. Becker, and R. Gillies. 2017. "California from Drought to Deluge." *Nature Climate Change 7*: 465–468. https://doi.org/10.1038/nclimate3330.

Xu, C., N. G. McDowell, F. R. Fisher, L. Wei, S. Sevanto, B. O. Christofferson, E. Weng, and R. S. Middleton. 2019. "Increasing Impacts of Extreme Droughts on Vegetation Productivity Under Climate Change." *Nature Climate Change 9*: 948–953. https://doi.org/10.1038/s41558-019-0630-6.

Yahdjian, L., and O. E. Sala. 2006. "Vegetation Structure Constrains Primary Production Response to Water Availability in the Patagonian Steppe." *Ecology 87*: 952–962. https://doi.org/10.1890/0012-9658(2006)87.

Zscheischler, J., S. Westra, B. J. Van Den Hurk, S. I. Seneviratne, P. J. Ward, A. Pitman, and X. Zhang. 2018. "Future Climate Risk from Compound Events." *Nature Climate Change 8*: 469–477. https://doi.org/10.1038/s41558-018-0156-3.

Zscheischler, J., O. Martius, S. Westra, E. Bevacqua, C. Raymond, R. M. Horton, B. van den Hurk, A. AghaKouchak, A. Jezequel, M. D. Mahecha, D. Maraun, A. M. Ramos, N. N. Ridder, W. Thiery, and E. Vignotto. 2020. "A Typology of Compound Weather and Climate Events." *Nature Reviews Earth & Environment 1*: 333–347. https://doi.org/10.1038/s43017-020-0060-z.

CHAPTER 4: ENVIRONMENTAL HETEROGENEITY IMPOSED BY PHOTOVOLTAIC ARRAY ALTERS GRASSLAND SOIL MICROBIAL COMMUNITIES[1]

4.1 Summary

The rapid expansion of photovoltaic (PV) energy production has generated concern over its potential ecosystem impacts. PV arrays induce unique microenvironmental conditions by altering resource availability and substantially impacting aboveground processes. However, the belowground consequences of PV development are understudied, limiting our understanding of overall ecosystem impacts. Here, we paired soil physiochemical, molecular, and functional analyses with aboveground measures to assess plant–soil–microbial responses to distinct microsites beneath a single-axis tracking PV system in a semi-arid C3 grassland. We hypothesized that each PV microsite would harbor a unique suite of soil physiochemical properties and microbiomes. We found only subtle differences in soil organic matter and pH, corresponding with aboveground productivity patterns, but other physiochemical properties remained unchanged. However, soil microbial community structure and function differed markedly across PV microsites and from a reference grassland plot. Within the array, microbial decomposition rates were highest where plant productivity and organic matter were greatest, but surprisingly lowest where soil moisture remained elevated throughout the growing season. Overall, these findings suggest that PV arrays create disparate patterns of soil microbial community structure and function, which may feedback to influence overall ecosystem functionality. Coarse measures of soil physiochemical properties, such as total carbon, may overlook key impacts of PV development.

[1] Siggers, J. A., Sturchio, M. A., Gordon, L., Mead, S., Smith, M. D., & Knapp, A. K. (2025). Environmental Heterogeneity Imposed by Photovoltaic Array Alters Grassland Soil Microbial Communities. *Global Change Biology*, 31(7), e70376.

4.2 Introduction

Transitioning to renewable and sustainable forms of energy generation is a critical step in avoiding the most extreme consequences of anthropogenic climate change (Olabi and Abdelkareem 2022). Solar photovoltaic (PV) arrays are considered to be the best immediate solution for reducing CO2 emissions by 2030 (Lee et al. 2023), yet there is often little incentive for solar developers to consider how PV facilities affect ecosystem services provided by underlying soils, plants, and animals (Armstrong et al. 2014; Moore-O'Leary et al. 2017; Grodsky 2021; Sturchio and Knapp 2023). Given the large spatial footprint of solar energy production, particularly in agriculturally important landscapes (i.e., croplands and grasslands; Adeh et al. 2019), where sustainable land use can be a challenge, legitimate concerns about long-term land stewardship under solar arrays must be addressed (Hernandez et al. 2014, 2019; Adeh et al. 2019; U.S. Department of Energy [DoE] 2021).

Agrivoltaics is an approach to solar energy generation that accommodates agricultural activities (e.g., row and specialty crops, grazing) between and beneath PV panels (Goetzberger and Zastrow 1982; Dupraz et al. 2011; Barron-Gafford et al. 2019). This is particularly appealing in grazed perennial grasslands, as vegetation is short-statured, irradiance is high, and there is less need to operate large machinery in close proximity to PV panels (Pascaris et al. 2022). Although the abiotic controls of grassland ecosystems have been studied in many contexts (e.g., drought, grazing, nitrogen deposition; Knapp et al. 2020; Irisarri et al. 2015; Wei et al. 2013), the environmental heterogeneity imparted by PV panels at small spatial scales represents novel conditions in landscapes typically defined by their relative homogeneity (Knapp and Sturchio 2024). For example, precipitation inputs in PV arrays are either deflected when rain is blocked from reaching the ground directly beneath panels or concentrated when rain is shed to

panel edges. In single-axis tracking arrays where panels track the sun across the sky (east–west), PV-induced environmental heterogeneity in both light availability to plants and alterations in soil moisture have been shown to substantially alter patterns of productivity, physiology, and phenology across climatologically disparate grasslands (Adeh et al. 2018; Andrew et al. 2021; Vervloesem et al. 2022; Kannenberg et al. 2023; Sturchio, Kannenberg, and Knapp 2024; Sturchio, Kannenberg, Pinkowitz, and Knapp 2024; Knapp and Sturchio 2024).

Generally, heterogeneity in light, temperature, and water availability strongly influences primary productivity (Knapp and Seastedt 1986; Möhl et al. 2020; Sala et al. 1988), which is often tightly linked to belowground communities and the processes they control (Wardle et al. 2004; Bardgett and Wardle 2010). For instance, elevated soil temperature can modify plant growth and rhizodeposition (Kuzyakov et al. 2007), while subtle shifts in soil moisture can favor particular functional groups of soil bacteria and fungi that may in turn influence plant nutrient availability (Kaisermann et al. 2015; Borowik and Wyszkowska 2016; Fierer 2017). Even without plants, abiotic alterations can be a primary determinant of belowground processes (Jackson et al. 2017). Although it is well known that PV arrays create uniquely dynamic environments, we currently lack a fundamental understanding of how altered abiotic drivers influence aboveground–belowground linkages and overall belowground processes within solar facilities.

Previous belowground investigations have focused on how PV arrays induce variation in soil moisture, soil temperature, and several other edaphic factors (Adeh et al. 2018; BarronGafford et al. 2019; Choi et al. 2020, 2023; Andrew et al. 2021; Carvalho et al. 2025). Soil nutrient availability and total carbon (C) have been shown to be consistently lower within PV arrays relative to nearby control sites, while other soil properties, like pH and organic matter

(OM) shift unpredictably (Choi et al. 2020, 2023; Lambert et al. 2021; Moscatelli et al. 2022). Such responses may be ecosystem dependent and driven by varying construction practices used to establish the arrays. Evaluations of in situ belowground biotic function, including soil respiration, soil microbial community structure, and overall microbial activity via extracellular enzyme assays, have also been performed in solar arrays, but only at limited microsites (between and beneath panels, Lambert et al. 2021; Moscatelli et al. 2022; Li et al. 2023; Carvalho et al. 2025; Scholten et al. 2025), thus overlooking the wider range of soil microenvironments within PV facilities (see Choi et al. 2020; Sturchio et al. 2022; Sturchio, Kannenberg, Pinkowitz, and Knapp 2024). Hence, there is a major gap in understanding the full spectrum of consequences for soil abiotic heterogeneity within PV arrays, contributing to a more general lack of understanding of how this projected land use change will alter belowground biological activity.

To better understand how PV-induced environmental heterogeneity alters key soil properties and processes that underpin biogeochemical cycling and ecosystem function, we paired soil functional assays with physiochemical and molecular analyses in a semi-arid, C3 dominated grassland. The array selected for our study was particularly valuable because a single graminoid species dominated all microsites, allowing us to isolate how abiotic environmental heterogeneity impacted soil processes in the absence of plant community compositional shifts. We assessed decomposition rates of organic compounds, quantified microbial biomass carbon (C) and nitrogen (N) and microbial community structure, and performed a suite of physiochemical analyses (e.g., pH, total C, electrical conductivity) to determine relationships between PV microsites and soil properties and processes. We hypothesized that PV-induced differences in soil physiochemical profiles would drive contrasting soil microbial community

structure and function across PV microsites, with the most substantial differences between microsites where the greatest previously documented differences in abiotic variation occur (e.g., west panel edge and beneath panels, Choi et al. 2020; Sturchio et al. 2022; Sturchio and Knapp 2023) relative to undisturbed grassland. Specifically, we expected that soil microbial biomass and decomposition rates would be highest along the west panel edge, where soil moisture is greatest throughout the growing season, and lowest beneath panels due to the lack of light, productivity, and precipitation inputs. We further expected that soil microbial community structure beneath panels would differ markedly from other PV microsites and control plots.

4.3 Methods

4.3.1 Study Site

Research was conducted at Jack's Solar Garden (JSG) in Longmont, Colorado, USA (40.12191, −105.12936). JSG was established in 2019 as a 1.2 MW solar energy production and research facility fabricated with single-axis tracking panels (tracking east–west). Panels are 2 m long (east–west) and mounted 1.8 m above the ground when flat, with 3.2 m of interspace between the western edge of a panel row and the eastern edge of the next (Figure 4.1). The land was not graded during array installation and overall disturbance was minimized such that grass cover is 100% throughout the array. The soils at the site are Nunn sandy clay loam (of the Nunn series) with 0%–1% slopes (Soil Survey Staff, Natural Resources Conservation Service, United States Department of Agriculture 2025). The soils are well-drained and taxonomically classified as fine, smectitic, mesic Aridic Argiustolls formed primarily from alluvial and aeolian deposition with a predominantly loamy alluvium parent material (National Cooperative Soil Survey 2025). The vegetation beneath panels is primarily dominated (> 90% cover) by a monoculture of Bromus inermis, a naturalized perennial C3 grass. Other species, such as *Medicago sativa*

(Alfalfa), *Dactylis glomerata* (C_3 Orchard grass), and *Tragopogon dubius* (C_3 forb), compose the majority of subordinate plant species, although they were not present in any of the experimental microsite plots. JSG was formerly managed as a hay farm until PV installation in 2019, when active management (e.g., mowing and fertilization) ended. The site is situated at 1508 m of elevation, with a semi-arid climate, a mean annual temperature of 9.7°C, and 365 mm of annual precipitation (Colorado Climate Center; http://ccc.atmos.colostate.edu/).

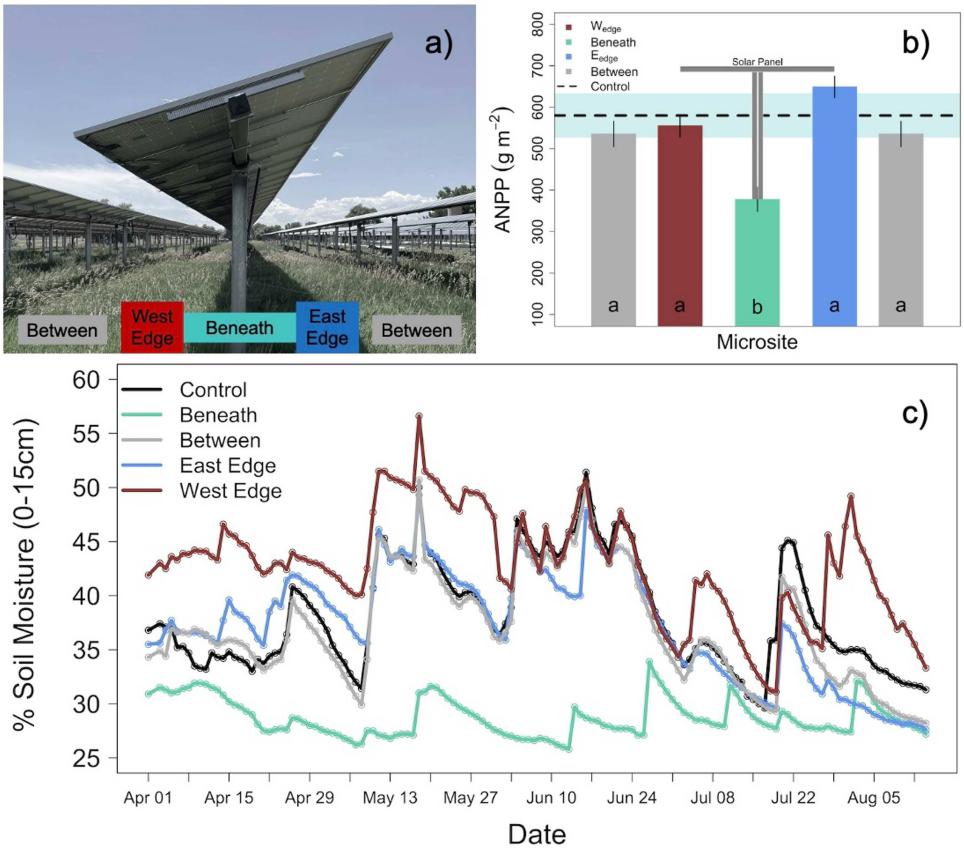

Figure 4.1. Distribution of experimental microsites, along with their impacts on ANPP and soil moisture. a): Experimental microsites (Between, West edge (W_{edge}), Beneath, East edge (E_{edge})) for sample collection in the perennial C_3 grassland at Jack's Solar Garden. Between microsites are shown twice to display spatial orientation of microsites, which is also included in subsequent figures. b): Microsite patterns of mean ANPP for 2023 are color coded to match Fig. 1a. Lines on vertical bars represent standard error from the mean. Letters in bars represent statistical differences ($p < 0.05$, Table A3.1). The control site mean ANPP is represented by a dashed horizontal line with a light blue band representing standard error from the mean, which is repeated in the figures below. c): Average growing season volumetric soil moisture (0-15cm).

4.3.2 Experimental Design

In May 2023, we established four 15.6m transects perpendicular to the rows of PV panels within a portion of JSG that is composed of undisturbed perennial grassland (Fig. A3.1). Each transect was split into three replicate sampling areas comprised of four unique PV microsites based on past studies in single-axis tracking arrays that have identified these as areas with unique light and precipitation inputs (Kannenberg et al. 2023; Sturchio, Kannenberg, and Knapp 2024; Sturchio, Kannenberg, Pinkowitz, and Knapp 2024; Sturchio and Knapp 2025; Fig. 4.1a). This resulted in 48 experimental microsite plots (1m×0.5m), with 12 per microsite treatment (Fig. A3.1, Sturchio and Knapp 2025). The between panel (*Between*, directly between PV support posts) microsites receive precipitation inputs similar to control plots but receive only ~70% of direct sunlight. Rainfall events at panel edges are concentrated due to runoff, but the spatial pattern of precipitation redistribution is time dependent. For example, morning rainfall is shed to the eastern panel edge (E_{edge}, 80 cm east of PV support posts) and afternoon rainfall is shed to the western panel edge (W_{edge}, 80 cm west of PV support posts). Total sunlight availability is also limited at panel edges, with E_{edge} and W_{edge} receiving ~47% and ~42% of total daily light inputs, respectively. Beneath panel microsites (*Beneath*, directly in line with PV support posts) receive the least rainfall and ~30% of total daily light inputs. Our external control (Control) plots (n=4) were located in an undisturbed area 20m outside of the solar array and ~100m from the nearest experimental microsite plot in an area of homologous soil type, slope, and management.

4.3.3 Environmental Measurements

Volumetric water content (VWC, denoted as soil moisture [SM]) was measured using CS616 Soil Moisture Sensors (Campbell Scientific, Logan, UT) at 15min increments from May to September 2023, hereafter considered the growing season. Each experimental microsite and

control plot had paired sensors at 0–15 cm depth (Fig. 4.1). Differences in photosynthetic photon flux density, air temperature, and relative humidity across microsites were previously characterized (Kannenberg et al. 2023; Sturchio, Kannenberg, Pinkowitz, and Knapp 2024), allowing us to infer these values. The mean air temperature on the sampling date was 22.7°C with light overcast conditions.

4.3.4 Soil and Plant Sampling

Destructive soil sampling only took place once on August 2, 2023, near peak primary production, to minimize disturbance and interference with other aspects of the study (i.e., biomass harvest). Three soil samples were collected from each experimental microsite (n=48) and control (n=4) plot (15cm depth×2.22cm diameter) using a steel soil probe (AMS Inc., ID, USA) and homogenized in the field to capture within-plot spatial heterogeneity. Immediately prior to bulk homogenization, samples for microbial analyses were collected from the interior of the core (5–10cm depth) using a sterilized metal spatula and homogenized, and each tool was cleaned thoroughly with 70% ethanol after each plot. Samples were collected, placed in a cooler, and immediately transported back to the Colorado State University (CSU) laboratory. The samples collected for microbial analysis were then immediately subset and transferred to −80°C storage for DNA preservation (~3g per sample) and remaining portions were refrigerated. All analyses requiring fresh soils (e.g., microbial biomass, MSIR) were conducted within a week of sample collection, and DNA was extracted from frozen samples within 2 weeks of collection. All subsequent soil analyses were conducted on a randomly selected subset of samples from experimental microsite and control plots. Soil cores (10cm depth×6cm diameter) were collected in replicate (n=3 per microsite treatment and control) on August 3, 2023, for bulk density measurements.

At the end of the growing season (late-September), all plots were sampled for aboveground net primary productivity (ANPP). We placed a 0.1-m2 quadrat in each plot and harvested all biomass to ground level. Harvested biomass was dried at 60°C for 72h, then weighed to the nearest 0.01 g. For experimental microsite plots (*n*=12 per microsite treatment), variability in sample size was due to interference by native fauna or logistical constraints. For Control plots (*n*=4), sample size was limited by available space.

4.3.5 Soil Physiochemical Analysis

Soil properties were assessed using conventional methodologies at the Colorado State University SPUR Soil, Water and Plant Testing Laboratory. Gravimetric soil moisture was measured by weighing 10g of fresh, sieved (2mm) soil to the nearest 0.01g, drying at 105°C for 48h, then reweighing. Soil pH and electrical conductivity were measured in a 1:1 (w:v) soil and water suspension using a pH and conductivity meter. Soil organic matter (SOM) was determined via loss on ignition (Robertson et al. 1999). Soil total C and N were determined via dry combustion on an elemental analyzer using dry soil samples (VELP CN 802, Italy). To prepare for soil total C and N analyses, soils were sieved (2mm) to remove roots, any remaining roots were extracted with tweezers, then soils were ground with a sterile mortar and pestle. Soil texture was determined via hydrometer and wet sieving methods to calculate the clay and sand fractions, respectively. Soil bulk density was calculated following the drying and weighing of soil cores (10cm×6cm), then dividing dry weight by core volume.

4.3.6 Microbial Biomass

Microbial biomass C and N were assessed via the chloroform fumigation extraction method (Brookes et al. 1985). Biological replicates were randomly selected to represent each experimental microsite treatment and controls (*n*=8 for E_{edge}, W_{edge}, and *Beneath*, *n*=4 for

Between, *n*=3 for Control), and 10g of fresh fumigated and unfumigated samples were extracted in 50mL of 0.5M K_2SO_4 after 30min of shaking. Dissolved organic C and total N were determined using a Schimadzu TOC-L (Schimadzu Corp, Japan). Microbial biomass C and N were calculated as the difference between fumigated and unfumigated samples with the coefficients k_{EN} of 0.54 and k_{EC} of 0.45. We then converted all measures to a per gram dry soil basis using our gravimetric soil water content calculations.

4.3.7 Microbial Substrate-Induced Respiration

Microbial Substrate-Induced Respiration (MSIR) rates were generated for randomly subsampled soils of each experimental microsite treatment and control (*n*=3 biological replicates in duplicate [*n*=6 per treatment]) using the MicroResp system (Campbell et al. 2003; Creamer et al. 2016). Colorimetric gel detector plates were generated using a cresol red indicator solution to be read on an Infinite 200 Pro plate reader (Tecan, Switzerland) at 570nm. Five substrates (plus water) were selected based on their common occurrence as native labile and recalcitrant (i.e., length of the C chain) organic carbon inputs. These were: D-(+)-glucose, α-cellulose, D-(+)-xylose, N-acetyl-D-glucosamine, and lignin (alkali). Water was a sixth substrate to provide basal respiration measurements. Soils (0.3 ± 0.03 g) were loaded into 96-well plates and stored at 4°C in the dark for 3 days to allow acclimation following disturbance. The five substrates were then added to the soils in six replicate 25μL aliquots. The plate was left open for a period of 15min to release any potential carbonates present that may obscure readings following the addition of acidic substrates (Creamer et al. 2016). Baseline colorimetry readings were collected from the indicator plates at 570nm prior to sealing. Indicator plates were then sealed onto deep-well plates and incubated at 20°C for 6h. Colorimetry values were then collected from the indicator plates to calculate respiration rates (μg CO_2-C g^{-1} h^{-1}) as the difference between final and initial values.

Overall substrate-induced respiration was calculated by subtracting basal respiration then summing the responses for each sample and substrate (Colombo et al. 2016).

4.3.8 Nutrient Probes

Plant root simulator (PRS) probes (Western Ag Innovations, Saskatoon, Saskatchewan, CA) were used to assess plant available macronutrients (N, P, and K) and micronutrients (Ca, Mg, Fe, Mn, Cu, Zn, B, S, Pb, Al, and Cd). PRS probes imitate plant uptake of ions via paired 10 cm^2 cation and anion exchange resin membranes inserted in the upper soil profile. We buried probes (n=2–3 pairs) in each plot at two points during the growing season. The first period (May 31–June 26) was chosen to represent the early growing season. The second period (August 2–September 5) was chosen to represent the late growing season. Each pair of probes was retrieved and sent to WesternAg Innovations for processing. The two to three pairs from each plot were eluted together within the laboratory.

4.3.9 Sequencing

Soil microbial DNA was extracted using the Qiagen DNeasy PowerSoil Pro Kit (Qiagen, Hilden, Germany) according to the manufacturer's specifications. All DNA extractions were done at Colorado State University. DNA samples were assessed for quality and quantity using a NanoDrop Lite Spectrophotometer (ThermoFisher Scientific, MA, USA) and Qubit 4 Fluorometer (Invitrogen). Extractions were reiterated if the 260/280 absorbance ratio was below 1.7 due to low DNA quality. Once all DNA extractions were successfully completed and quality checked, they were stored at −20°C until the samples were sent to the CIRES Fierer's Microbial Community Sequencing Lab at the University of Colorado Boulder (Boulder, Colorado) for library preparation and sequencing. DNA was amplified using a SimpliAmp Thermocycler (ThermoFisher Scientific). Illumina MiSeq (Illumina Inc., CA, USA) 2×150bp chemistry at 500

cycles was used for paired-end amplicon sequencing of the 16S V4 (515F/806R primers; Apprill et al. 2015; Parada et al. 2015) and 2×250bp chemistry at 500 cycles was used for paired-end amplicon sequencing of the ITS (ITS1/ITS2; Caporaso et al. 2012) regions, with no-template and extraction controls included in each run.

4.3.10 Bioinformatic Processing

Raw data were received in FASTQ format and demultiplexed using QIIME2 2023.5 software (Bolyen et al. 2019). Sequences were assessed for quality following demultiplexing, merged, then denoised using the DADA2 plug-in (Bokulich et al. 2013; Callahan et al. 2016). Low-quality sequences ($Q < 25$) were filtered out. Taxonomy was assigned for all sequences using the feature-classifier QIIME2 plug-in (Bokulich et al., 2018). We assigned taxonomy to 16S sequences against the GreenGenes2 database (McDonald et al. 2023) and ITS sequences against the UNITE database (Nilsson et al. 2019) at 99% similarity, generating operational taxonomic units (OTUs). Mitochondrial and chloroplast reads were removed using the taxa-filter table plug-in (Bolyen et al. 2019). Feature table and taxonomic assignments were exported for downstream analysis in R software (R Core Team, 2023).

4.3.11 Statistical Analysis

Samples were separately analyzed for bacterial/archaeal (16S) and fungal (ITS) communities. OTUs under 20 total reads were removed from analyses to minimize contaminant and sequencing errors (Cao et al. 2021). Samples were rarefied at 11,000 reads for 16S rRNA and 26,000 reads for ITS rRNA. These rarefaction values were chosen to retain the maximum number of samples and allow comparison of samples with differing sequencing depths. Rarefied OTU tables were used for alpha diversity calculations, but not for other downstream analyses. The ‘mctoolsr,’ ‘vegan,’ and ‘phyloseq’ R packages were used to analyze microbial communities

(McMurdie and Holmes 2013; Oksanen et al. 2013; Leff 2017). For alpha diversity analysis, richness and Shannon diversity indices were calculated and compared with generalized linear models (GLMs) using microsite as a predictor variable. For beta diversity analysis, Bray–Curtis distances were calculated and ordinated using constrained analysis of principal coordinates (CAPs) with microsite as the constraining variable.

Permutational multivariate analysis of variance (PERMANOVA) models and pairwise comparisons with 'pairwiseAdonis' were used to investigate differences in microbial community structure corresponding with microsite (Arbizu 2020). To determine which taxa were differentially abundant between microsites, we used ANCOM-BC with microsite as the predictor, prevalence cutoff of 0.10, and alpha of 0.05 (Lin and Peddada 2020). Shared taxa were determined using the core_members() function in the 'microbiome' package with a detection threshold of 0.001 and prevalence threshold of 0.10 (Lahti and Shetty 2019). Environmental variables, soil edaphic properties, plant available nutrients, microbial biomass, and MSIR rates were all analyzed in GLMs and analyses of variance (ANOVAs) using microsite as a predictor variable. Spearman rank correlation coefficients were calculated for the dominant microbial taxa, soil properties, and ANPP. All analyses were performed using R version 4.3.0 (R Core Team 2017).

4.4 Results

4.4.1 Aboveground Productivity

Aboveground productivity was highest in E_{edge} (649.03 ± 32.07 g m^{-2}), although not significantly higher than Control ANPP. In contrast, aboveground productivity was significantly reduced Beneath panels relative to the Control (378.2 ± 17.56 and 580.20 ± 52.90 g m^{-2}, respectively) ($F = 11.5194$, $p < 0.001$, Fig. 3.1, Tables A3.1 and A3.2).

4.4.2 Soil Physiochemistry

Soils at the site of the solar array were classified as clay loam with 39.1% clay, 20.3% silt, and 40.6% sand. Soil pH ranged from 6.97 to 7.82 across microsites and was slightly lower in E_{edge} relative to Control (7.27 ± 0.069 vs. 7.74 ± 0.1196, respectively) ($F = 3.9613$, $p = 0.018$, Tables A3.1 and A3.2). Soil organic matter ranged from 0.98% to 1.35% and was significantly higher on the E_{edge} relative to Between (1.22% ± 0.03% vs. 1.03% ± 0.04%, respectively) ($F = 3.4208$, $p = 0.030$, Tables A3.1 and A3.2) but did not differ between other microsites. Soil moisture differed between microsites following a pattern previously observed at the same site ($p < 0.001$; Tables A3.1 and A3.2). Bulk density, total C, total N, and EC did not differ across microsite treatments or control (Tables A3.1 and A3.2).

Growing season soil nutrient availability indicated distinct microsite dynamics across the early (May and June) and late (July and August) growing season. Early growing season nutrient availability was assessed within the microsites directly affected by PV panels (i.e., Beneath, E_{edge}, W_{edge}, Table A3.3). Of the macronutrients, only P ($F = 16.052$, $p < 0.001$) and K ($F = 86.443$, $p < 0.001$) differed by microsite (Tables A3.3 and A3.4). Of the micronutrients, Ca, Mg, Fe, Cu, Zn, S, Al, and Cd all significantly differed by microsite (Tables A3.3 and A3.4). Late growing season nutrient availability was assessed across all microsites (including between panels) and the control plots and showed even fewer differences by microsite; Of the macronutrients, only K differed across microsites (Tables A3.3 and A3.5). Of the micronutrients, only Pb and Cd differed across microsites. Overall, soil nutrient availability generally decreased across PV microsites throughout the growing season (Table A3.3).

4.4.3 Soil Biotic Properties

4.4.3.1 Microbial Biomass

Microbial biomass carbon (MBC) was lowest in W_{edge} and Between microsites (409 ± 39.3 and 483 ± 55.6 μg C g^{-1} soil, respectively, Fig. 4.2), while highest in Control and Beneath microsites (889 ± 64.3 and 858 ± 39.3 μg C g^{-1} soil, respectively, Fig. 4.2) ($F = 22.088$, $p < 0.001$, Tables A3.1 and A3.2). Microbial biomass nitrogen (MBN) was lowest in W_{edge} and Between (62.3 ± 3.18 and 76.6 ± 4.50 μg C g^{-1} soil, respectively, Fig. 4.2), and highest in Control and Eedge (116.6 ± 5.20 and 86.5 ± 4.03 μg C g^{-1} soil, respectively, Fig. 4.2) ($F = 21.343$, $p < 0.001$, Tables A3.1, A3.2), whereas microbial biomass C:N ratios were lowest in Between and Wedge (6.37 ± 0.31 and 6.59 ± 0.21 μg C g^{-1} soil, respectively, Fig. 4.2) and highest in Beneath and Control (10.16 ± 0.57 and 7.65 ± 0.56 μg C g^{-1} soil, respectively, Fig. 4.2, Table A3.2).

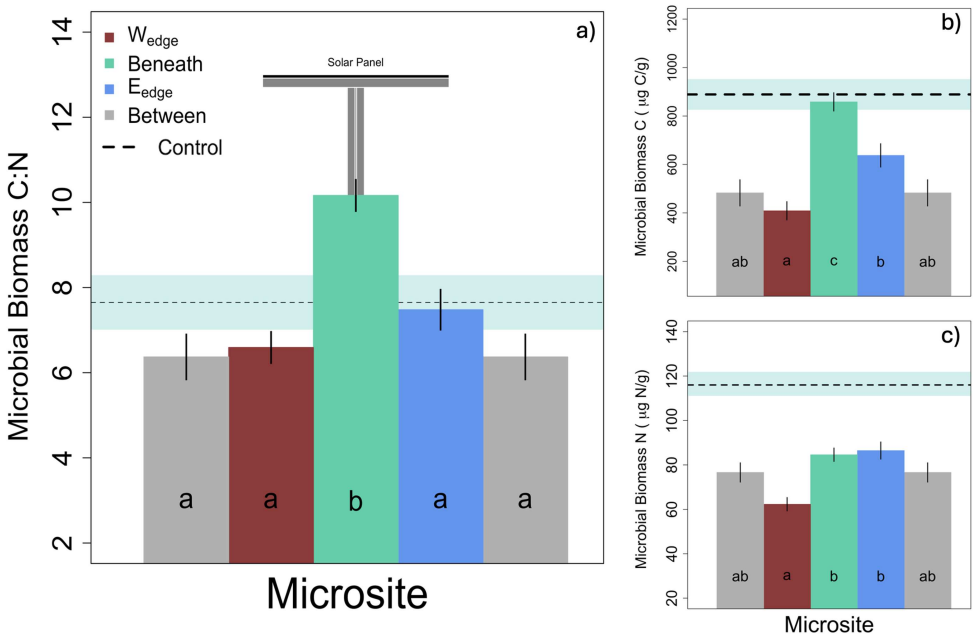

Figure 4.2: Microbial biomass across microsites. a): Microbial biomass carbon to nitrogen molar ratios. b): Microbial biomass C measured in µg g^{-1} dry soil. c): Microbial biomass N measured in µg g^{-1} dry soil. Lines on vertical bars represent standard error from the mean. Different letters within the bars indicate values that are statistically different ($p < 0.05$, Table A3.1). The control sample means are represented by a dashed horizontal line with a light blue band representing standard error from the mean.

4.4.3.2 Multiple Substrate Induced Respiration (MSIR, MicroResp)

Similar to MBC and MBN, overall MSIR rates were significantly lower in W_{edge} (1.30 ± 0.27 µg g^{-1} h^{-1} CO_2-C) relative to all other microsites, with highest rates observed in E_{edge} and Control (7.08 ± 1.22 and 6.51 ± 1.53 µg g^{-1} h^{-1} CO_2-C, respectively) ($F = 3.6452$, $p = 0.012$, Tables A3.1 and A3.6). Basal (water) respiration displayed alternative trends, with rates significantly lowest in Control (1.12 ± 0.09 µg g^{-1} h^{-1} CO_2-C) relative to all other microsites and highest rates observed in the E_{edge} microsite (1.78 ± 0.07 µg g^{-1} h^{-1} CO_2-C) ($F = 7.1546$, $p < 0.001$). The E_{edge} microsites consistently displayed the highest respiration rates across every substrate, while the lowest rates were substrate dependent (Fig. 4.3; Table A3.6).

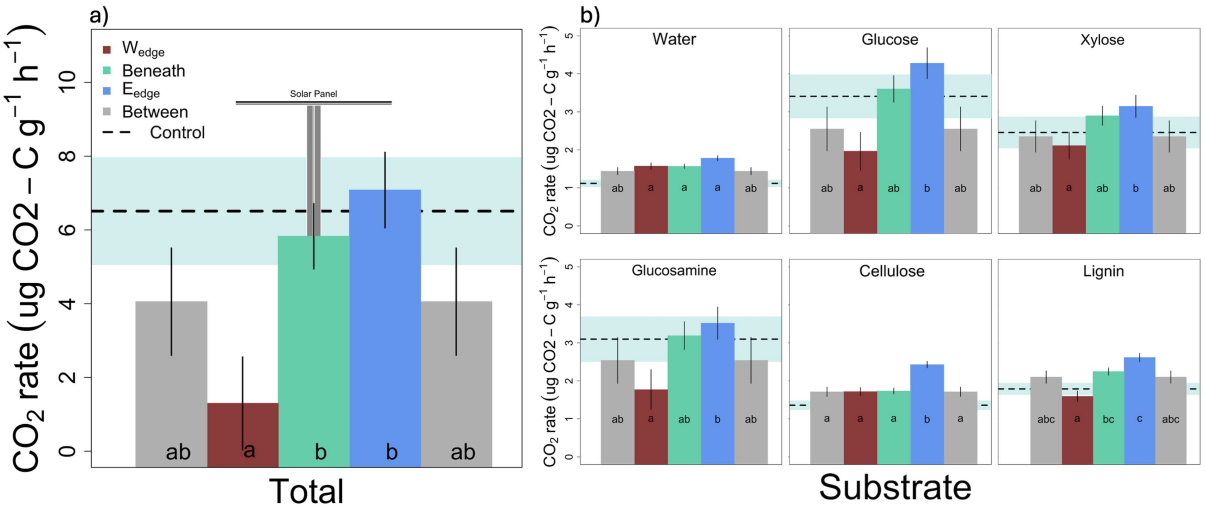

Figure 4.3: Mean response of soil respiration to six substrates across microsites. a): Cumulative mean respiration responses to all six substrates (i.e., total respiration) after subtracting water controls (i.e., basal respiration). b): Soil respiration rates under substrate addition of increasingly recalcitrant organic substrates. Individual bars follow spatial distribution of microsite sampling scheme (Fig. 4.1). Lines on vertical bars represent standard error from the mean. Different letters within the bars indicate values that are statistically different ($p < 0.05$). The control sample means are represented by a dashed horizontal line with a light blue band representing standard error from the mean.

4.4.4 Soil Microbial Community Composition

4.4.4.1 Alpha Diversity

There were no significant differences in bacterial and archaeal Shannon diversity across microsites (Fig. 4.4; Table A3.5). However, Between and Control microsites had the highest Shannon diversity (5.29 ± 0.05 and 5.27 ± 0.11, respectively), and Beneath and E_{edge} microsites had the lowest Shannon diversity (5.17 ± 0.04 and 5.22 ± 0.03, respectively).

There were no significant differences in fungal Shannon diversity across microsites, although trends were more pronounced relative to bacteria/archaea and differed substantially

(Fig. 4.4; Table A3.5). The E_{edge} and Beneath microsites had the highest Shannon diversity (3.86 ± 0.09 and 3.85 ± 0.14, respectively), and Between and W_{edge} had the lowest Shannon diversity (3.52 ± 0.05 and 3.70 ± 0.13, respectively).

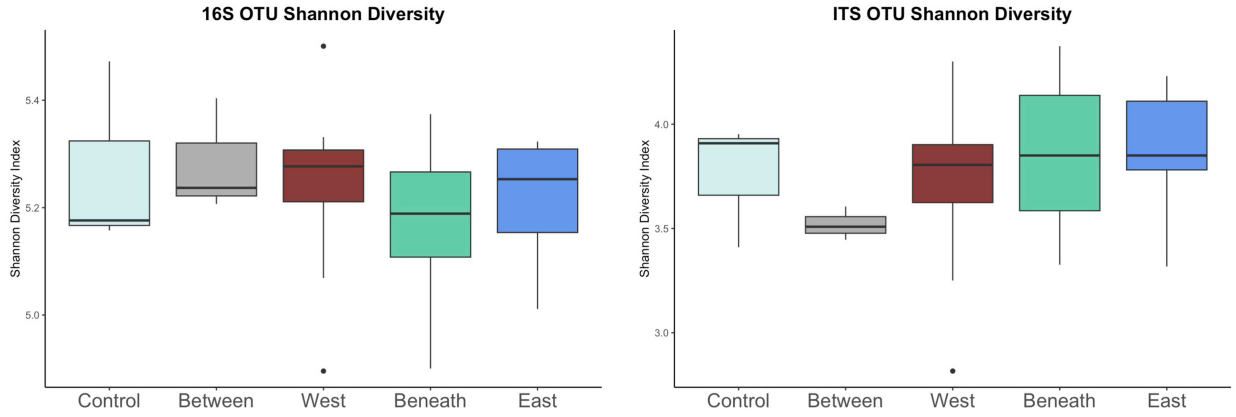

Figure 4.4: Left) Shannon diversity of bacteria, archaea, and Right) fungi. Boxes represent the median and interquartile range. Whiskers represent the maximum and minimum values. There are no significant differences for either amplicon.

4.4.4.2 Beta Diversity

Prokaryotic (bacterial and archaeal) communities differed by microsite (pseudo-F = 2.2415, $p < 0.001$, Fig. 4.5; Table A3.5). Differences were most pronounced between the Control and W_{edge} ($p = 0.06$), Beneath ($p = 0.05$), and E_{edge} ($p = 0.03$) microsites according to pairwise analyses. Analysis of the E_{edge} and Between communities also suggested differences in composition ($p = 0.09$).

Fungal communities also differed by microsite (pseudo-F = 1.3506, $p < 0.001$, Fig. 4.5; Table S5). Differences were most pronounced between the Control and W_{edge} ($p = 0.025$),

Beneath (p = 0.026), and E_{edge} (p = 0.025) microsites according to pairwise analyses. In brief, Control prokaryotic and fungal communities differed substantially from those of microsites that are most directly influenced by panels (i.e., E_{edge}, Beneath, W_{edge}).

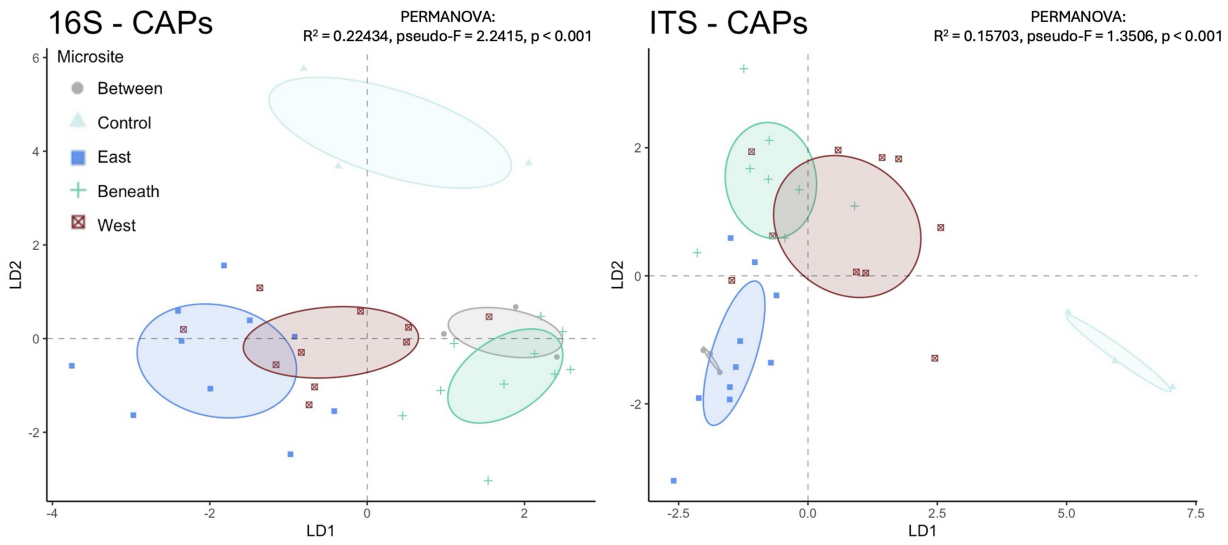

Figure 4.5: Ordinations for canonical analysis of principal coordinates (CAP) illustrating the impact of microsite heterogeneity on Left) soil bacterial, archaeal, and Right) fungal communities. CAP analyses based on Bray-Curtis dissimilarities. Permutational multivariate analysis of variance (PERMANOVA) model results displayed in upper corner of each panel. CAP was conducted following detection of the significant microsite effects via PERMANOVA (p < 0.05).

4.4.4.3 Taxonomic Differences

The most abundant bacterial and archaeal classes across all samples included Nitrososphaeria (20.7%), Vicinamibacteria (14.9%), Verrucomicrobiae (10.5%), Planctomycetia (8.5%), Alphaproteobacteria (6.4%), Bacteroidia (5.9%), and Actinomycetia (5.2%) by relative abundance (see Fig. A3.2 for phylum-level breakdown). The top 10% of dominant OTUs accounted for 66.1% of total reads, with the ammonia-oxidizing archaea *Nitrosocosmicus hydrocola* accounting for 12.3% of total reads alone. 189 OTUs were shared across all microsites; 81 were unique to Control, 86 unique to Between, 59 unique to E_{edge}, 45 unique to Beneath, and 24 unique to W_{edge} (Fig. 4.6). Amongst the dominant bacterial and archaeal classes, Verrucomicrobiae differed by microsite (p = 0.002, relative abundances in Between = 4.3%, Control = 8.3%, E_{edge} = 8.3%, Beneath = 5.4%, W_{edge} = 7.4%), along with Planctomycetia (p = 0.009, relative abundances in Between = 9.2%, Control = 8.8%, E_{edge} = 9.7%, Beneath = 7.5%, W_{edge} = 9.1%). The most enriched bacterial and archaeal taxa in the E_{edge} were Fibrobacteraceae, Enterobacteraceae, and Pedosphaerales relative to the W_{edge}. Conversely, the most enriched bacterial and archaeal taxa in the W_{edge} were family WHTK01, family Pan216, and Solirubrobacterales relative to the E_{edge} (Fig. 4.7). These explicit comparisons were made based on our hypothesized and observed differences in decomposition rates.

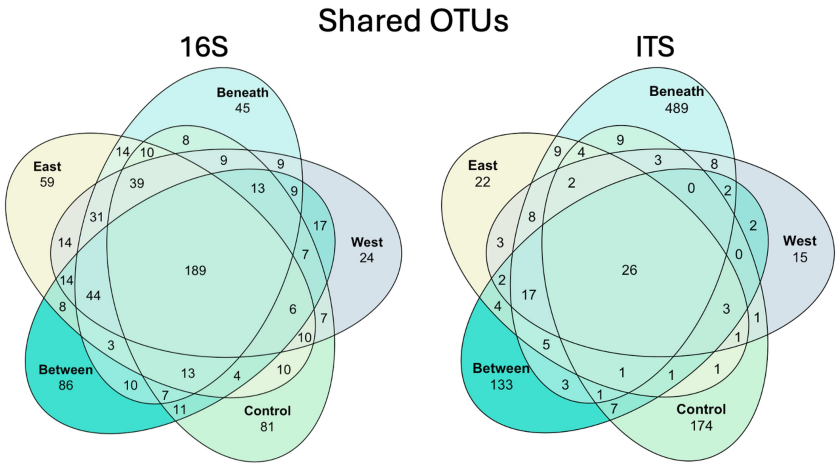

Figure 4.6: Number of shared and unique OTUs between microsites. Values associated only with a single microsite indicate OTUs that are unique to that microsite. Values in overlapping circles indicate taxa that are shared between microsites.

The most abundant fungal classes across all samples included Mortierellomycetes (18.3%), Pezizomycetes (13.5%), Agaricomycetes (13.5%), Tremellomycetes (10.1%), Leotiomycetes (9.9%), and Glomeromycetes (5.6%) by relative abundance (see Fig. A3.3 for phylum-level breakdown). The top 10% of dominant OTUs accounted for 76.8% of total reads, with the most dominant OTU, *Pulvinula* sp., accounting for 5.1% of total reads alone. 26 OTUs were shared across all microsites; 176 were unique to Control, 133 unique to Between, 22 unique to E_{edge}, 489 unique to Beneath, and 14 unique to W_{edge} (Figs. 4.6, A3.4). Amongst the dominant fungal classes, Agaricomycetes differed by microsite ($p = 0.002$, relative abundances in Between = 12.2%, Control = 12.6%, E_{edge} = 13.9%, Beneath = 3.4%, W_{edge} = 6.8%), along with Dothideomycetes ($p = 0.08$, relative abundances in Between = 2.9%, Control = 7.8%, E_{edge} = 15.4%, Beneath = 16.9%, W_{edge} = 16.9%). The most enriched fungal taxa in the E_{edge} were Xylaria, Peniophoraceae, and Phaeosphaeriaceae relative to the W_{edge}. Conversely, the most enriched fungal taxa in the W_{edge} were Dioszegia, Pyrenochaetopsis, and Lycoperdon relative to the E_{edge} (Fig. 4.7).

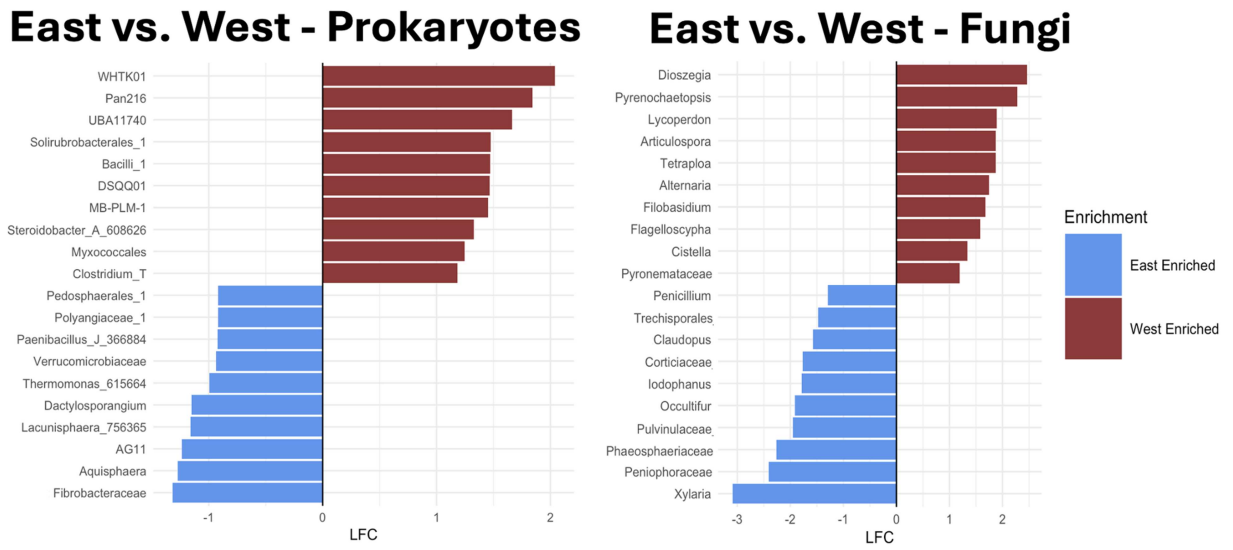

Figure 4.7: Differentially abundant taxa in the East and West edge microsites. Left): Bacterial and archaeal taxa that are enriched in the E_{edge} (blue) and W_{edge} (red) at the genus level or finest available taxonomic resolution. Right): Fungal taxa that are enriched in the E_{edge} (blue) and W_{edge} (red) at the genus level or finest available taxonomic resolution. Differential abundance analysis was conducted with the ANCOM-BC R package, and logfold changes are visualized along the x-axis.

4.5 Discussion

We assessed how a single-axis tracking PV array altered soil microbial communities and physiochemical properties in a semi-arid grassland. We found that PV-induced heterogeneity promoted unique soil microbial community structure across PV microsites and relative to non-PV controls, with overall differences largely dictated by shifts in the relative abundance of fungal taxa. We also found that, within the array, microbial biomass was highest beneath panels, where the most unique fungal taxa were located, while microbial activity (measured as substrate decomposition) was highest along the eastern panel edge (E_{edge}), where organic matter (OM) and aboveground net primary production (ANPP) were highest. Subtle differences in soil

physiochemical profiles contributed to patterns of soil microbial community structure and activity, but the lack of major profile shifts indicates the importance of PV array construction practices that avoid disturbance and conserve existing biological function.

Spatial differences in plant productivity and soil moisture within the PV array were consistent with previous findings in a semi-arid climate, where E_{edge} plants were most productive, while W_{edge} soils remained the wettest throughout the growing season (Sturchio et al. 2022, Kannenberg et al. 2023, Sturchio et al. 2024b). As expected, beneath panels remained driest and had the lowest ANPP. Because of these trends, we anticipated that soil microbial biomass would differ most substantially across W_{edge} and beneath panel microsites. Our hypothesis was supported by the magnitude of differences, however, the directionality of this relationship, where microbial biomass (C and N) was greatest beneath panels, was unexpected (Fig. 4.2). The exceptionally wet 2023 growing season (536 mm, + 46% greater than long term average), where SM did not drop below 25% beneath panels, may have prevented water limitation and thus facilitated microbial proliferation. Another proposed mechanism for increased microbial biomass accumulation beneath panels is greater belowground C allocation under persistent shading (Bahn et al. 2013, Moscatelli et al. 2022), although others have found the opposite response to increased shading (Möhl et al. 2020). Surprisingly, microbial biomass was higher in control plots than any PV microsite (Fig. 4.2). Given the control plots are unimpeded by PV panels, they undergo the longest daily photoperiods, potentially increasing production of plant photosynthetic products and altering root exudate composition and concentration (Vives-Peris et al. 2020). Unique exudate composition or increased concentrations could enhance microbial biomass production in control plots relative to PV microsites. The lower microbial biomass within a PV array is corroborated by Lambert et al. (2021) who found lower microbial

biomass in a PV array relative to reference pinewood and shrubland, though the PV array had been graded during construction.

Microbial activity did not consistently parallel patterns of microbial biomass, rather it was more closely related to changes in soil physiochemical properties. The E_{edge} harbored the highest microbial activity (Fig. 4.3), likely influenced by the relatively high OM and ANPP and neutral pH. These findings are consistent with previous assessments of microbial activity in natural ecosystems indicating pH and organic C as primary determinants of activity (Creamer et al. 2016, Fierer & Jackson 2006, Nielsen et al. 2010). Although OM is a proxy of organic C, relatively high OM, ANPP, moderate SM, and neutral pH at the E_{edge} generated an environment ideal for turnover of organic compounds within the array. The rapid degradation of both labile (e.g., glucose) and recalcitrant (e.g., lignin) compounds indicates that E_{edge} microbial communities contain a wide array of metabolic pathways (Neely et al. 1991). Interestingly, W_{edge} had the lowest microbial activity, likely due to extended periods of > 40% SM that may have caused waterlogging and oxygen limitation, which may have reduced microbial biomass, limited microbial activity, and altered community structure in the semi-arid system that is accustomed to drier, aerobic soils (Mentzer et al. 2006, Blagodatsky & Smith, 2012, Banerjee et al. 2016, Liu et al. 2023).

In natural systems, differences in microbial activity and metabolic diversity have been attributed to shifts in microbial community composition (Hernandez and Hobbie, 2010, Xun et al. 2015). In further support of our hypothesis, microbial community composition differed across PV microsites, with the most notable differences between PV and non-PV control communities. Although prokaryotic communities were predominantly composed of the globally ubiquitous soil phyla, Acidobacteria, Thermoproteota, Actinobacteria, Planctomycetes, and Proteobacteria (Figs.

A3.2, A3.5, Delgado-Baquerizo et al. 2018), shifts in the relative abundance of the phyla Verrucomicrobia and Planctomycetia drove differentiation between communities. These findings contrast with those of a semi-arid grassland in China, where Actinobacteria and Proteobacteria were the primary drivers of compositional shifts (Bai et al. 2022). Furthermore, prokaryotic communities were dominated by the ammonia-oxidizing archaea, *Nitrososocosmicus hydrocola*, which is likely attributable to the history of N fertilization at the site (Huang et al. 2021, Han et al. 2024). Fungal communities were also dominated by ubiquitous phyla, Ascomycota, Basidiomycota, and Mortierellomycota (Tedersoo et al. 2014, Fig. A3.3), but a class-level analysis suggested that shifts in Agaricomycetes and Dothideomycetes were responsible for driving overall fungal community differences. Although pairwise comparisons did not indicate significant differences in fungal community structure beneath panels and other microsites, the immense number of unique OTUs beneath panels (Fig. 4.6) suggest that this microsite may promote fungal diversity, which could be driven by the hypothesized reallocation of plant photosynthates (Bahn et al. 2013, Moscatelli et al. 2022), differences in soil moisture and nutrient content (Kaisermann et al. 2015), or unique aboveground-belowground interactions not present in other PV microsites. Interestingly, these findings contrast with Liu et al. (2023), where control fungal communities show no clear differentiation between those within an arid PV array.

Prior studies assessing soil responses to PV arrays tended to focus on soil physiochemical properties that are likely to be negatively impacted by the extreme disturbance associated with PV installation (Lambert et al. 2021, Choi et al. 2024). Without major intervention, these properties, such as total C, are unlikely to return to pre-disturbance conditions for years to decades (Jackson et al. 2017). While soil physiochemical properties may not differ drastically across PV microsites if minimally invasive construction practices are leveraged, soil biological

processes, major controls over ecosystem C-cycling, nutrient cycling, and overall functionality, can still differ across relatively small spatial scales (Liu et al. 2023, Leroy et al. 2025). For example, the fungal genus, *Xylaria*, was enriched along the E_{edge} (relative to W_{edge}), promoting higher rates of recalcitrant substrate decomposition (Fig. 4.5b, Osono et al. 2011). Our findings corroborate recent studies of soil microbial activity in PV arrays (Moscatelli et al. 2022, Liu et al. 2023, Lambert et al. 2024), suggesting that, even across different ecosystems, PV arrays substantially alter belowground functionality. Collectively, these findings provide evidence of PV-induced environmental heterogeneity contributing to soil microbial niche differentiation, which may be increasingly evident under more extreme climatic conditions (Sturchio and Knapp, 2023).

The recent surge of studies assessing ecosystem impacts of PV arrays has been invaluable for informing the sustainable development of renewable energy infrastructure, yet the complexity of ecological interactions necessitates scalable approaches that can integrate data from disparate ecosystem types (e.g., simulation models, Paschalis et al. 2025). To understand how this form of land-use change may impact carbon and nutrient cycling, such approaches should leverage case studies that capture the impacts of various PV array designs, construction practices, and management types globally (Bacon et al. 2024). The data presented here suggest that landscape-scale models and future case studies should consider the unique processes underway at different PV microsites. While these data highlight the importance of taking a minimally invasive approach (e.g., no land grading) to PV array construction to preserve ecosystem functionality and limit the need for restoration practices, we further suggest that restoration approaches within PV arrays take advantage of the contrasting conditions present across PV microsites, which may facilitate the establishment of different plant communities, enhanced soil biodiversity, and

potentially soil C sequestration (Lambert et al. 2024, Krasner et al. 2025, Sturchio & Knapp, 2025).

4.6 Conclusion

The rapid pace and scale of PV array installations has generated concern regarding the ecosystem consequences of such a large-scale land use change (Cook 2011, Hernandez et al. 2014). Here, we show that, following a minimally invasive array construction, PV-induced changes in microenvironmental conditions can substantially alter soil microbial community structure and function and, to a lesser degree, soil physiochemical properties, across relatively small (m^2) spatial scales. Although microsite differences in most soil physiochemical properties were modest, microbial community structure and function was strongly influenced by the heterogeneity induced by PV panels. PV-driven shifts in soil functionality have the potential to drive large-scale changes in ecosystem functionality, from altered plant nutrient availability to C fluxes. Considering the diversity of PV construction practices and designs, it is imperative that we conduct further investigations of belowground responses to better understand how global C and nutrient cycles will respond to this form of land use change. We suggest future studies pair analyses of soil properties with soil microbial structure and function to provide clearer insight into short and long-term processes that cannot be gauged by any single measure. These approaches should leverage metagenomics, metatranscriptomics, and other -omics technology where possible to generate a more holistic picture of soil food web contributions to belowground functionality. We further recommend that sampling be conducted across discrete PV microsites that are likely to provide distinct ecosystem functions (e.g., W_{edge}, E_{edge}, Beneath, Between), rather than a single PV microsite (i.e., beneath panels). PV arrays also provide abundant potential to investigate the environmental controls over plant-soil interactions. Given this growing form of

land use is primed to become a primary source of energy production globally (Nijsse et al. 2023), accelerating belowground research and emphasizing more sustainable construction practices must be a priority.

LITERATURE CITED

Adeh, E., J. S. Selker, and C. W. Higgins. 2018. "Remarkable Agrivoltaic Influence on Soil Moisture, Micrometeorology and Water-Use Efficiency." *PloS One* 13, no. 11: e0203256. https://doi.org/10.1371/journal.pone.0203256

Adeh, E. H., S. P. Good, M. Calaf, and C. W. Higgins. 2019. "Solar PV Power Potential is Greatest over Croplands." *Scientific Reports* 9, no. 1: 1-6. https://doi.org/10.1038/s41598-019-47803-3

Andrew, A. C., C. W. Higgins, M. A. Smallman, M. Graham, and S. Ates. 2021. "Herbage Yield, Lamb Growth and Foraging Behavior in Agrivoltaic Production System." *Frontiers in Sustainable Food Systems* 5, 659175. https://doi.org/10.3389/fsufs.2021.659175

Apprill, A., S. McNally, R. Parsons, and L. Weber. 2015. "Minor Revision to V5 Region SSU rRNA 806R Gene Primer Greatly Increases Detection of SAR11 Bacterioplankton." *Aquatic Microbial Ecology* 75, no. 2: 129-137. https://doi.org/10.3354/ame

Arbizu, M. 2020. "pairwiseAdonis: Pairwise Multilevel Comparisons using Adonis." *R package version 0.4*.

Armstrong, A., S. Waldron, J. Whitaker, and N. J. Ostle. 2014. "Wind Farm and Solar Park Effects on Plant-Soil Carbon Cycling: Uncertain Impacts of Changes in Ground-Level Microclimate." *Global Change Biology* 20, no. 6: 1699-1706. https://doi.org/10.1111/gcb.12437

Bacon, T., T. Ohlert, C. Toy, J. A. Siggers, and M. A. Sturchio. 2024. "Network Science can Improve the Sustainable Development of Solar Energy." *Environmental Research: Energy* 1, no. 4: 043002. https://doi.org/10.1088/2753-3751/ad99dc

Bahn, M., F. A. Lattanzi, R. Hasibeder, et al. 2013. "Responses of Belowground Carbon Allocation Dynamics to Extended Shading in Mountain Grassland." *New Phytologist* 198, no. 1: 116-126. https://doi.org/10.1111/nph.12138

Bai, Z., A. Jia, Z. Bai, et al. 2022. "Photovoltaic Panels have Altered Grassland Plant Biodiversity and Soil Microbial Diversity." *Frontiers in Microbiology* 13, 1065899. https://doi.org/10.3389/fmicb.2022.1065899

Banerjee, S., B. Helgason, L. Wang, T. Winsley, B. C. Ferrari, and S. D. Siciliano. 2016. "Legacy Effects of Soil Moisture on Microbial Community Structure and N2O Emissions." *Soil Biology and Biochemistry* 95, 40-50. https://doi.org/10.1016/j.soilbio.2015.12.004

Bardgett, R. D., and D. A. Wardle. 2010. "Aboveground-Belowground Linkages: Biotic Interactions, Ecosystem Processes, and Global Change." Oxford University Press.

Barron-Gafford, G. A., M. A. Pavao-Zuckerman, R. L. Minor, et al. 2019. "Agrivoltaics Provide Mutual Benefits across the Food-Energy-Water Nexus in Drylands." *Nature Sustainability* 2, no. 9: 848-855. https://doi.org/10.1038/s41893-019-0364-5

Blagodatsky, S. and P. Smith. 2012. “Soil Physics Meets Soil Biology: Towards Better Mechanistic Prediction of Greenhouse Gas Emissions from Soil.” *Soil Biology and Biochemistry* 47, 78-92. https://doi.org/10.1016/j.soilbio.2011.12.015

Bokulich, N. A., S. Subramanian, J. J. Faith, et al. 2013. “Quality-filtering Vastly Improves Diversity Estimates from Illumina Amplicon Sequencing.” *Nature Methods* 10, no. 1: 57-59. https://doi.org/10.1038/nmeth.2276

Bokulich, N. A., B. D. Kaehler, J. R. Rideout, et al. 2018. “Optimizing Taxonomic Classification of Marker-Gene Amplicon Sequences with QIIME2’s q2-feature-classifier Plugin.” *Microbiome* 6, 1-17. https://doi.org/10.1186/s40168-018-0470-z

Bolyen, E., J. R. Rideout, M. R. Dillon, et al. 2019. “Reproducible, Interactive, Scalable and Extensible Microbiome Data Science using QIIME2.” *Nature Biotechnology* 37, no. 8: 852-857. https://doi.org/10.1038/s41587-019-0209-9

Borowik, A. and J. Wyszkowska. 2016. “Soil Moisture as a Factor Affecting the Microbiological and Biochemical Activity of Soil.” *Plant Soil Environment* 62, no. 6: 250-255. doi: 10.17221/158/2016-PSE

Brookes, P. C., A. Landman, G. Pruden, and S. D. Jenkinson. 1985. “Chloroform Fumigation and the Release of Soil Nitrogen: A Rapid Direct Extraction Method to Measure Microbial Biomass Nitrogen in Soil.” *Soil Biology and Biochemistry* 17, no. 6: 837-842. https://doi.org/10.1016/0038-0717(85)90144-0

Callahan, B. J., P. J. McMurdie, M. J. Rosen, A. W. Han, A. J. A. Johnson, and S. P. Holmes. 2016. “DADA2: High-Resolution Samples Inference from Illumina Amplicon Data.” *Nature Methods* 13, no. 7: 581-583. https://doi.org/10.1038/nmeth.3869

Campbell, C. D., S. J. Chapman, C. M. Cameron, M. S. Davidson, and J. M. Potts. 2003. “A Rapid Microtiter Plate Method to Measure Carbon Dioxide Evolved from Carbon Substrate Amendments so as to Determine the Physiological Profiles of Soil Microbial Communities by Using Whole Soil.” *Applied and Environmental Microbiology* 69, no. 6: 3593-3599. https://doi.org/10.1128/AEM.69.6.3593-3599.2003

Cao, Q., X. Sun, K. Rajesh, et al. 2021. “Effects of Rare Microbiome Taxa Filtering on Statistical Analyses.” *Frontiers in Microbiology* 11, 607325. https://doi.org/10.3389/fmicb.2020.607325

Carvalho, F., H. Montag, L. Bentley, et al. 2025. “Plant and Soil Responses to Ground-Mounted Solar Panels in Temperate Agricultural Systems.” *Environmental Research Letters* 20, no. 2: 024003. https://doi.org/10.1088/1748-9326/ada45b

Choi, C. S., A. E. Cagle, J. Macknick, D. E. Bloom, J. S. Caplan, and S. Ruvi. 2020. “Effects of Revegetation on Soil Physical and Chemical Properties in Solar Photovoltaic Infrastructure.” *Frontiers in Environmental Science* 8, 140. https://doi.org/10.3389/fenvs.2020.00140

Choi, C. S., J. Macknick, Y. Li, D. Bloom, J. McCall, and S. Ravi. 2023. “Environmental Co-Benefits of Maintaining Native Vegetation with Solar Photovoltaic Infrastructure.” *Earth’s Future* 11, no. 6: e2023EF003542. https://doi.org/10.1029/2023EF003542

Choi, C. S., J. Macknick, J. McCall, R. Bertel, and S. Ravi. 2024. “Multi-year Analysis of Physical Interactions between Solar PV Arrays and Underlying Soil-Plant Complex in Vegetated Utility-Scale Systems.” *Applied Energy* 365, 123227. https://doi.org/10.1016/j.apenergy.2024.123227

Cook, P. 2011. “Infrastructure, Rural Electrification and Development.” *Energy for Sustainable Development* 15, 304-313. https://doi.org/10.1016/j.esd.2011.07.008

Colombo, F., C. A. Macdonald, T. C. Jeffries, J. R. Powell, and B. K. Singh. 2016. “Impact of Forest Management Practices on Soil Bacterial Diversity and Consequences for Soil Processes.” *Soil Biology and Biochemistry* 94, 200-210. https://doi.org/10.1016/j.soilbio.2015.11.029

Creamer, R. E., D. Stone, P. Berry, and I. Kuiper. 2016. “Measuring Respiration Profiles of Soil Microbial Communities across Europe using MicroRespTM Method.” *Applied Soil Ecology* 97, 36-43. https://doi.org/10.1016/j.apsoil.2015.08.004

Delgado-Baquerizo, M., A. M. Oliverio, T. E. Brewer, et al. 2018. “A Global Atlas of the Dominant Bacteria Found in Soil.” *Science* 359, no. 6373, 320-325. https://doi.org/10.1126/science.aap9516

DOE U.S. Department of Energy 2021 Solar futures study (Department of Energy, Office of Energy Efficiency and Renewable Energy, Washington D.C. Sept) (available at: www.energy.gov/eere/solar/solar-futures-study)(Accessed 10 October 2024)

Dupraz, C., H. Marrou, G. Talbot, L. Dufour, A. Nogier, and Y. Ferard. 2011. “Combining Solar Photovoltaic Panels and Food Crops for Optimizing Land Use: Towards New Agrivoltaic Schemes.” *Renewable Energy* 36, no. 10, 2725-2732. https://doi.org/10.1016/j.renene.2011.03.005

Fierer, N. 2017. “Embracing the Unknown: Disentangling the Complexities of the Soil Microbiome.” *Nature Reviews Microbiology* 15, 579-590. https://doi.org/10.1038/nrmicro.2017.87

Fierer, N., and R. B. Jackson. 2006. “The Diversity and Biogeography of Soil Bacterial Communities.” *Proceedings of the National Academy of Sciences* 103, no. 3: 626-631. https://doi.org/10.1073/pnas.0507535103

Fierer, N., M. S. Strickland, D. Liptzin, M. A. Bradford, and C. C. Cleveland. 2009. “Global Patterns in Belowground Communities.” *Ecology Letters* 12, 1238-1249. https://doi.org/10.1111/j.1461-0248.2009.01360.x

Goetzberger, A., and A. Zastrow. 1982. “On the Coexistence of Solar-Energy Conversion and Plant Cultivation.” *International Journal of Solar Energy* 1, no. 1: 55-69. https://doi.org/10.1080/01425918208909875

Grodsky, S. M. 2021. “Matching Renewable Energy and Conservation Targets for a Sustainable Future.” *One Earth* 4, no. 7: 924-926. https://doi.org/10.1016/j.oneear.2021.07.001

Han, S., S. Kim, C. J. Sedlacek, et al. 2024. “Adaptive Traits of Nitrodocosmicus Clade Ammonia-Oxidizing Archaea.” *Environmental Microbiology* 15, no. 11: e02169-24. https://doi.org/10.1128/mbio.02169-24

Hernández, D. L., and S. E. Hobbie. 2010. “The Effects of Substrate Composition, Quantity, and Quality on Microbial Activity.” *Plant and Soil* 335, 397-411. https://doi.org/10.1007/s11104-010-0428-9

Hernandez, R. R., S. B. Easter, M. Murphy-Mariscal, et al. 2014. “Environmental Impacts of Utility-Scale Solar Energy.” *Renewable and Sustainable Energy Reviews* 29, 766-779. https://doi.org/10.1016/j.rser.2013.08.041

Hernandez, R. R., A. Armstrong, J. Burney, et al. 2019. “Techno-Ecological Synergies of Solar Energy for Global Sustainability.” *Nature Sustainability* 2, no. 7: 560-568. https://doi.org/10.1038/s41893-019-0309-z

Huang, L., S. Chakrabarti, J. Cooper, A., et al. 2021. “Ammonia-Oxidizing Archaea are Integral to Nitrogen Cycling in a Highly Fertile Agriculture Soil.” *ISME Communications* 1, 19. https://doi.org/10.1038/s43705-021-00020-4

Irisarri, J. G. N., J. D. Derner, L. M. Porensky, D. J. Augustine, J. L. Reeves, and K. E. Mueller. 2015. “Grazing Intensity Differentially Regulates ANPP Response to Precipitation in North American Semiarid Grasslands.” *Ecological Applications* 26, no. 5: 1370-1380. https://doi.org/10.1890/15-1332

Jackson, R. B., K. Lajtha, S. E. Crow, G. Hugelius, M. G. Kramer, and G. Piñeiro. 2017. “The Ecology of Soil Carbon: Pools, Vulnerabilities, and Biotic and Abiotic Controls.” *Annual Reviews of Ecology, Evolution, and Systematics* 48, 419-445. https://doi.org/10.1146/annurev-ecolsys-112414-054234

Kaisermann, A., P. A. Maron, L. Beaumelle, and J. C. Lata. 2015. “Fungal Communities are More Sensitive Indicators to Non-Extreme Soil Moisture Variations than Bacterial Communities.” *Applied Soil Ecology* 86, 158-164. https://doi.org/10.1016/j.apsoil.2014.10.009

Kannenberg, S. A., M. A. Sturchio, M. D. Venturas, and A. K. Knapp. 2023. “Grassland Carbon-Water Cycling is Minimally Impacted by a Photovoltaic Array.” *Communications Earth & Environment* 4, no. 1: 238. https://doi.org/10.1038/s43247-023-00904-4

Knapp, A. K., A. Chen, R. J. Griffin-Nolan, et al. 2020. “Resolving the Dust Bowl Paradox of Grassland Responses to Extreme Drought.” *Proceedings of the National Academy of Sciences* 117, no: 36, 22249-22255. https://doi.org/10.1073/pnas.1922030117

Knapp, A. K., and T. R. Seastedt. 1986. “Detritus Accumulations Limits Productivity of Tallgrass Prairie.” *Bioscience* 36, no. 10: 662-668. https://doi.org/10.2307/1310387

Knapp, A. K., and M. A. Sturchio. 2024. “Ecovoltaics in an Increasingly Water-Limited World: An Ecological Perspective.” *One Earth* 7, no. 10: 1705-1712. https://doi.org/10.1016/j.oneear.2024.09.003

Krasner, N. Z., J. Fox, A. Armstrong, et al. 2025. “Impacts of Photovoltaic Solar Energy on Soil Carbon: A Global Systematic Review and Framework.” *Renewable and Sustainable Energy Reviews* 208, 115032. https://doi.org/10.1016/j.rser.2024.115032

Kuzyakov, Y., P. W. Hill, and D. L. Jones. 2007. “Root Exudate Components Change Litter Decomposition in a Simulated Rhizosphere Depending on Temperature.” *Plant and Soil* 290, 293-305. https://doi.org/10.1007/s11104-006-9162-8

Lahti, L., and S. Shetty. 2019. “Microbiome R Package.”

Lambert, Q., A. Bischoff, S. Cueff, A. Cluchier, and R. Gros. 2021. “Effects of Solar Park Construction and Solar Panels on Soil Quality, Microclimate, CO2 Effluxes, and Vegetation under a Mediterranean Climate.” *Land Degradation & Development* 32, no. 18: 5190-5202. https://doi.org/10.1002/ldr.4101

Lambert, Q., A Bischoff, and R. Gros. 2024. “Effects of Habitat Restoration and Solar Panels on Soil Properties and Functions in Solar Parks.” *Applied Soil Ecology*, 203, 105614. https://doi.org/10.1016/j.apsoil.2024.105614

Lee, H., K. Calvin, D. Dasgupta, et al. 2023. IPCC, 2023: Climate Change 2023: Synthesis Report, Summary for Policymakers. Contribution of Working Groups I, II, and III to the Sixth Assessment Report of the Intergovernmental Panel on Climate Change [Core Writing Team, H. Lee and J. Romero (eds.)]. IPCC, Geneva, Switzerland.

Leff, J. W. 2017. “mctoolsr: Microbial Community Data Analysis Tools. R Package Version 0.1.1.2.”

Leroy, V., G. Decocq, P. Noirot-Cosson, and R. Marrec. 2025. “Impacts of Punctual Solar Trackers on Soil Biodiversity in Agricultural Lands.” *Geoderma* 453, 117147. https://doi.org/10.1016/j.geoderma.2024.117147

Li, C., J. Liu, J. Bao, T. Wu, and B. Chai. 2023. “Effect of Light Heterogeneity Caused by Photovoltaic Panels on the Plant-Soil-Microbial System in Solar Park.” *Land* 12, no. 2: 367. https://doi.org/10.3390/land12020367

Lin, H., and S. D. Peddada. 2020. “Analysis of Compositions of Microbiomes with Bias Correction.” *Nature Communications* 11, 3514. https://doi.org/10.1038/s41467-020-17041-7

Liu, Z., T. Peng, S. Ma, et al. 2023. “Potential Benefits and Risks of Solar Photovoltaic Power Plants on Arid and Semi-Arid Ecosystems: An Assessment of Soil Microbial and Plant Communities.” *Frontiers in Microbiology* 14, 1190650. https://doi.org/10.3389/fmicb.2023.1190650

McDonald, D., Y. Jiang, M. Balaban, et al. 2023. “Greengenes2 unifies microbial data in a single reference tree.” *Nature Biotechnology* 42, no. 5: 715-718. https://doi.org/10.1038/s41587-023-01845-1

McMurdie, P. J., and S. Holmes. 2013. “Phyloseq: An R Package for Reproducible Interactive Analysis and Graphics of Microbiome Census Data.” *PloS One* 8, no. 4: e61217. https://doi.org/10.1371/journal.pone.0061217

Mentzer, J. L., R. M. Goodman, and T. C. Balser. 2006. “Microbial Response over Time to Hydrologic and Fertilization Treatments in a Simulated Wet Prairie.” *Plant and Soil* 284, 85-100. https://doi.org/10.1007/s11104-006-0032-1

Möhl, P., E. Hiltbrunner, and C. Körner. 2020. “Halving Sunlight Reveals No Carbon Limitation of Aboveground Biomass Production in Alpine Grassland.” *Global Change Biology* 26, no. 3: 1857-1872. https://doi.org/10.1111/gcb.14949

Moscatelli, M. C., R. Marabottini, L. Massaccesi, and S. Marinari. 2022. “Soil Properties Changes after Seven Years of Ground Mounted Photovoltaic Panels in Central Italy Coastal Area.” *Geoderma Regional* 29, e00500. https://doi.org/10.1016/j.geodrs.2022.e00500

Moore-O’Leary, K. A., R. R. Hernandez, D. S. Johnston, et al. 2017. “Sustainability of Utility-Scale Solar Energy – Critical Ecological Concepts.” *Frontiers in Ecology and the Environment* 15, no. 7: 385-394. https://doi.org/10.1002/fee.1517

National Cooperative Soil Survey. NCSS Soil Characterization Database (Lab Data Mart). Available online. Accessed June 9, 2025.

Neely, C. L., M. H. Beare, W. L. Hargrove, and D. C. Coleman. 1991. “Relationships between Fungal and Bacterial Substrate-Induced Respiration, Biomass and Plant Residue Composition.” *Soil Biology and Biochemistry* 23, no. 10: 947-954. https://doi.org/10.1016/0038-0717(91)90175-J

Nielsen, U. N., G. H. Osler, C. D. Campbell, D. F. Burslem, and R. van der Wal. 2010. “The Influence of Vegetation Type, Soil Properties and Precipitation on the Composition of Soil Mite and Microbial Communities and the Landscape Scale.” *Journal of Biogeography* 37, no. 7: 1317-1328. https://doi.org/10.1111/j.1365-2699.2010.02281.x

Nijsse, F. J. M. M., J. Mercure, N. Ameli, et al. 2023. “The Momentum of the Solar Energy Transition.” *Nature Communications* 14, 6542. https://doi.org/10.1038/s41467-023-41971-7

Nilsson, R. H., K. H. Larsson, A. F. S. Taylor, et al. 2019. “The UNITE Database for Molecular Identification of Fungi: Handling Dark Taxa and Parallel Taxonomic Classifications.” *Nucleic Acids Research* 47, no. D1: D259-264. https://doi.org/10.1093/nar/gky1022

Oksanen, J., F. G. Blanchet, R. Kindt, et al. 2013. “Package ‘Vegan’”. Community Ecology Package, Version 2, no. 9: 1-295.

Olabi, A. G., and M. A. Abdelkareem. 2022. “Renewable Energy and Climate Change.” *Renewable and Sustainable Energy Reviews* 158, 112111. https://doi.org/10.1016/j.rser.2022.112111

Osono, T., C. To-Anun, Y. Hagiwara, and D. Hirose. 2011. “Decomposition of Wood, Petiole and Leaf Litter by Xylaria Species from Northern Thailand.” *Fungal Ecology* 4, no. 3: 210-218. https://doi.org/10.1016/j.funeco.2010.11.003

Parada, A. E., D. M. Needham, and J. A. Furham. 2015. “Every Base Matters: Assessing Small Subunit rRNA Primers for Marine Microbiomes with Mock Communities, Time Series and Global Field Samples.” *Environmental Microbiology* 18, no. 5: 1403-1414. https://doi.org/10.1111/1462-2920.13023

Pascaris, A. S., C. Schelly, M. Rouleau, and J. M. Pearce. 2022. “Do Agrivoltaics Improve Public Support for Solar? A Survey on Perceptions, Preferences, and Priorities.” *Green*

Technology, Resilience, and Sustainability 2, no. 1: 8. https://doi.org/10.1007/s44173-022-00007-x

Paschalis, A., S. Bonetti, and S. Fatichi. 2025. "Controls of Ecohydrological Grassland Dynamics in Agrivoltaics Systems." *Earth's Future* 13, e2024EF005183. https://doi.org/10.1029/2024EF005183

R Core Team. 2017. R: A Language and Environment for Statistical Computing. Vienna, Austria: R Foundation for Statistical Computing. https://www.R-project.org/.

Robertson, G. P., P. Sollins, B. G. Ellis, and K. Lajtha. 1999. "Exchangeable Ions, pH, and Cation Exchange Capacity." Standard Soil Methods for Long-Term Ecological Research 2, 462.

Sala, O. E., W. J. Parton, L. A. Joyce, and W. K. Lauenroth. 1988. "Primary Production of the Central Grassland Region of the United States." *Ecology* 69, no. 1: 40-45. https://doi.org/10.2307/1943158

Scholten, L., R. G. M. de Goede, A. Edlinger, B. B. Van Aken, and G. B. De Deyn. 2025. "Sharing the Light, Impact of Solar Parks on Plant Productivity, Soil Microbes and Soil Organic Matter." *Plants, People, Planet* 2025. https://doi.org/10.1002/ppp3.70011

Soil Survey Staff, Natural Resources Conservation Service, United States Department of Agriculture. Official Soil Series Descriptions. Available Online. Accessed June 9, 2025.

Sturchio, M. A., J. E. Macknick, G. A. Barron-Gafford, et al. 2022. "Grassland Productivity Responds Unexpectedly to Dynamic Light and Soil Water Environments Induced by Photovoltaic Arrays." *Ecosphere* 13, no. 12: e4334. https://doi.org/10.1002/ecs2.4334

Sturchio, M. A., and A. K. Knapp. 2023. "Ecovoltaic Principles for a More Sustainable, Ecologically Informed Solar Energy Future." *Nature Ecology and Evolution* 7, no. 11: 1746-1749. https://doi.org/10.1038/s41559-023-02174-x

Sturchio, M. A., S. A. Kannenberg, and A. K. Knapp. 2024a. "Agrivoltaic Arrays Can Maintain Semi-Arid Grassland Productivity and Extend the Seasonality of Forage Quality." *Applied Energy* 356, 122418. https://doi.org/10.1016/j.apenergy.2023.122418

Sturchio, M. A., S. A. Kannenberg, T. A. Pinkowitz, and A. K. Knapp. 2024b. "Solar Arrays Create Novel Environments that Uniquely Alter Plant Responses." *Plants, People, Planet* 6, no. 6: 1522-1533. https://doi.org/10.1002/ppp3.10554

Sturchio, M. A., and A. K. Knapp. 2025. "Evidence of Photovoltaic Aridity Mitigation in Semi-Arid Grasslands." *Environmental Research Letters* 20, 064047. https://doi.org/10.1088/1748-9326/add94d

Tedersoo, L., M. Bahram, S. Polme, et al. 2014. "Global Diversity and Geography of Soil Fungi." *Science* 346, no 6213: 1256688. https://doi.org/10.1126/science.1256688

Vervloesem, J., E. Marcheggiani, M. A. M. Choudhury, and B. Muys. 2022. "Effects of Photovoltaic Solar Farms on Microclimate and Vegetation Diversity." *Sustainability* 14, no. 12: 7493. https://doi.org/10.3390/su14127493

Wardle, D. A., R. D. Bardgett, J. N. Klironomos, H. Setala, W. H. van der Putten, and D. H. Wall. 2004. “Ecological Linkages Between Aboveground and Belowground Biota.” *Science* 304, 1629-1633. https://doi.org/10.1126/science.1094875

Wei, C., Q. Yu, E. Bai, et al. 2013. “Nitrogen Deposition Weakens Plant-Microbe Interactions in Grassland Ecosystems.” *Global Change Biology* 19, no. 12: 3688-3697. https://doi.org/10.1111/gcb.12348

Xun, W., T. Huang, J. Zhao, et al. 2015. “Environmental Conditions rather than Microbial Inoculum Composition Determine the Bacterial Composition, Microbial Biomass and Enzymatic Activity of Reconstructed Soi Microbial Activities.” *Soil Biology and Biochemistry* 90, 10-18. https://doi.org/10.1016/j.soilbio.2015.07.018

CHAPTER 5: CONCLUSIONS

Climate change has already compromised ecosystem stability globally, with ecological impacts projected to intensify with continued atmospheric warming (IPCC 2023, Swain et al. 2025). Increasingly frequent and severe hydroclimatic extremes, such as droughts and deluges, are anticipated to be a key manifestation of climate change (Fischer & Knutti 2016, Chen et al. 2025). Concerningly, our understanding of the ecological consequences of shifting precipitation regimes is severely lacking, inhibiting our ability to understand and predict future ecosystem trajectories. Simultaneously, efforts to limit atmospheric warming and sustain a growing population entail substantial land use changes, such as solar energy development, which further alter plant-soil-microbial interactions and emergent ecosystem functionality (Armstrong et al. 2014). Hence, there is a clear imperative to understand how ecosystems may respond to shifting precipitation regimes and land use change. In this dissertation I addressed questions related to the legacy effects of extreme drought on soil microbiomes, the contemporaneous impacts of extreme drought and deluge on grassland functionality, and the consequences of solar energy development for plant-soil-microbial interactions.

5.1 Research Summary

My findings suggest that extreme drought, deluges, and solar energy development have vast, often unexpected, impacts on grassland ecosystems. My first study (Chapter 2) showed that extreme drought results in legacy effects of altered rhizosphere soil microbial community structure across disparate grassland types. Legacies were present when chronic (extended) drought was imposed, though not following intense (acute) drought. Further, no legacies were evident in the bulk soil. Any evidence of soil microbial drought legacies was largely unexpected

given the rapid turnover time and relatively high frequency of water limitation in the grassland systems. Indeed, finding legacy effects solely in rhizosphere communities that experienced chronic drought stress indicates the importance of considering drought severity and soil niche when investigating the consequences on plant-soil-microbial interactions. There are likely underlying mechanisms of drought-induced shifts in plant functionality, such as root architectural shifts and hydraulic changes, that may alter their interactions with rhizosphere organisms long after the drought ends (de Vries et al. 2023).

The potential for extreme precipitation events (or "deluges") to accelerate ecosystem recovery from drought is critically underexplored. In my second study (Chapter 3), I found that a deluge event could not 'rescue' a semi-arid grassland from extreme, multi-year drought. Instead, compound drought and deluge stimulated carbon losses from the ecosystem and did not prompt recovery of plant productivity (ANPP). Contrary to a previous study, where a deluge event partially rescued ANPP from drought within a single growing season (Hoover et al. 2022), it is likely that the second year of extreme drought severely depleted the dominant plant species' non-structural carbohydrates and meristematic density, inhibiting the ability for plant communities to capitalize on the deluge event. Given the likelihood of increasingly frequent and severe precipitation anomalies, the interaction between different drought severities and unique deluge timing/intensity must be further explored.

Another predominant driver of altered precipitation regimes is land use change, particularly solar energy development. The expansion of photovoltaic (PV) arrays is occurring rapidly, and little is known about how these immense arrays impact their host ecosystems (Sturchio & Knapp 2023). My final study (Chapter 4) investigated the effects of PV-induced heterogeneity in abiotic factors (i.e., precipitation, light) on plant-soil-microbial interactions. I

found that the unique microclimates created by PV panels shift soil moisture and ANPP, which in turn influence microbial community structure and function. For instance, under the east edge of panels, where ANPP is the highest and soil moisture is elevated, relatively high soil organic matter and a unique suite of microbial taxa drove increased decomposition rates. Thus, PV arrays introduce environmental heterogeneity that will impact ecosystem structure and function across trophic levels. The ecological impacts of PV arrays must be thoroughly investigated across ecosystem types, plant communities, construction approaches and management strategies as this energy source is rapidly deployed around the world.

5.2 Implications and Future Directions

My dissertation work explored a range of grassland responses to global change drivers. As precipitation regimes becomes increasingly volatile under climate change, studies must shed light on the contemporaneous and lasting impacts of precipitation extremes. Though I found drought legacy effects on soil microbial community structure, future work must investigate legacy effects on soil functionality and ecosystem processes across scales (Canarini et al. 2021, Müller and Bahn 2022, Oram et al. 2025). Both experimental and theoretical approaches must be employed to disentangle the processes that lead to, and do not lead to, drought legacy effects. For instance, greenhouse studies may be leveraged to carefully manipulate the extent of water limitation, plant community composition, microbial community composition, and soil properties, along with myriad other factors (e.g., microbial drought history; see de Vries et al. 2023) that may determine how plant-soil-microbial interactions respond to drought and persist post-drought. Mechanistic understanding from greenhouse studies must be paired with field studies that employ spatiotemporally rigorous investigations of legacy effects under unique drought severities and ecosystem types. Such studies will deepen our understanding of recovery

trajectories versus truly persistent drought legacy effects. As individual studies accumulate, syntheses must attempt to link pattern to process and inform when and where to anticipate drought legacy effects, along with the implications for future ecosystem functionality (e.g., Evans et al. 2022). Given our findings, I suggest that forthcoming studies should leverage multiple experimental sites with contrasting climate regimes to tease apart the influence of precipitation patterns, drought history, plant communities, and other underexplored factors, including drought-induced shifts in soil structure (e.g., Thotakuri et al. 2025).

Similarly, drought and deluge events are likely to jointly impact ecosystems with varying degrees of water limitation, plant communities, soil types, and myriad other factors that demand further exploration. Field studies, remote sensing, and modeling efforts would be especially impactful in determining ecological responses to compound hydroclimatic extremes (Swain et al. 2025). Field studies, like Chapter 3, allow researchers to measure responses that are difficult to accurately derive from satellite products or model outputs. For instance, the photosynthetic responses that occurred following the deluge did not translate to increased productivity, which could drive substantial disagreement between measured and modeled responses. Incorporation of remote sensing products that rely on Solar-Induced Fluorescence (SIF) rather than traditional measures of vegetation greenness, like Normalized Difference Vegetation Index (NDVI) may help to limit this disagreement (Magney et al. 2019), but ground-based measurements are still a necessity. Further, these studies should prioritize ecosystems where models tend to converge on enhanced likelihood of increased precipitation intensity, such as high-latitude regions and monsoonal regions (Pfahl et al. 2017, IPCC 2023), to aid in accurately parameterizing Earth system models.

Meanwhile, simultaneous changes in energy production introduce further uncertainty regarding sustained ecosystem functionality. Global change drivers are often as varied as the ecosystems they impact; for instance, PV arrays can have as many unique designs as developers can imagine. Hence, the context dependency is a challenge that we must see as an opportunity. Connecting with PV energy developers to inform array construction and experimentally investigate the ecological impacts of different array designs will be necessary to overcome such context dependency (Sturchio & Knapp 2023). Further, arrays are being built upon understudied ecosystems globally, providing an unprecedented opportunity to investigate the abiotic controls over ecological community structure, biogeochemical cycling, and other ecosystem properties and functions. We must leverage this rapid expansion of renewable energy to address both applied ecological questions – such as how solar panel spacing impacts rangeland productivity and forage quality – and fundamental theoretical questions, such as how do PV-induced alterations in light availability impact plant photosynthesis and subsequently modify root exudate composition and concentration. Moreover, how PV arrays may mitigate (or exacerbate) the ecological consequences of precipitation extremes is virtually unexplored (Knapp and Sturchio 2024). In many ways, this technology may be a particularly effective tool in mitigating the detrimental impacts of climate change.

A predictive understanding of global change requires a shift in focus from investigating isolated, short-term drivers to the interactive effects of multiple stressors, especially across longer time scales and unique ecosystems. Field studies will always remain an indispensable component of ecological research, and we must be willing to expand our research approaches to meet the needs of a rapidly changing world.

LITERATURE CITED

Armstrong, A., S. Waldron, J. Whitaker, and N. J. Ostle. 2014. "Wind Farm and Solar Park Effects on Plant-Soil Carbon Cycling: Uncertain Impacts of Changes in Ground-Level Microclimate." *Global Change Biology* 20, no. 6: 1699-1706. https://doi.org/10.1111/gcb.12437.

Canarini, A., H. Schmidt, L. Fuchslueger, V. Martin, C. W. Herbold, D. Zezula, ... and A. Richter. 2021. "Ecological Memory of Recurrent Drought Modifies Soil Processes via Changes in Soil Microbial Community." *Nature Communications* 12, no. 1: 5308. https://doi.org/10.1038/s41467-021-25675-4.

Chen, L., P. Brun, P. Buri, S. Fatishi, A. Gessler, M. J. McCarthy, ... and D. N. Karger. 2025. "Global Increase in the Occurrence and Impact of Multiyear Droughts." *Science* 387: 278–284. https://doi.org/10.1126/science.adr2589.

De Vries, F., J. Lau, C. Hawkes, and M. Semchenko. 2023. "Plant–Soil Feedback Under Drought: Does History Shape the Future?" *Trends in Ecology & Evolution* 38, no. 8: 708–718. https://doi.org/10.1016/j.tree.2023.02.004.

Evans, S. E., S. D. Allison, and C. V. Hawkes. 2022. "Microbes, Memory and Moisture: Predicting Microbial Moisture Responses and Their Impact on Carbon Cycling." *Functional Ecology* 36, no. 6: 1430–1441. https://doi.org/10.1111/1365-2435.14041.

Fischer, E. M., and R. Knutti. 2016. "Observed Heavy Precipitation Increase Confirms Theory and Early Models." *Nature Climate Change 6*: 986–991. https://doi.org/10.1038/nclimate3110.

Hoover, D. L., O. L. Hajek, M. D. Smith, K. Wilkins, I. J. Slette, and A. K. Knapp. 2022. "Compound Hydroclimatic Extremes in a Semi-Arid Grassland: Drought, Deluge, and the Carbon Cycle." *Global Change Biology* 28: 2611–2621. https://doi.org/10.1111/gcb.16081.

IPCC. 2023. "Summary for Policymakers." In: *Climate Change 2023: Synthesis Report. Contribution of Working Groups I, II and III to the Sixth Assessment Report of the Intergovernmental Panel on Climate Change* [Core Writing Team, H. Lee and J. Romero (eds.)]. IPCC, Geneva, Switzerland: 1–34. https://doi.org/10.59327/IPCC/AR6-9789291691647.001.

Knapp, A. K., and M. A. Sturchio. 2024. "Ecovoltaics in an increasingly water-limited world: An ecological perspective." *One Earth* 7, no. 10: 1705-1712. https://doi.org/10.1016/j.oneear.2024.09.003.

Magney, T. S., Bowling, D. R., Logan, B. A., Grossmann, K., Stutz, J., Blanken, P. D., Burns, S. P., Cheng, R., Garcia, M. A., Kohler, P., and S. Lopez. 2019. "Mechanistic Evidence for

Tracking the Seasonality of Photosynthesis with Solar-Induced Fluorescence." *Proceedings of the National Academy of Sciences* 116, no. 24: 11640-11645. https://doi.org/10.1073/pnas.1900278116.

Müller, L. M., and M. Bahn. 2022. "Drought Legacies and Ecosystem Responses to Subsequent Drought." *Global Change Biology* 28, no. 17: 5086–5103. https://doi.org/10.1111/gcb.16270.

Oram, N. J., N. Praeg, R. D. Bardgett, F. Brennan, T. Caruso, P. Illmer, ... and F. T. de Vries. 2025. "Drought Intensity Shapes Soil Legacy Effects on Grassland Plant and Soil Microbial Communities and Their Responses to Future Drought." *Global Change Biology* 31, no. 9: e70495. https://doi.org/10.1111/gcb.70495.

Pfahl, S., O'Gorman, P. A., and E. M. Fischer. 2017. "Understanding the Regional Pattern of Projected Future Changes in Extreme Precipitation." *Nature Climate Change* 7, no. 6: 423-427. https://doi.org/10.1038/nclimate3287.

Sturchio, M. A., and A. K. Knapp. 2023. "Ecovoltaic Principles for a More Sustainable, Ecologically Informed Solar Energy Future." *Nature Ecology and Evolution* 7, no. 11: 1746-1749. https://doi.org/10.1038/s41559-023-02174-x.

Swain, D. L., A. F. Prein, J. T. Abatzoglou, C. M. Albano, M. Brunner, N. S. Diffenbaugh, et al. 2025. "Hydroclimate Volatility on a Warming Earth." *Nature Reviews Earth & Environment* 6: 35–50. https://doi.org/10.1038/s43017-024-00624-z.

Thotakuri, G., M. Dor, M. Smith, A. Guber, and A. Kravchenko. 2025. "Soil Pore-Size Distributions and Selected Biochemical Properties in Short-Grass Steppe Under Long-Term Drought." *Journal of Environmental Management 391*: 126557. https://doi.org/10.1016/j.jenvman.2024.126557.

APPENDIX 1

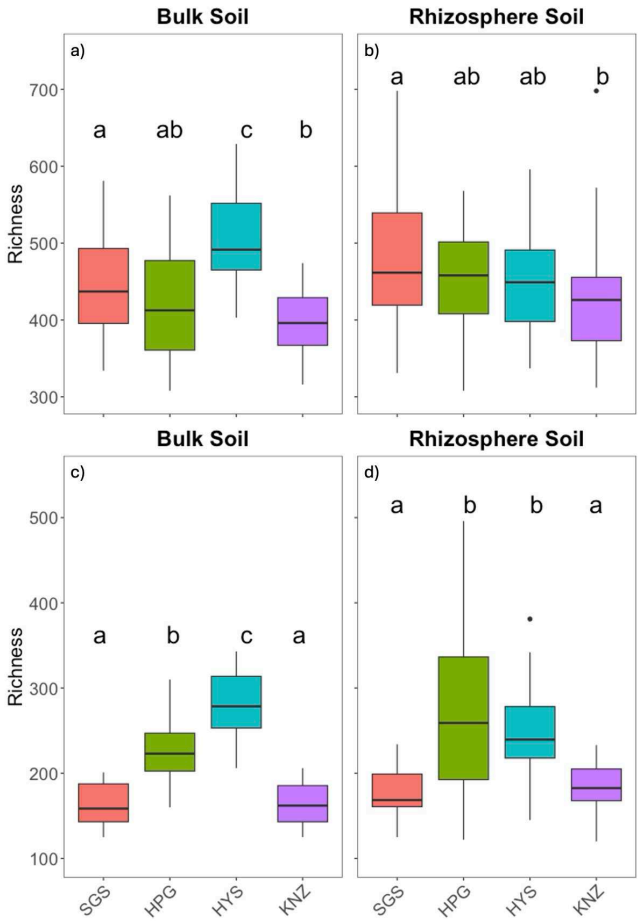

Figure A1.1: a) Prokaryotic bulk soil and b) rhizosphere soil richness by site. c) Fungal bulk soil and d) rhizosphere soil richness by site. Significant differences are indicated by letters above each box.

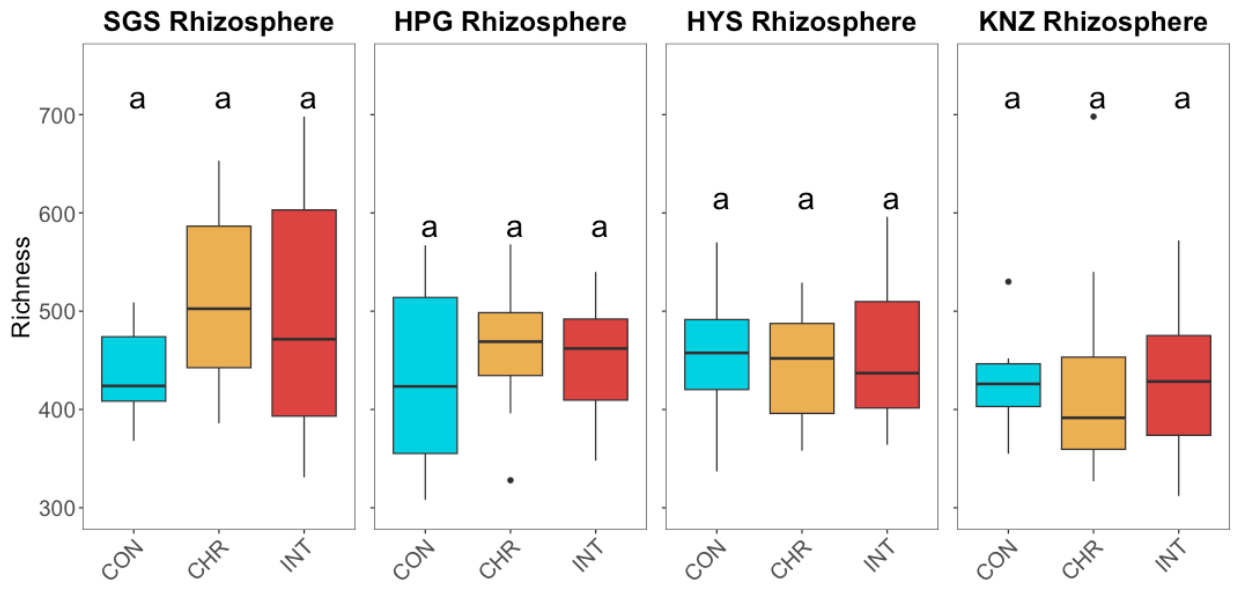

Figure A1.2: Prokaryotic rhizosphere soil richness by treatment. There are no significant differences across treatments at any site.

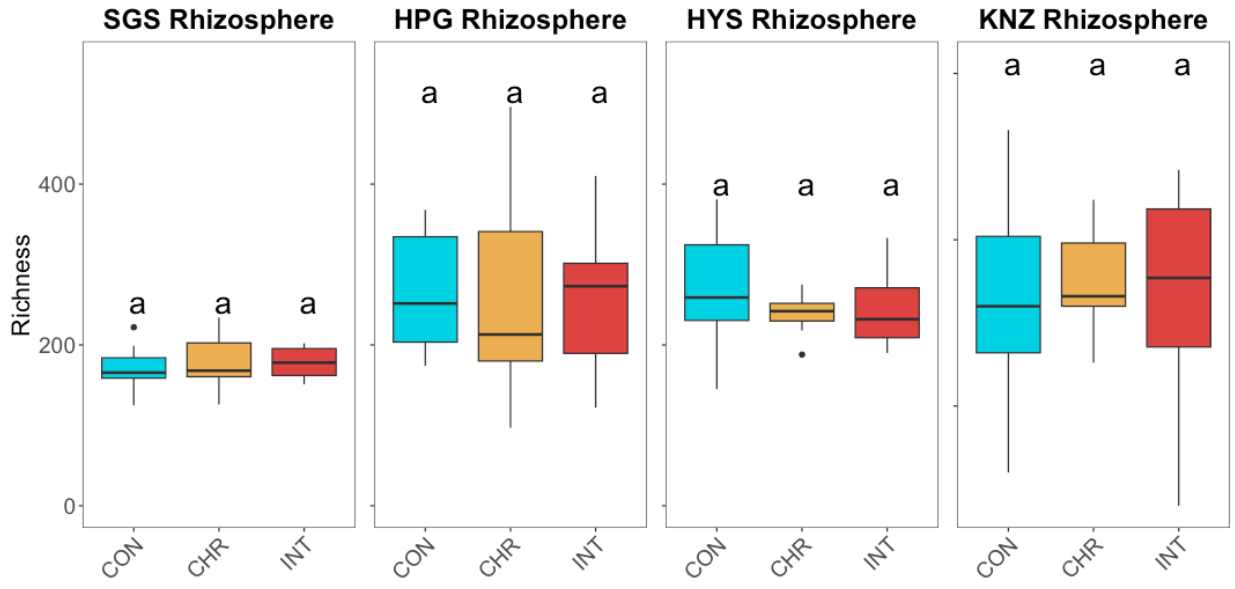

Figure A1.3: Fungal rhizosphere soil richness by treatment. There are no significant differences across treatments at any site.

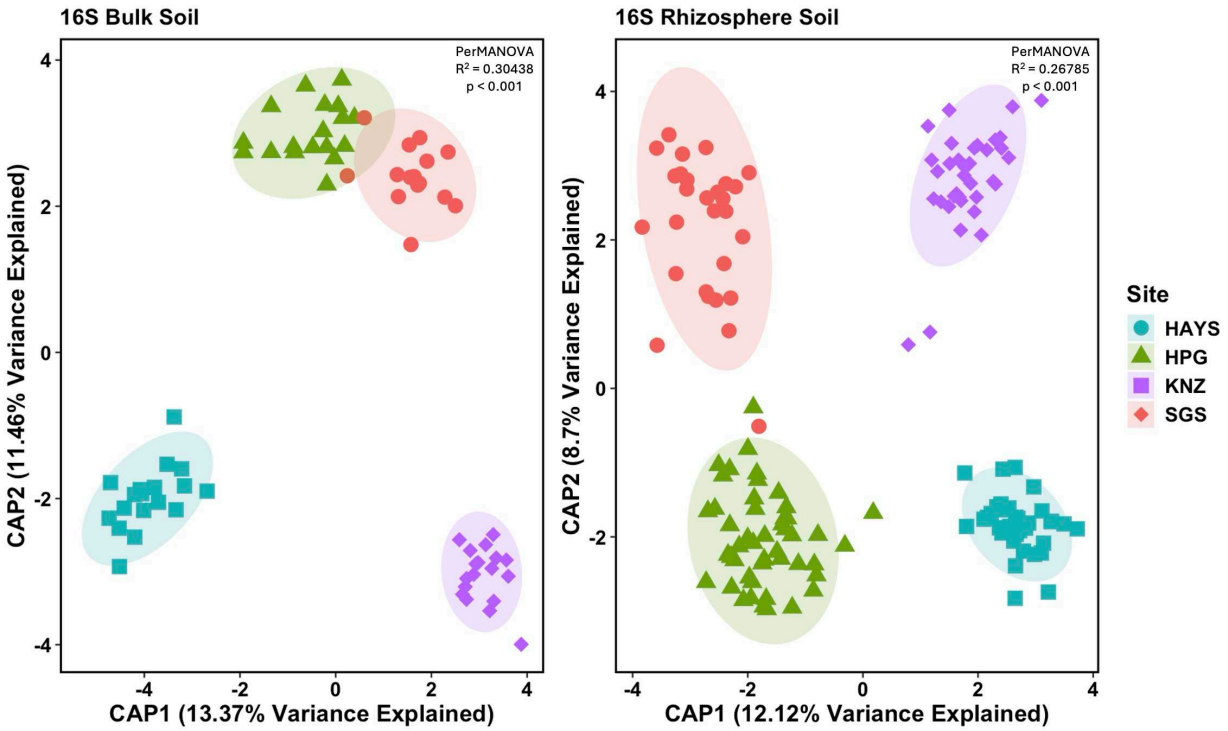

Figure A1.4: Constrained analysis of principal coordinates (CAPs) ordinations demonstrating the impact of site on bulk soil prokaryotic (left) and rhizosphere soil prokaryotic (right) communities. Permutational multivariate analysis of variance (PERMANOVA) model results are shown in upper corner of each panel. CAPs were conducted following detection of the significant site-level treatment effects via PERMANOVA ($p<0.05$).

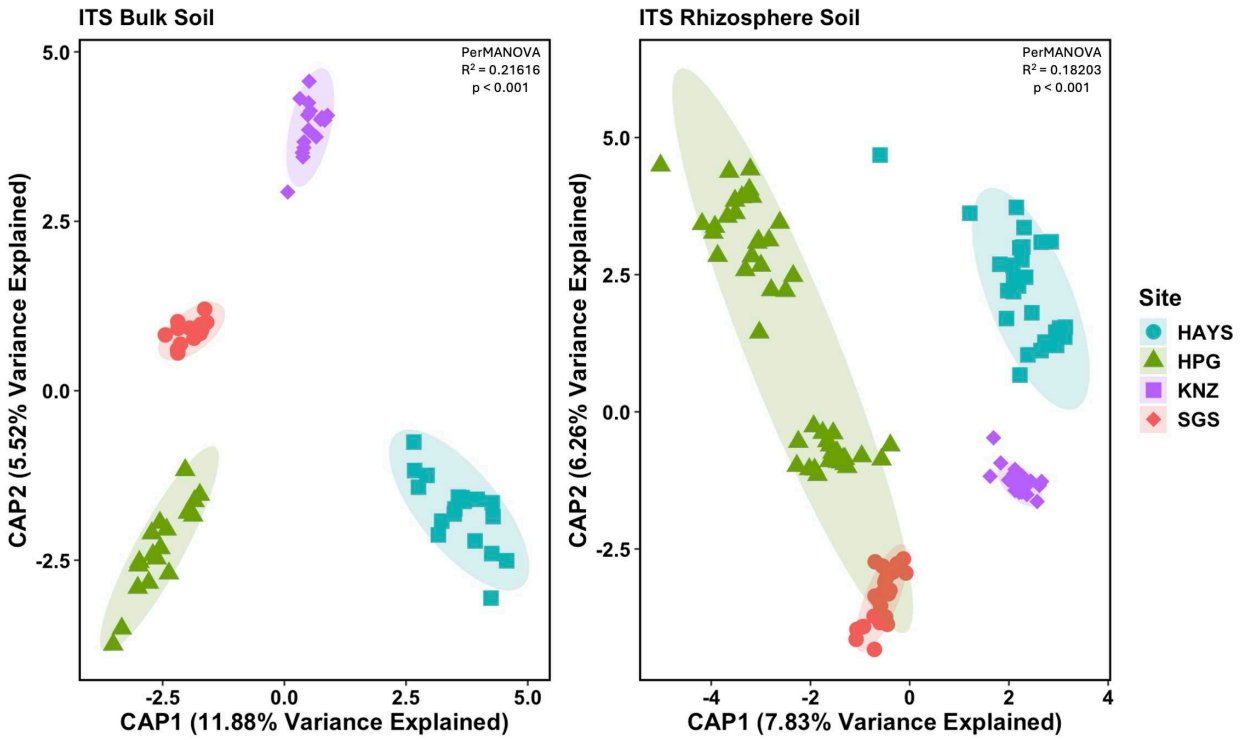

Figure A1.5: Constrained analysis of principal coordinates (CAPs) ordinations demonstrating the impact of site on bulk soil fungal (left) and rhizosphere soil fungal (right) communities. Permutational multivariate analysis of variance (PERMANOVA) model results are shown in upper corner of each panel. CAPs were conducted following detection of the significant site-level treatment effects via PERMANOVA ($p<0.05$).

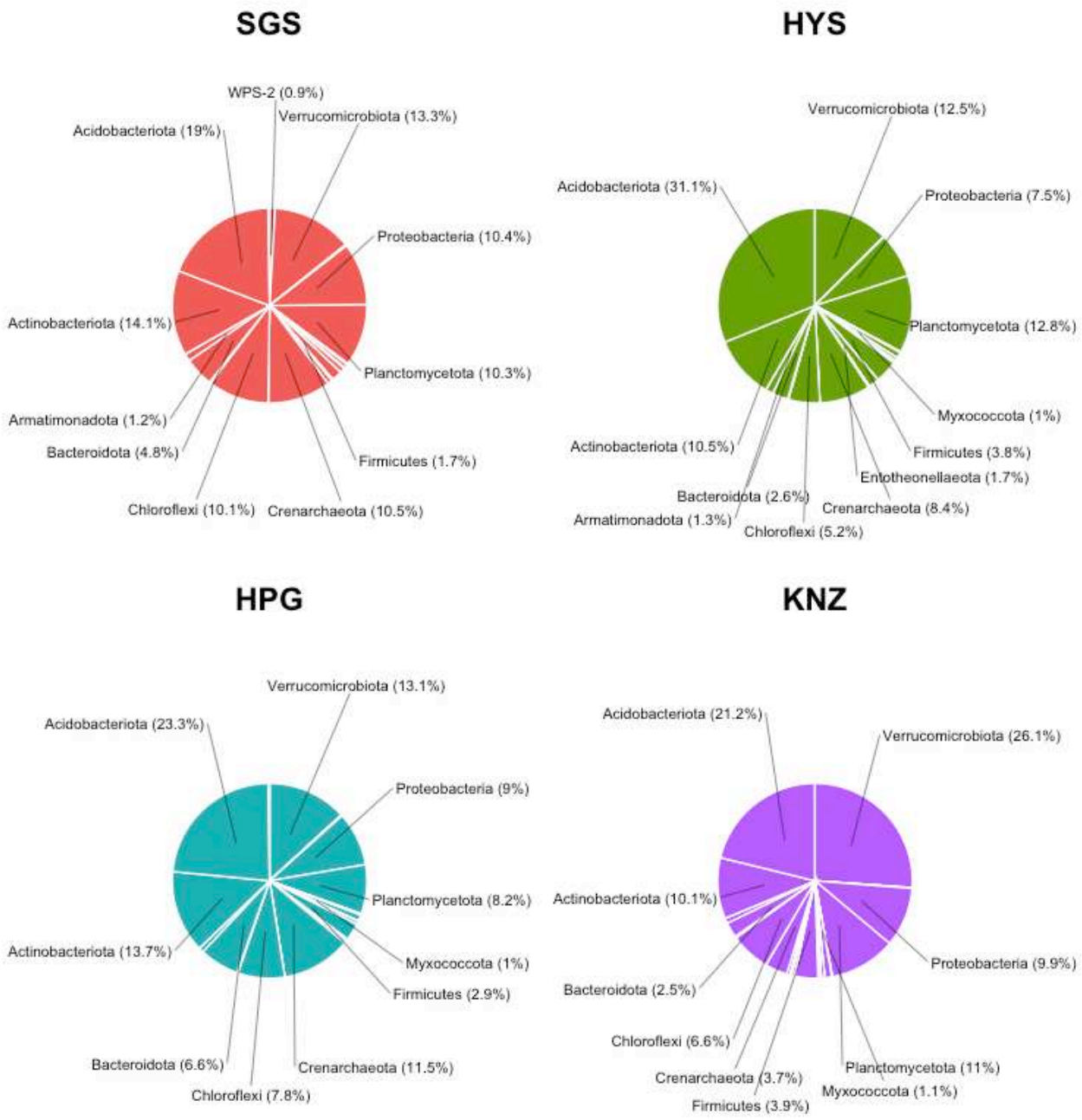

Figure A1.6: Relative abundance of prokaryotic phyla averaged across all samples at the site level. Only phyla with relative abundance > 0.9% are labeled.

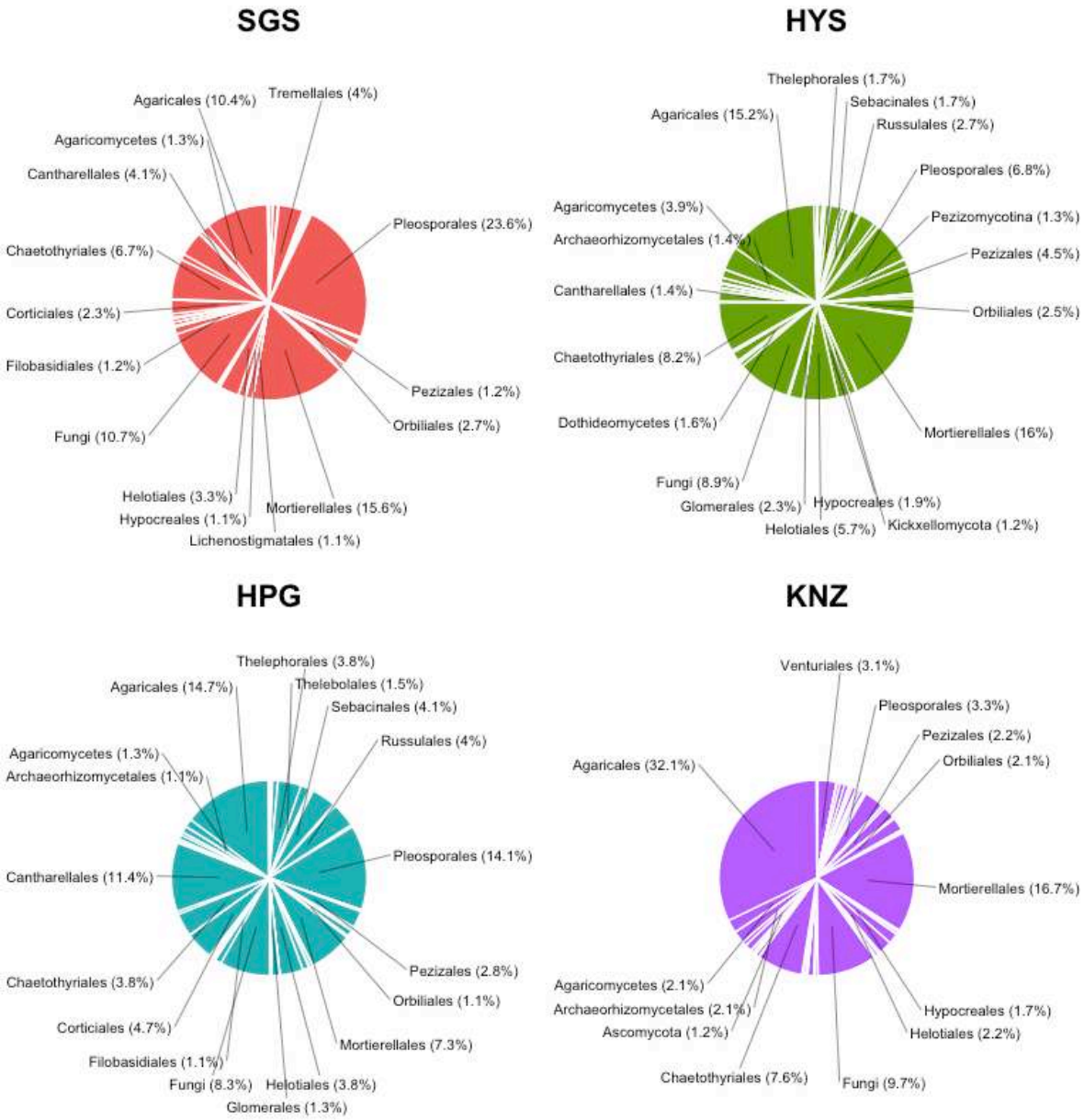

Figure A1.7: Relative abundance of fungal orders averaged across all samples at the site level. Only orders with relative abundance > 0.9% are labeled.

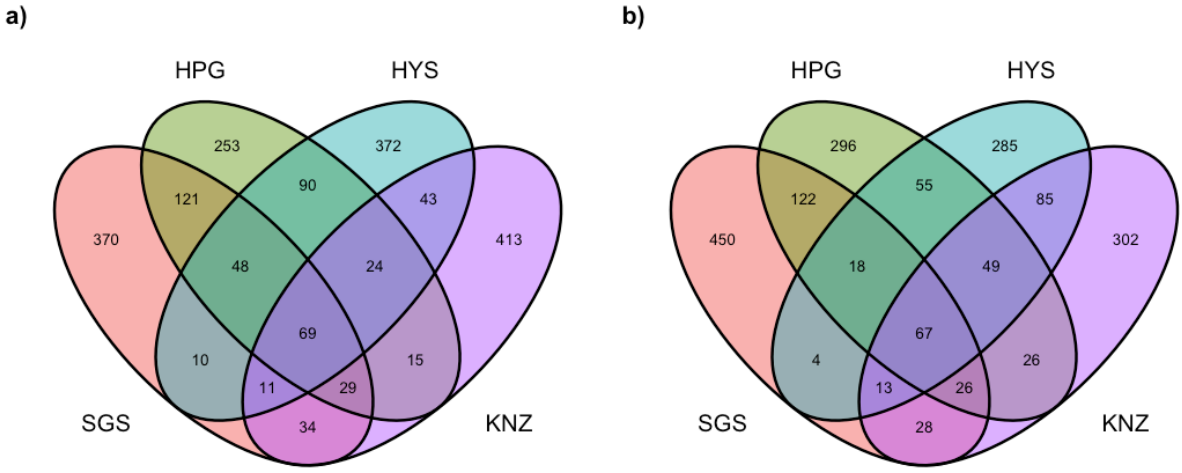

Figure A1.8: a) Shared bulk soil prokaryotic taxa across sites, regardless of treatment, and b) Shared rhizosphere soil prokaryotic taxa across sites, regardless of treatment. Comparisons are made at the ASV level.

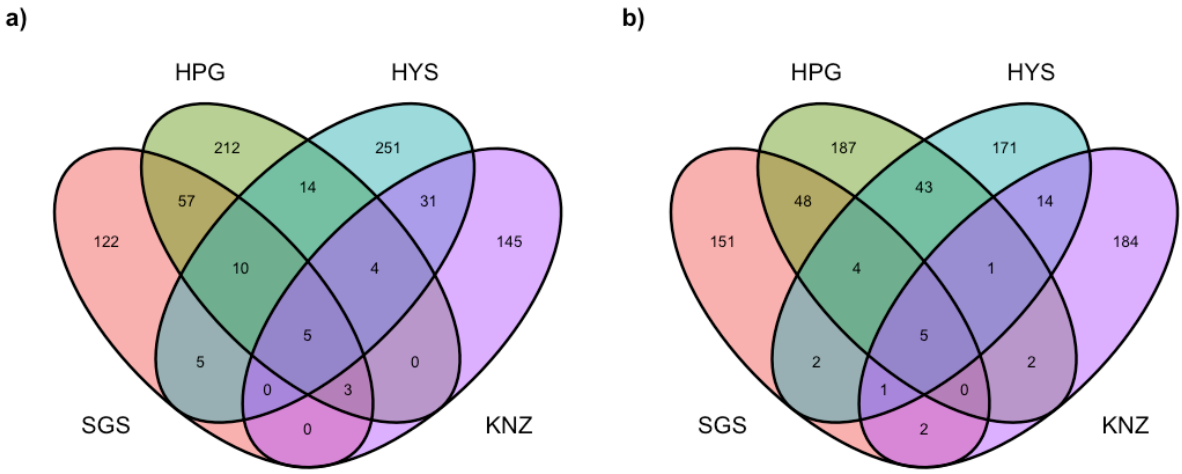

Figure A1.9: a) Shared bulk soil fungal taxa across sites, regardless of treatment, and b) Shared rhizosphere soil fungal taxa across sites, regardless of treatment. Comparisons are made at the ASV level.

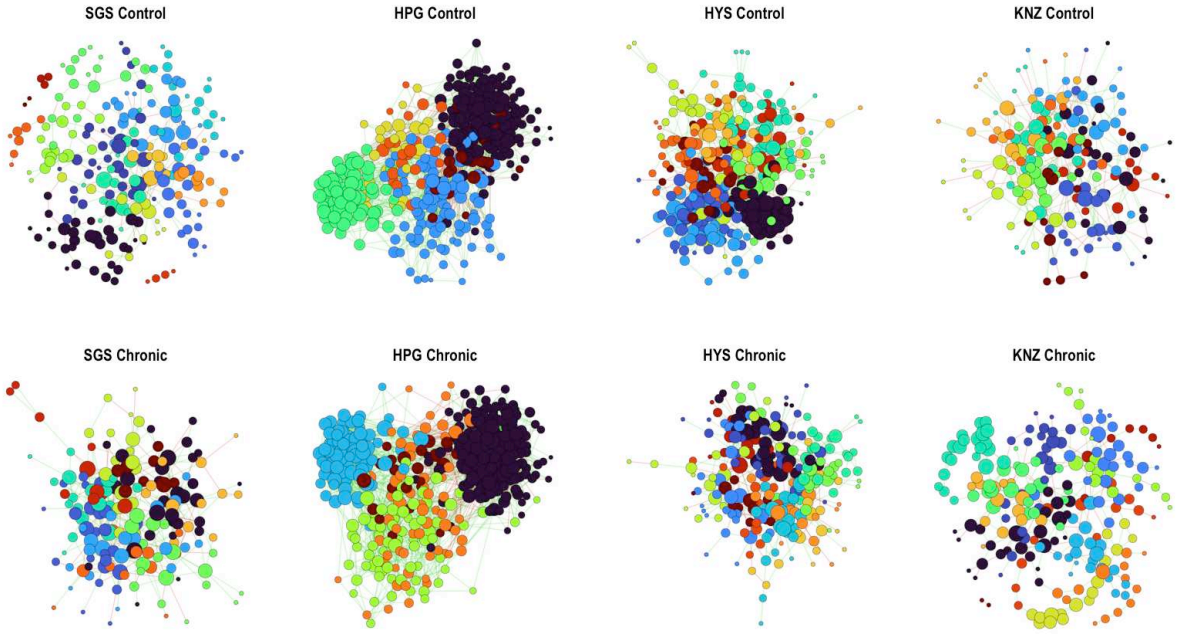

Figure A1.10: Soil rhizosphere prokaryotic co-occurrence networks for Control (CON) and Chronic drought (CHR) treatments at each study site. Individual nodes (circles) represent prokaryotic ASVs. Edges (lines) indicate positive (green) or negative (red) associations among ASVs. Node colors indicate distinct modules, representing clusters of tightly associated nodes.

Table A1.1: The influence of site, treatment, and their interactions on changes in prokaryotic and fungal richness based on linear mixed model.

		Prokaryotes		**Fungi**	
Niche	**Driver**	F-value	*p*	F-value	*p*
Bulk	Site	10.3726	0.0001	35.2954	0.0001
	Treatment	1.1415	0.3265	0.1083	0.8975
	Site:Treatment	0.7809	0.5883	0.2449	0.9593
Rhizosphere	Site	2.5164	0.0610	16.5745	0.0001
	Treatment	1.3909	0.2525	0.1531	0.8582
	Site:Treatment	0.6322	0.7042	0.1773	0.9826

Table A1.2: The influence of site, treatment, and their interactions on changes in prokaryotic and fungal Shannon diversity based on linear mixed model.

		Prokaryotes		**Fungi**	
Niche	**Driver**	F-value	*p*	F-value	*p*
Bulk	Site	24.8654	0.0001	40.8141	0.0001
	Treatment	1.0657	0.3513	0.8755	0.4225
	Site:Treatment	0.5719	0.7510	1.4405	0.2165
Rhizosphere	Site	1.6414	0.1829	4.1659	0.004
	Treatment	0.7707	0.4948	0.8137	0.446
	Site:Treatment	0.5866	0.7405	1.1193	0.355

Table A1.3: Beta-dispersion (BetaDisper) test results of treatment effects on rhizosphere microbial communities. Beta-dispersion testing was conducted on Aitchison distance matrices by treatment at the site level. Significant *p*-values indicate overdispersion of one treatment relative to others.

Site	**Prokaryotes**	**Fungi**
SGS	*p = 0.502*	*p* = 0.642
HPG	*p* = 0.059	*p* = 0.367
HYS	*p* = 0.091	*p = 0.251*
KNZ	*p* = 0.911	*p* = 0.999

APPENDIX 2

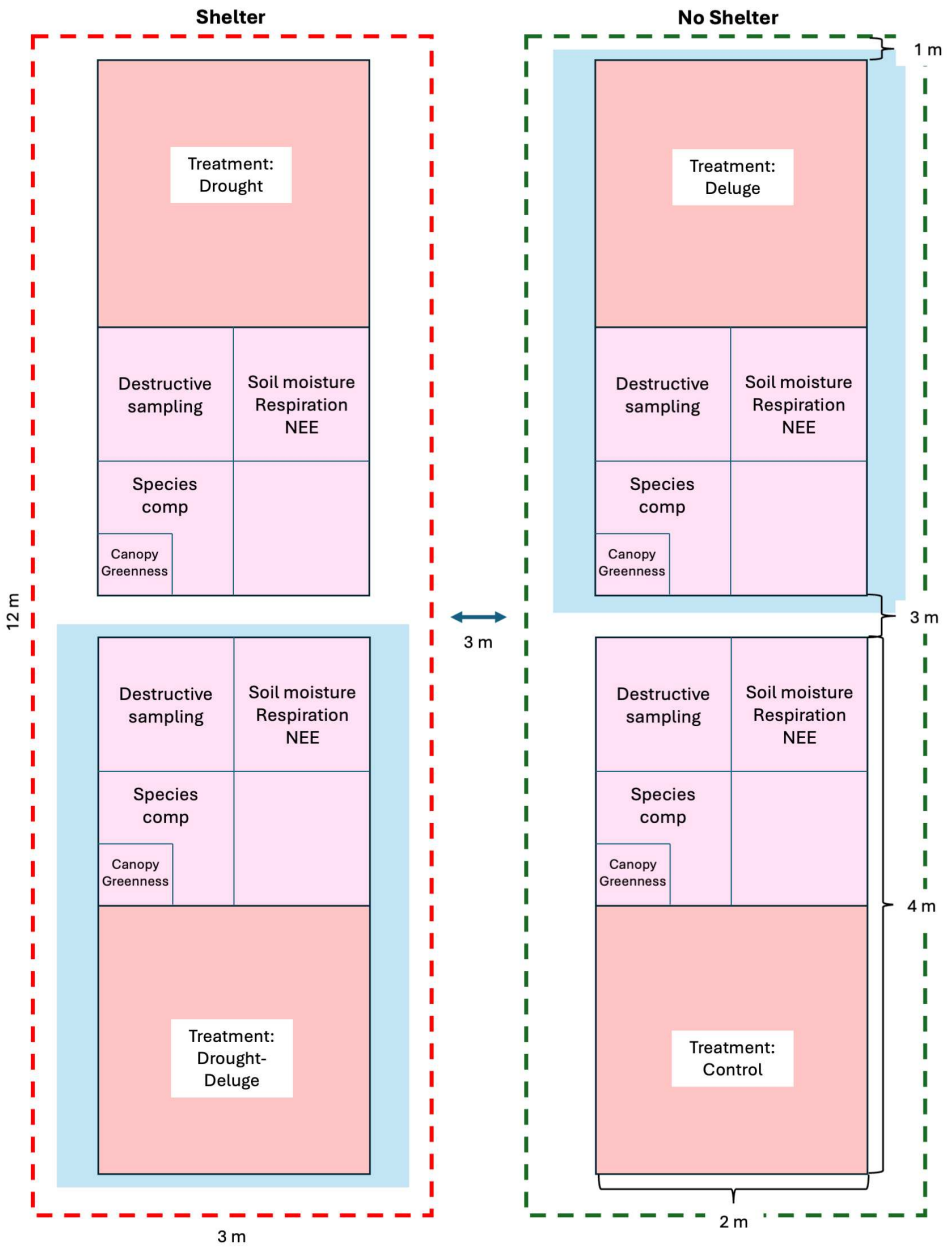

Figure A2.1: Conceptual diagram of an experimental block. Each block consists of two plots that were randomly assigned to receive a drought (Shelter) or no drought (No Shelter). Within each plot, a subplot was randomly assigned to receive the deluge event or not, resulting in four subplots that correspond with a unique treatment (Control, Drought, Deluge, Drought-Deluge). Each subplot was 2 x 4 m, with a 2 x 2 m sampling area (*light pink*) that was composed of four unique 1 x 1 m subplots, designated for 1) non-destructive sampling (species comp (not shown) and canopy greenness), 2) NEE, soil respiration, and soil moisture measurements, 3) destructive sampling, and 4) an extra destructive sampling area. Ten blocks were designated in replicate across the experimental pasture.

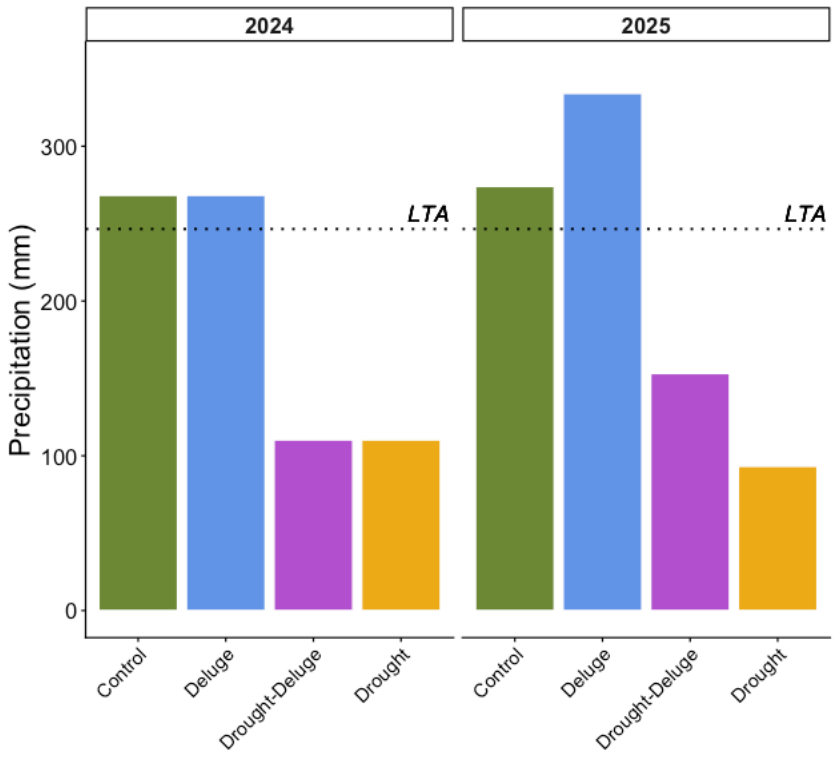

Figure A2.2: Growing season (April 15-September 30) precipitation totals for 2024 and 2025. Totals in 2024 account for manual water additions, and totals in 2025 account for the deluge addition. The dotted horizontal line corresponds to the long-term average precipitation at this field site (246.5 mm, 1990-2021).

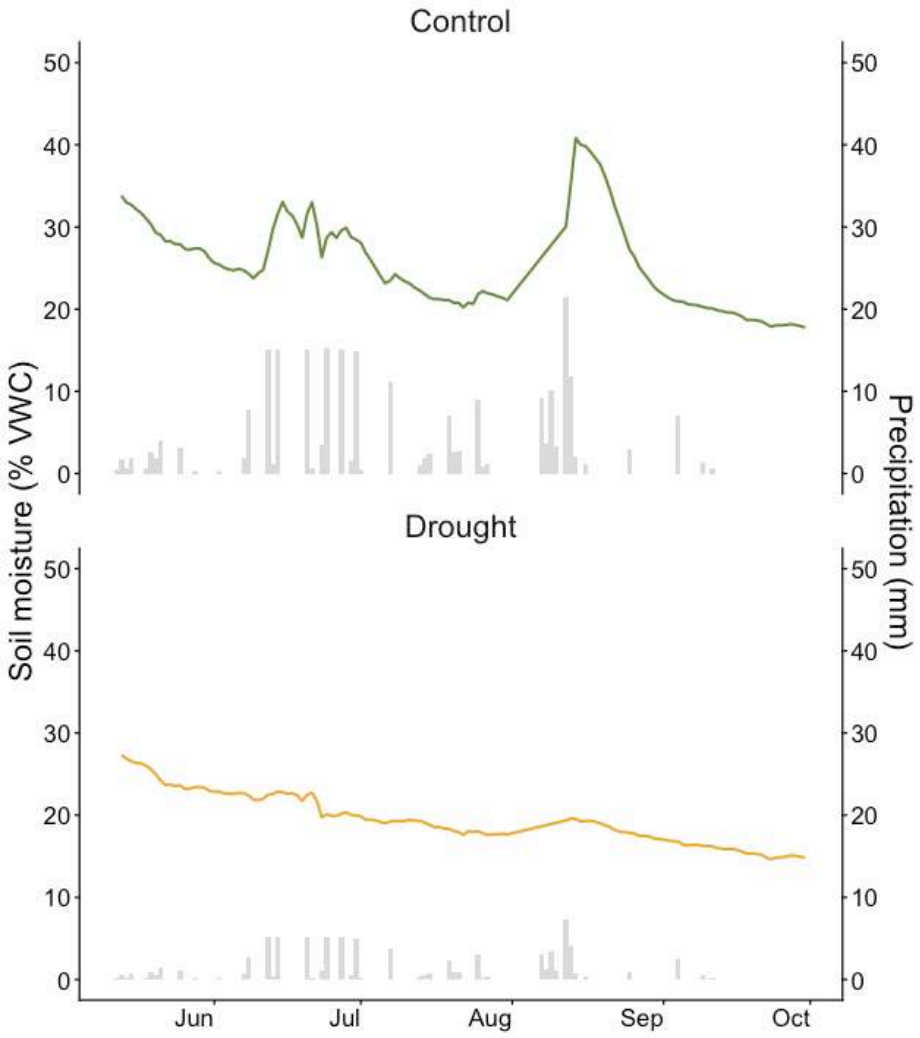

Figure A2.3: Soil moisture and precipitation inputs during the first growing season (May 13-September 30). Soil moisture sensors were not fully installed until May 13, shortening the timeframe relative to the second growing season. VWC = volumetric water content.

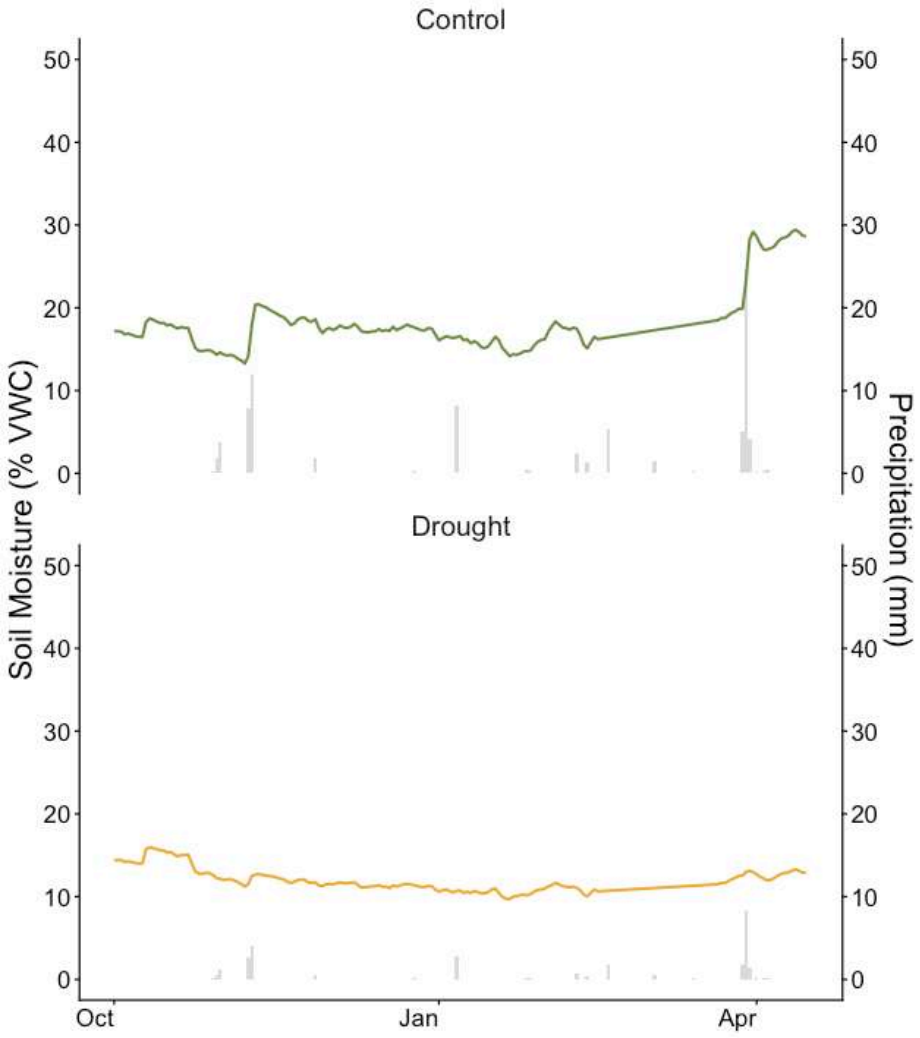

Figure A2.4: Soil moisture and precipitation inputs between the first and second growing seasons (September 30-April 15). VWC = volumetric water content.

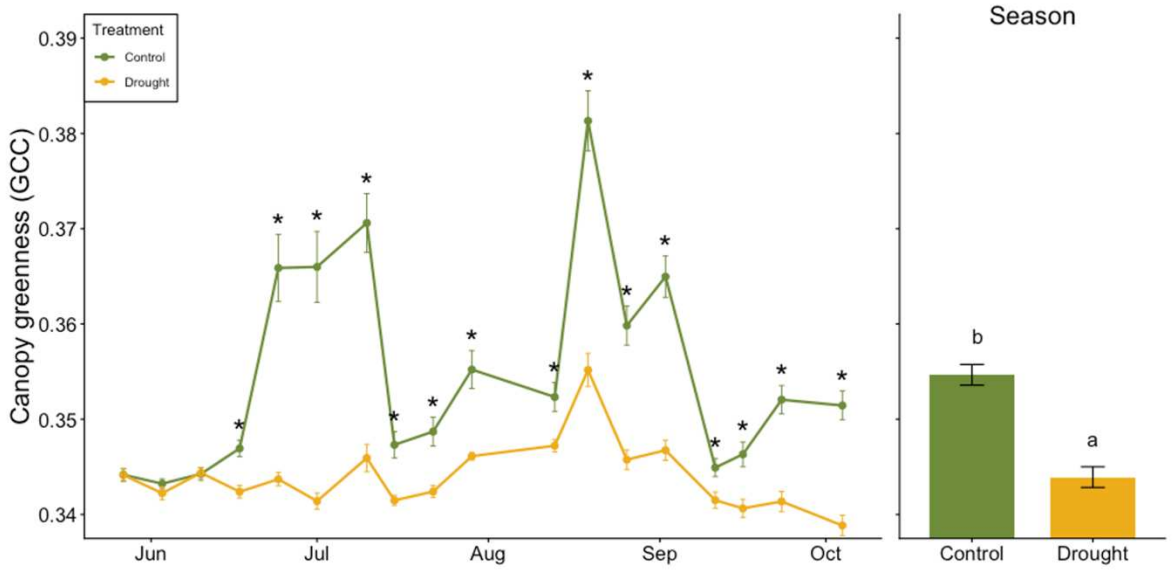

Figure A2.5: Canopy greenness, as measured with green chromatic coordinate index (GCC), during the first growing season. Left) Patterns of greenness through time. Right) Average greenness for each treatment. Error bars indicate ± 1 SE, and asterisks/letters indicate significant ($p < 0.05$) treatment differences.

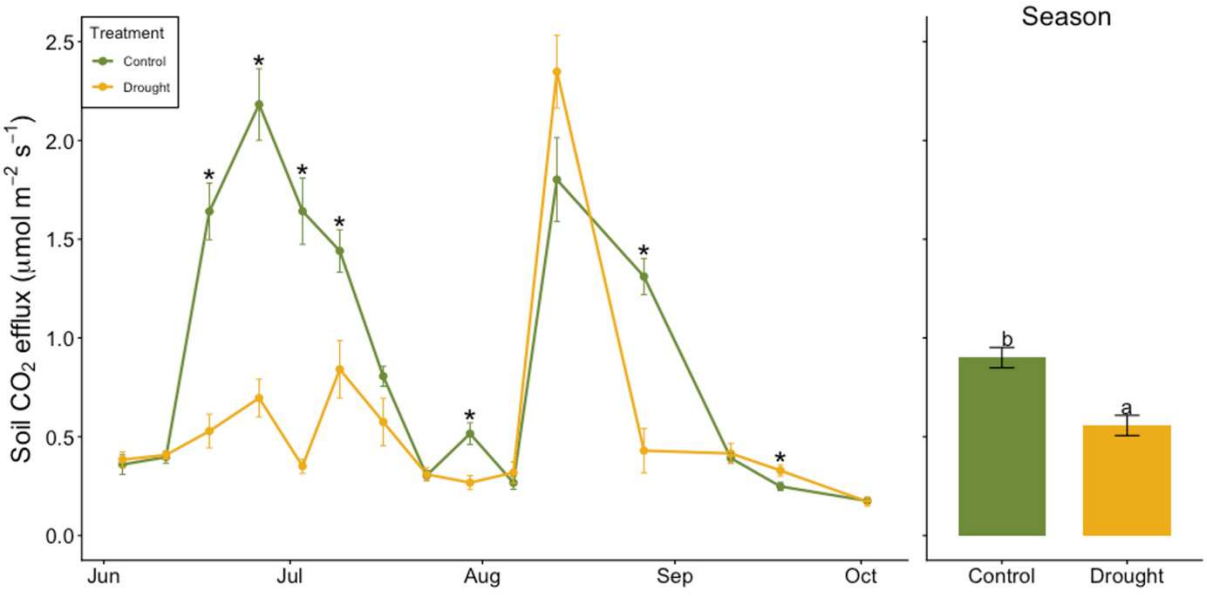

Figure A2.6: Left) Effects of drought treatment on soil respiration (soil CO_2 efflux) patterns during the first growing season. Right) Average soil respiration for each treatment. Error bars indicate ± 1 SE, and asterisks/letters indicate significant ($p < 0.05$) treatment differences.

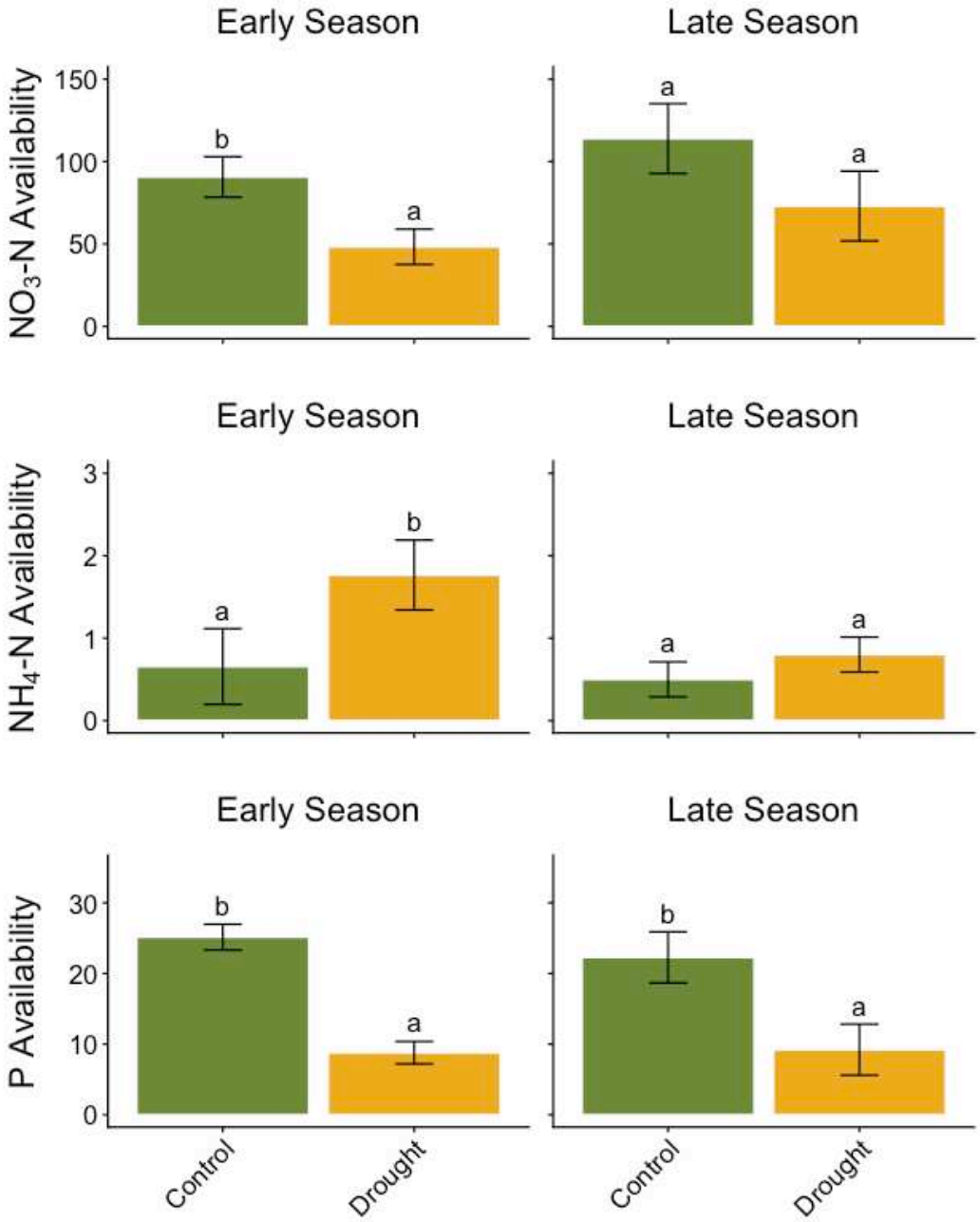

Figure A2.7: Soil nutrient availability for each treatment measured by plant root simulator probes (see Methods) during the first growing season. Probes were buried during the early (June 4-July 4) and late (July 26-August 27) growing season periods to capture seasonal trends in nutrient availability. Nutrients are measured in units of (μg/10cm^2/burial length). Error bars indicate ± 1 SE, and letters indicate significant ($p < 0.05$) treatment differences.

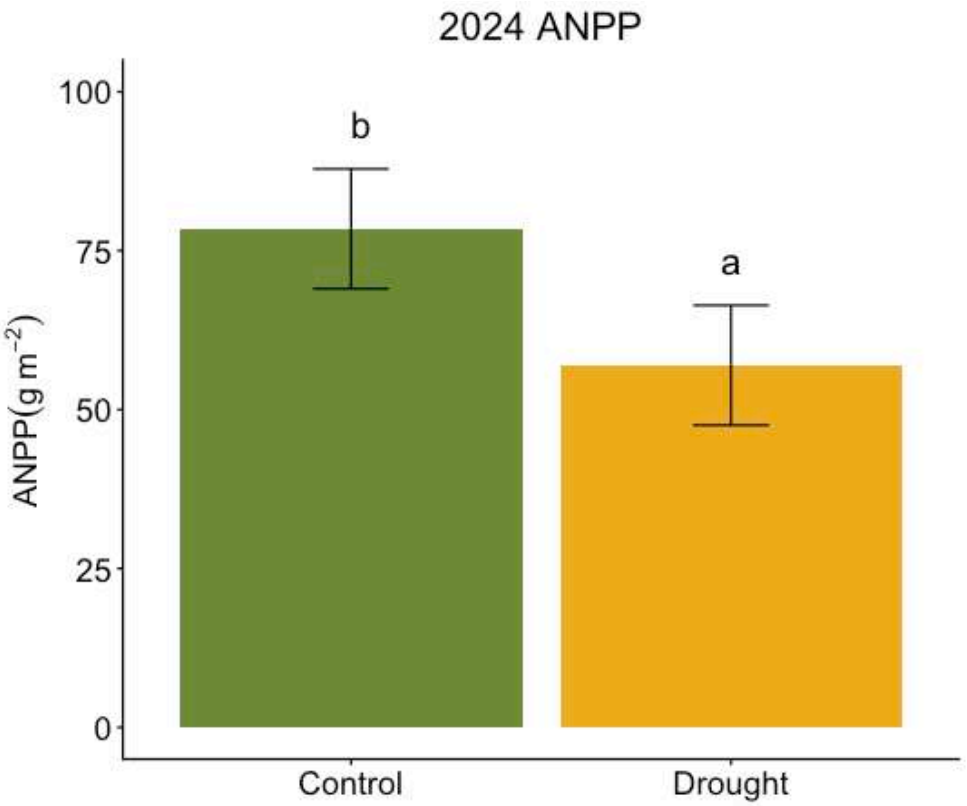

Figure A2.8: Effects of the drought treatment on aboveground net primary productivity (ANPP) during the first growing season of the experiment. Error bars indicate ± 1 SE, and letters indicate significant ($p < 0.05$) treatment differences.

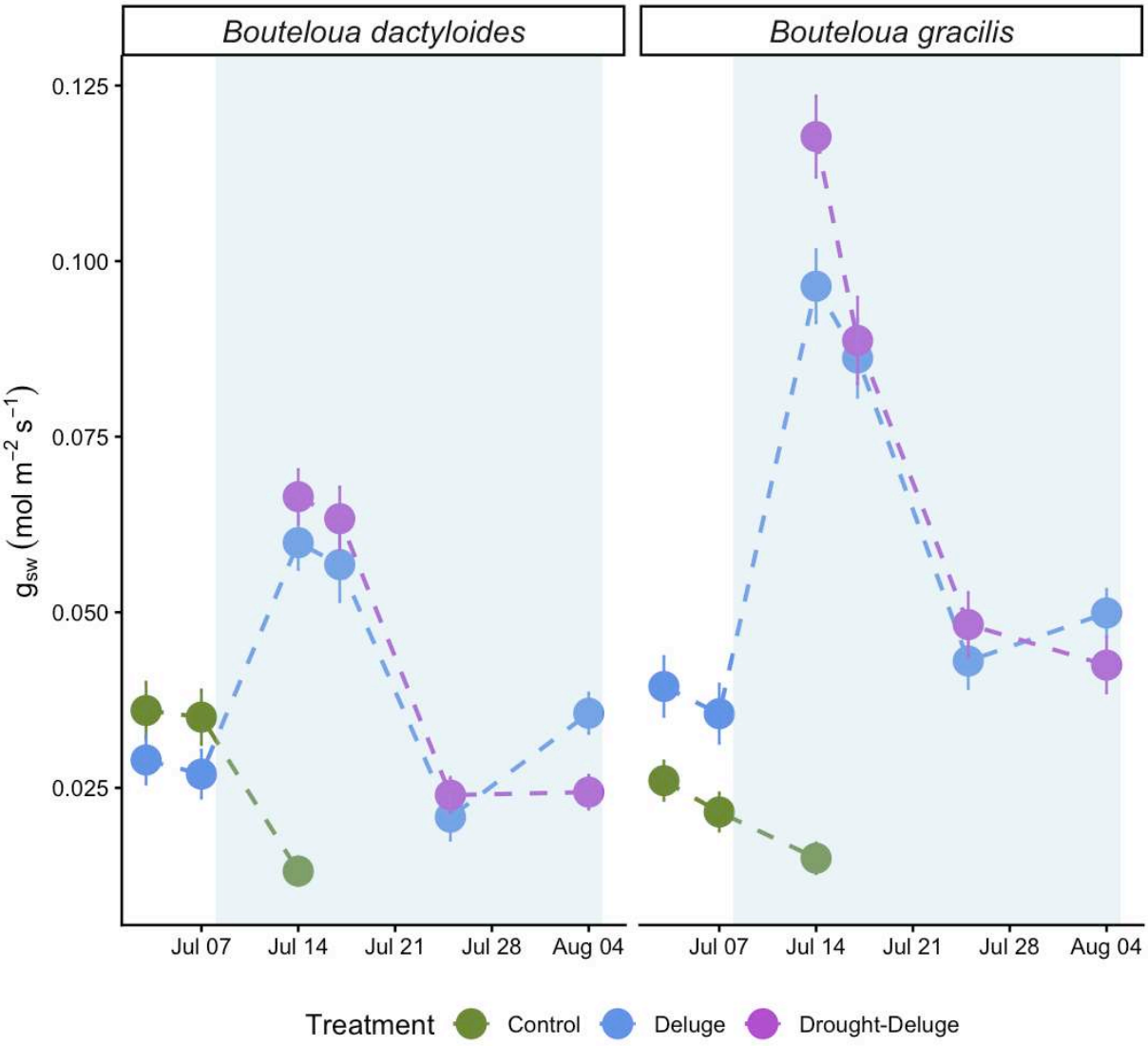

Figure A2.9: Patterns of leaf stomatal conductance to water vapor (g_{sw}) for *Bouteloua dactyloides* and *Bouteloua gracilis* in Control, Deluge, and Drought-Deluge treatments. Pre-deluge measurements were taken at two timepoints, and post-deluge measurements were taken at three timepoints. Measurements were only taken for the Control treatment once post-deluge given a lack of photosynthetically active leaf tissue at the time.

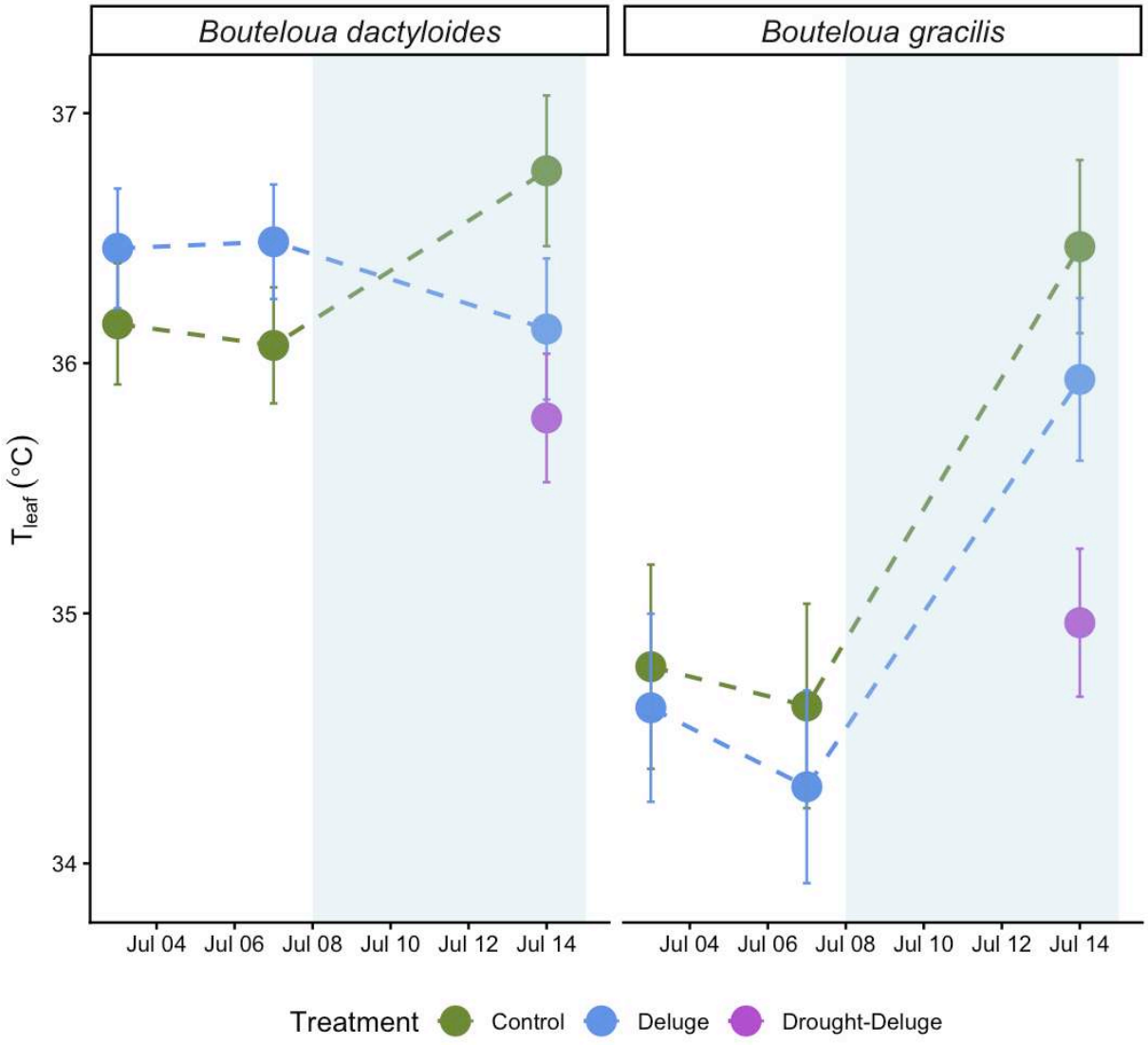

Figure A2.10: Patterns of leaf temperature for *Bouteloua dactyloides* and *Bouteloua gracilis* in Control, Deluge, and Drought-Deluge treatments. Pre-deluge measurements were taken at two timepoints, and post-deluge measurements were taken once.

Table A2.1: Growing season (April 15-September 30) precipitation amounts per year and treatment. These values include manual additions in both 2024 and 2025.

	2024	**2025**
Control	268.27 mm	274.06 mm
Deluge	268.27 mm	334.06 mm
Drought	110.26 mm	93.18 mm
Drought-Deluge	110.26 mm	153.18 mm
Long-Term Average	246.54 mm	246.54 mm

Table A2.2: Summary of the mixed model Analysis of Variance (ANOVA) results for each ecosystem measure from 2024. History indicates if the plots experienced drought or control conditions during the 2024 growing season. Date indicates individual dates for repeated measures (greenness, soil respiration, soil moisture) and seasonal periods for distinct measures (soil NO_3-N, NH_4-N, P). Reported values are the degrees of freedom (numerator, denominator), the *F*-statistic, and *p*-value. Significant *p*-values (< 0.05) are bolded.

2024						
Greenness				**Soil NH4-N**		
Term	**df**	**F**	***p***	**df**	**F**	***p***
History	1, 29	53.99	< 0.001	1, 33	4.9757	0.03264
Date	17, 634	60.24	< 0.001	1, 33	3.2571	0.08041
History * Date	17, 634	25.72	< 0.001	1, 33	1.5567	0.22096
Soil Respiration				**Soil P**		
Term	**df**	**F**	***p***	**df**	**F**	***p***
History	1, 29	26.422	< 0.001	1, 33	30.0115	< 0.001
Date	14, 510	82.1332	< 0.001	1, 33	0.1706	0.6823
History * Date	14, 510	24.4232	< 0.001	1, 33	0.542	0.542
Soil NO3-N				**ANPP**		
Term	**df**	**F**	***p***	**df**	**F**	***p***
History	1, 36	6.0404	0.01893	1, 29	3.6849	0.03027
Date	1, 36	2.0027	0.16562			
History * Date	1, 36	0.0019	0.96508			
Soil Moisture						
Term	**df**	**F**	***p***			
History	1, 25	47.8774	< 0.001			

Table A2.3: Summary of the mixed model Analysis of Variance (ANOVA) results for each ecosystem measure from 2025. History indicates if the plots experienced drought or control conditions during the 2024 growing season. Event indicates if the plots experienced the deluge event or not during the 2025 growing season. Date indicates individual dates for repeated measures (greenness, soil respiration, soil moisture, GPP, NEE, ER, g_{sw}) and seasonal periods for distinct measures (soil NO_3-N, NH_4-N, P, TC, TN, OM). Reported values are the degrees of freedom (numerator, denominator), the *F*-statistic, and *p*-value. Significant *p*-values (< 0.05) are bolded. GPP = Gross Primary Production, NEE = Net Ecosystem Exchange, ER = Ecosystem Respiration, g_{sw} = Stomatal Conductance, TC = Soil Total Carbon, TN = Soil Total Nitrogen, OM = Soil Organic Matter.

2025									
Greenness				**Soil NO3-N**			**Soil NH4-N**		
Term	**df**	**F**	***p***	**df**	**F**	***p***	**df**	**F**	***p***
History	1, 27	0.67	0.42	1, 28	63.05	**< 0.001**	1, 32	4.16	0.050
Event	1, 27	0.30	0.59	1, 28	18.86	**< 0.001**	1, 32	1.30	0.263
Date	26, 907	44.41	**< 0.001**	1, 28	1.02	0.321	1, 32	0.21	0.650
History * Event	1, 27	0.27	0.611	1, 28	6.58	0.016	1, 32	0.03	0.866
History * Date	26, 907	12.16	**< 0.001**	1, 28	0.91	0.348	1, 32	0.00	1.000
Event * Date	26, 907	10.19	**< 0.001**	1, 28	38.19	**< 0.001**	1, 32	0.21	0.650
History * Event * Date	26, 907	1.31	0.136	1, 28	17.64	**< 0.001**	1, 32	0.03	0.866
Soil Respiration				**Soil P**			**Soil TC**		
Term	**df**	**F**	***p***	**df**	**F**	***p***	**df**	**F**	***p***
History	1, 27	46.12	**< 0.001**	1, 32	4.16	0.050	1, 32	0.53	0.472
Event	1, 27	38.24	**< 0.001**	1, 32	1.30	0.263	1, 32	0.00	0.977
Date	19, 628	23.87	**< 0.001**	1, 32	0.21	0.650	1, 32	5.85	0.021
History * Event	1, 27	3.33	0.079	1, 32	0.03	0.866	1, 32	1.99	0.168
History * Date	19, 628	30.35	**< 0.001**	1, 32	0.00	1.000	1, 32	0.06	0.814
Event * Date	19, 628	21.46	**< 0.001**	1, 32	0.21	0.650	1, 32	0.12	0.735
History * Event * Date	19, 628	4.12	**< 0.001**	1, 32	0.03	0.866	1, 32	0.00	0.953
GPP				**NEE**			**ER**		
Term	**df**	**F**	***p***	**df**	**F**	***p***	**df**	**F**	***p***
History	1, 12	19.81	0.001	1, 12	15.46	0.002	1, 12	10.59	0.007
Event	1, 12	5.74	0.034	1, 12	3.19	0.099	1, 12	3.33	0.093
Date	14, 214	7.12	**< 0.001**	14, 214	7.35	**< 0.001**	14, 214	7.43	**< 0.001**

History * Event	1, 12	3.34	0.093	1, 12	1.61	0.229	1, 12	2.29	0.156
History * Date	14, 214	3.68	< 0.001	14, 214	3.57	< 0.001	14, 214	3.68	< 0.001
Event * Date	14, 214	15.55	< 0.001	14, 214	8.68	< 0.001	14, 214	15.32	< 0.001
History * Event * Date	14, 214	6.67	< 0.001	14, 214	4.81	< 0.001	14, 214	4.59	< 0.001
Soil TN				**Soil OM**			**ANPP**		
Term	**df**	**F**	***p***	**df**	**F**	***p***	**df**	**F**	***p***
History	1, 28	0.02	0.886	1, 28	0.45	0.507	1, 27	131.92	< 0.001
Event	1, 28	0.00	1.000	1, 28	3.49	0.072	1, 27	0.09	0.767
Date	1, 28	2.54	0.122	1, 28	0.94	0.340			
History * Event	1, 28	0.76	0.392	1, 28	2.01	0.167	1, 27	0.04	0.847
History * Date	1, 28	0.02	0.886	1, 28	0.67	0.418			
Event * Date	1, 28	0.00	1.000	1, 28	2.95	0.097			
History * Event * Date	1, 28	0.00	1.000	1, 28	0.27	0.605			
g_{sw} (*B. gracilis*)				**g_{sw} (*B. dactyloides*)**					
Term	**df**	**F**	***p***	**df**	**F**	***p***			
History	1, 149	0.89	0.347	1, 123	2.29	0.133			
Event	1, 78	123.44	< 0.001	1, 76	52.75	<0.001			
Date	4, 761	23.01	< 0.001	4, 749	16.94	<0.001			
History * Date	3, 762	3.38	0.018	3, 752	1.93	0.124			
Event * Date	1, 762	0.00	0.988	1, 749	0.03	0.867			

Daily Plant Water Relations

Measurements of stomatal conductance (g_{sw}) were made at three timepoints throughout the day (10:00, 13:00, 13:00, 15:00, and 17:00 h) on dates both prior to the deluge event (July 3rd & 7th) and following the deluge event (July 14th, 17th, 25th, and August 4th) using a portable porometer/fluorometer (LI-600, LI-COR, Inc., Lincoln NE, USA). Three replicate measurements were taken per species (*B. dactyloides* and *B. gracilis*) per plot at each timepoint. Only the Control, Deluge, and Drought-Deluge treatments were sampled due to a lack of photosynthetically active plant tissue in the Drought treatment. Leaf senescence in the Control treatment was responsible for the cessation of g_{sw} measurements following July 14th measurement campaign. Daily mean g_{sw} was calculated by averaging measurements across timepoints for each sampling date. Grass g_{sw} has been shown to be variable along leaf blades (Ocheltree et al. 2012), so as a precautionary measure, all g_{sw} measurements were taken from a standardized point on *B. dactyloides* and *B. gracilis* leaves.

Methods A2.1: Methodological description for plant physiological measurements taken before and after the deluge event.

Plant Physiological Responses

The two focal plants, *B. gracilis* and *B. dactyloides*, displayed similar g_{sw} responses to the deluge event in both the Deluge and Drought-Deluge treatments (Fig. A2.9). Both species had elevated g_{sw} for two weeks following the deluge event, before returning to pre-deluge levels (Fig. A2.9). *B. gracilis* g_{sw} doubled that of *B. dactyloides* and remained higher throughout the duration of our measurements (Fig. A2.9). Elevated g_{sw} corresponded with decreased T_{leaf} for both species following the deluge event (Fig. A2.10).

Results A2.1: The response of stomatal conductance (g_{sw}) and leaf temperature (T_{leaf}) of the two dominant grass species, *Bouteloua gracilis* and *Bouteloua dactyloides*, to the deluge event.

APPENDIX 3

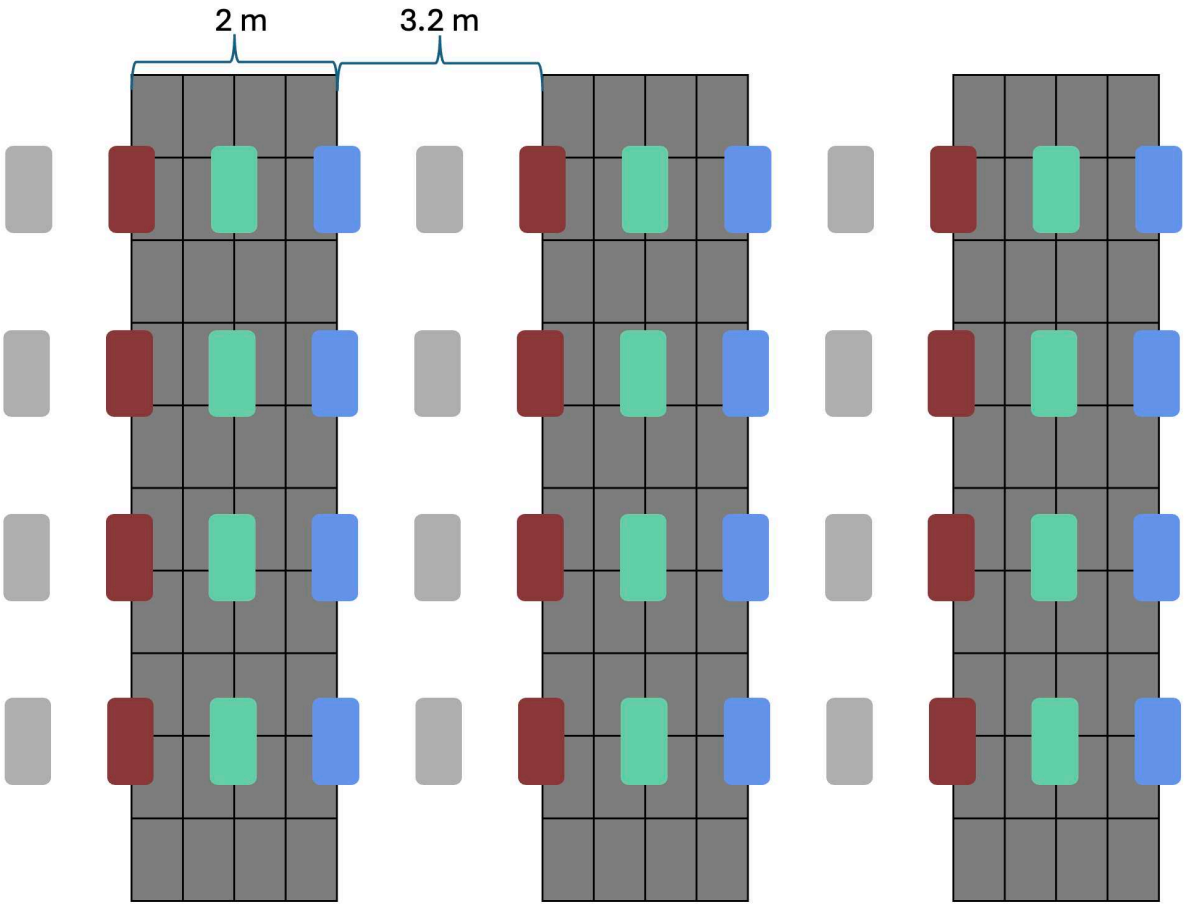

Figure A3.1: Conceptual figure of sampling scheme. Experimental microsites are color coded to match the primary manuscript. *Between* is grey, W_{edge} is red, *Beneath* is green, and E_{edge} is blue.

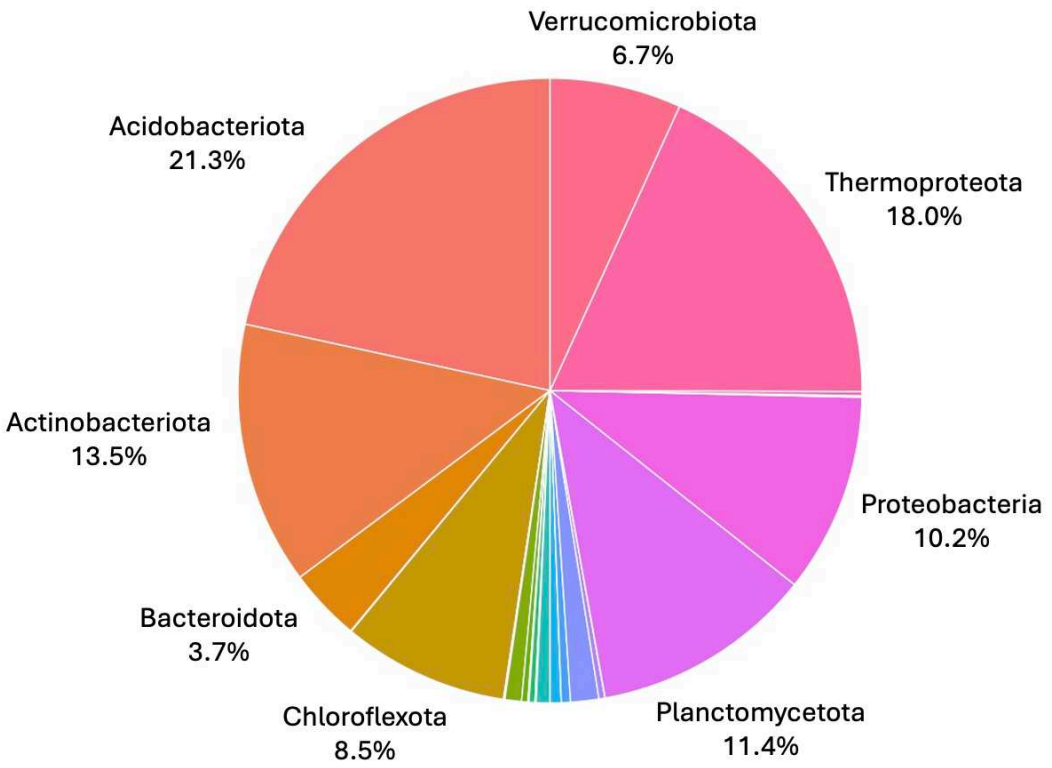

Figure A3.2: Relative abundance of dominant bacterial/archaeal phyla averaged across all samples.

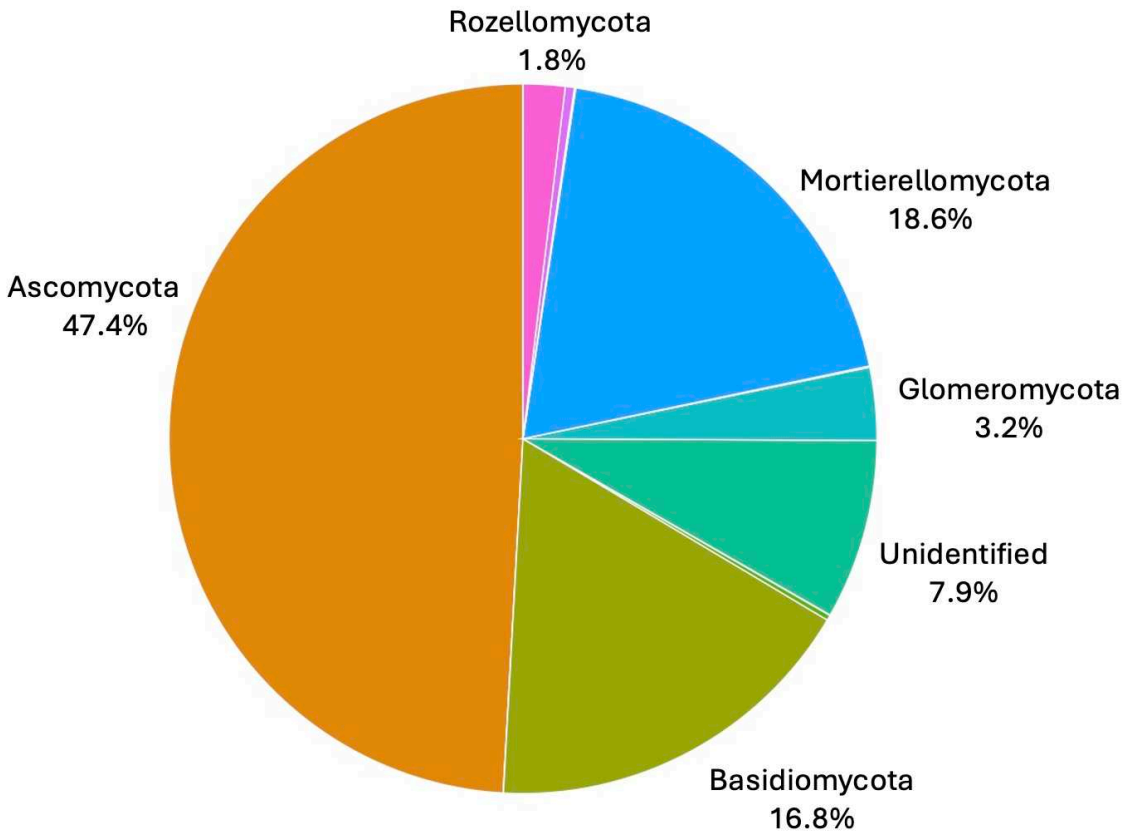

Figure A3.3: Relative abundance of dominant fungal phyla averaged across all samples.

Figure A3.4: Differentially abundant taxa in the Beneath panel and Control microsites. a): Bacterial and archaeal taxa that are enriched in Beneath (aquamarine) and Control (cyan) at the order level. b): Fungal taxa that are enriched in Beneath (aquamarine) and Control (cyan) at the order level. Differential abundance analysis was conducted with the ANCOM-BC R package, and logfold changes are visualized along the x-axis.

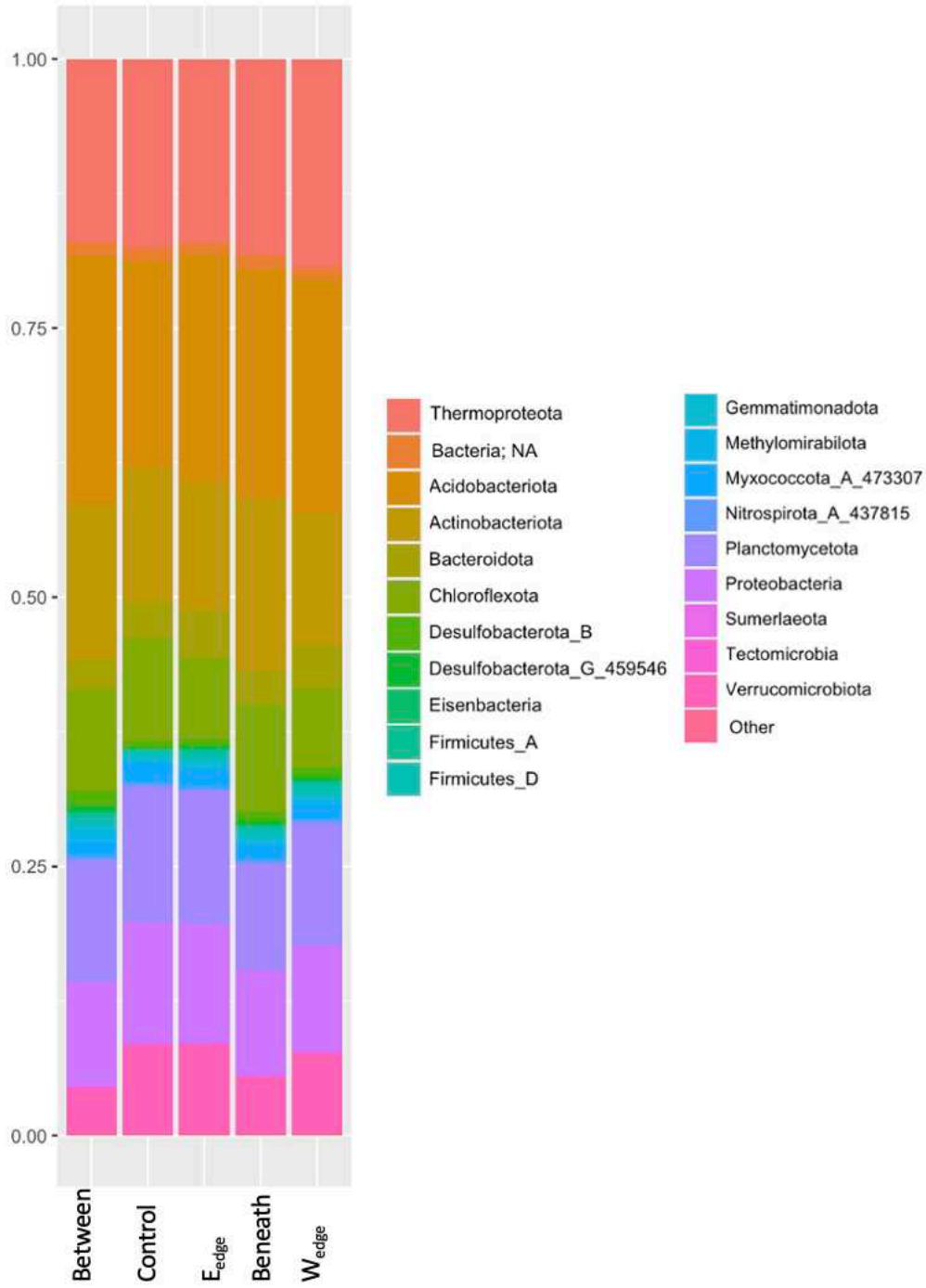

Figure A3.5: Relative abundance of the 20 most abundant prokaryotic phyla in each microsite.

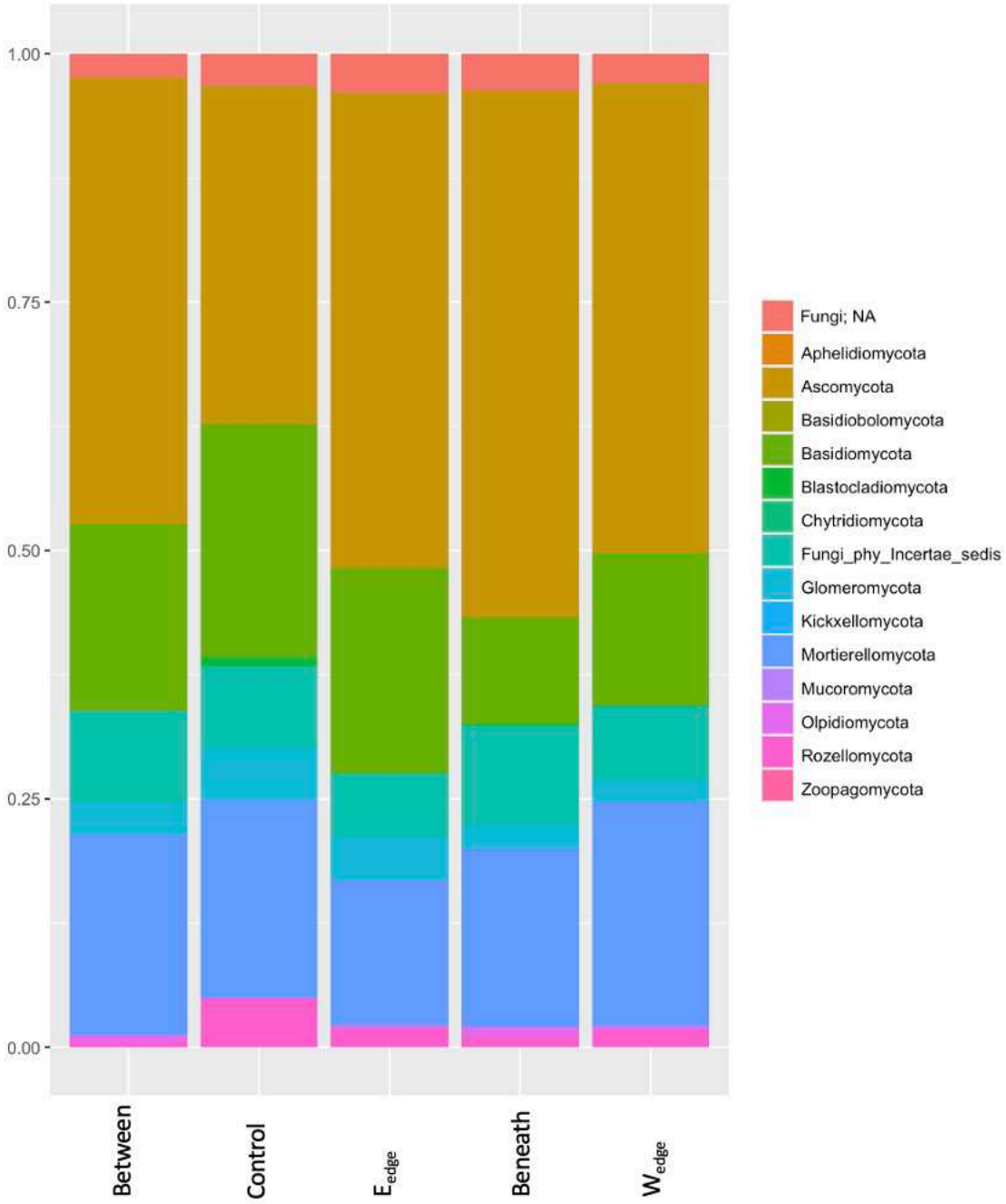

Figure A3.6: Relative abundance of the 14 most abundant fungal phyla in each microsite.

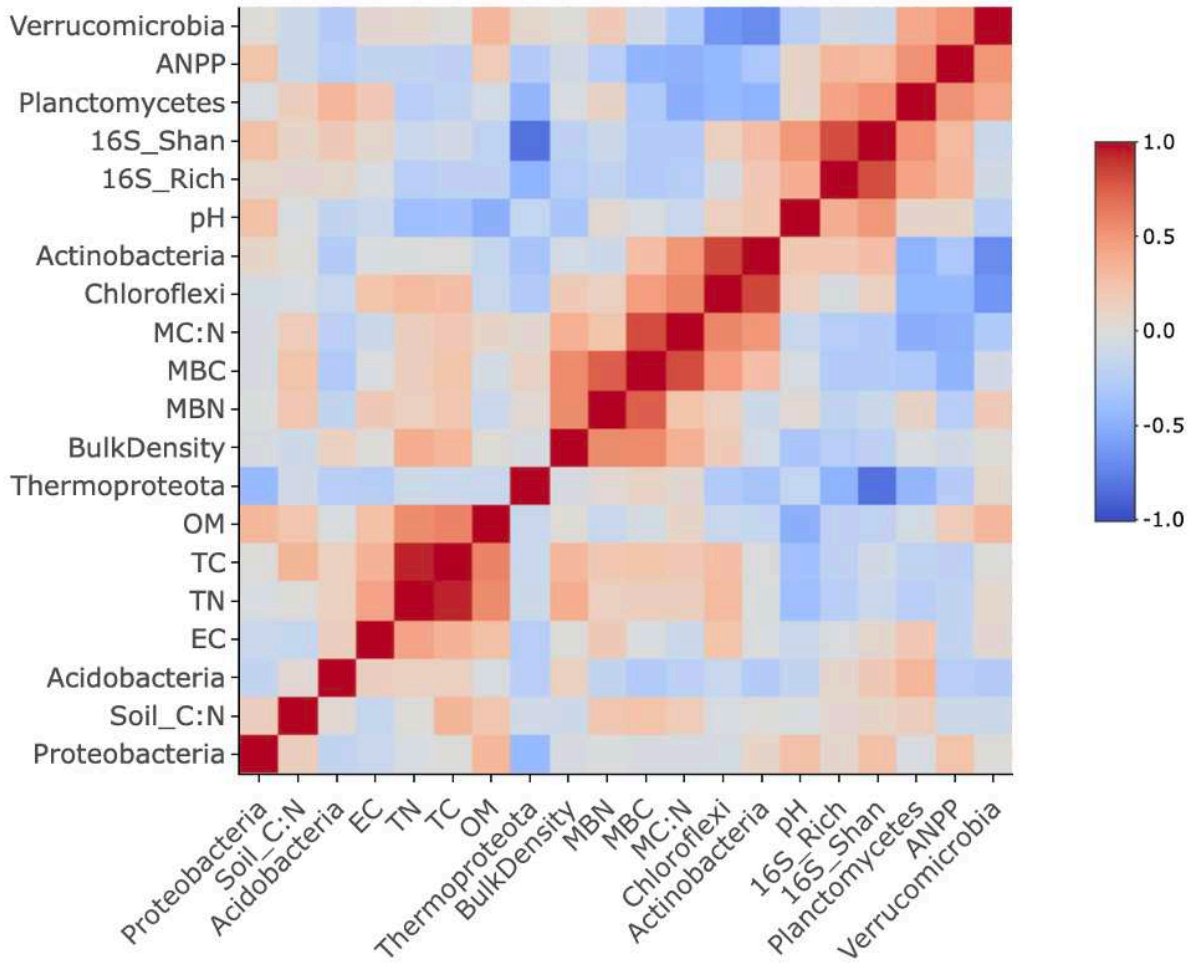

Figure A3.7: Spearman rank correlation analysis of dominant bacterial and archaeal phyla and soil properties. ANPP = Aboveground Net Primary Productivity, 16S_Shan = Shannon diversity of bacteria & archaea, 16S_Rich = Richness of bacteria & archaea, MC:N = Microbial biomass C:N ratio, MBC = Microbial biomass C, MBN = Microbial biomass N, OM = Organic Matter, TC = Total C, TN = Total N, Soil_C:N = Soil C:N ratio.

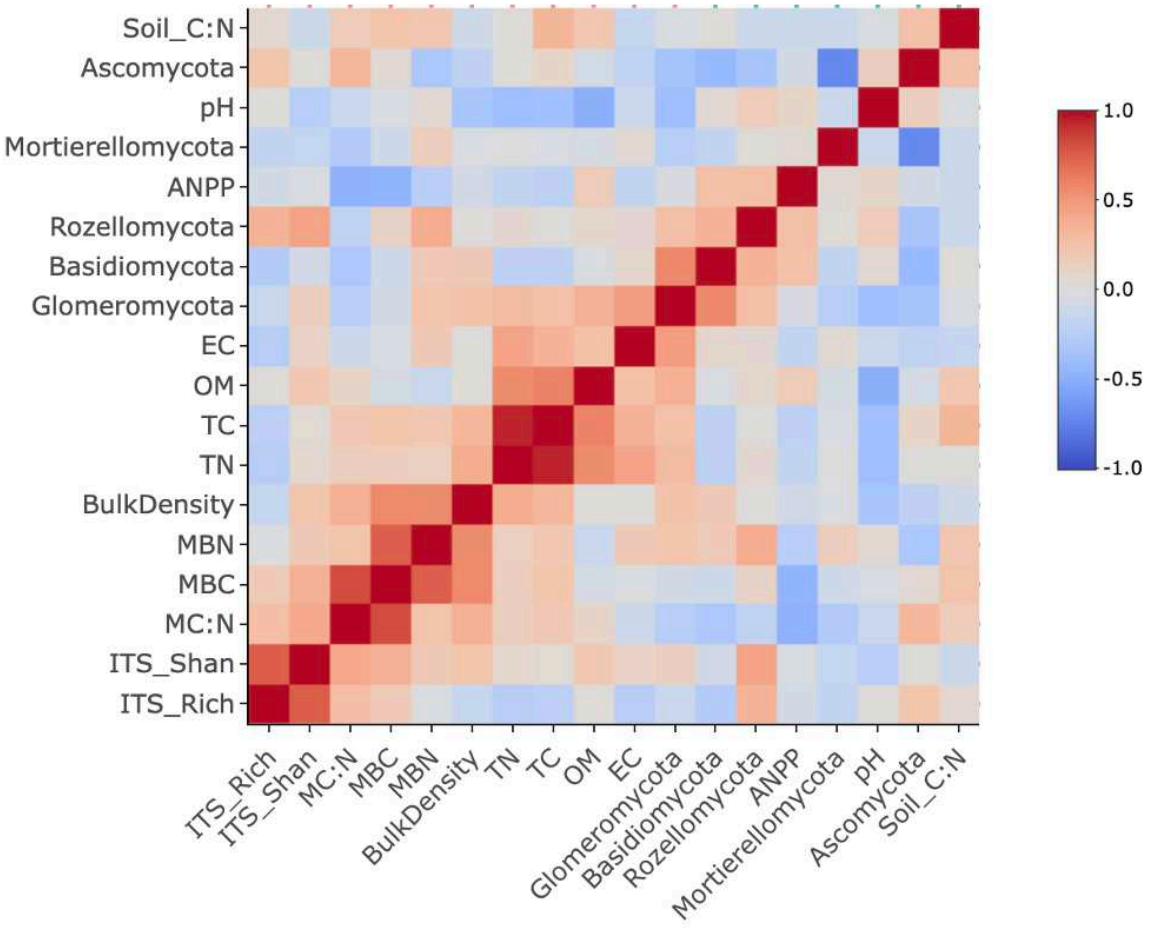

Figure A3.8: Spearman rank correlation analysis of dominant fungal phyla and soil properties. ANPP = Aboveground Net Primary Productivity, ITS_Shan = Shannon diversity of fungi, ITS_Rich = Richness of fungi, MC:N = Microbial biomass C:N ratio, MBC = Microbial biomass C, MBN = Microbial biomass N, OM = Organic Matter, TC = Total C, TN = Total N, Soil_C:N = Soil C:N ratio.

Table A3.1: ANOVA tests of environmental and soil physiochemical properties, microbial biomass, and MicroResp substrate induced respiration rates using microsite as a predictor. *p<0.05; **p<0.01; ***p<0.001.

Response Variable	Microsite	
	df	F
ANPP	4	11.5194***
Organic Matter	4	3.4208*
Electrical Conductivity	4	0.5925
Total C	4	1.489
Total N	4	0.9818
pH	4	3.9613*
Microbial Biomass C	4	22.088***
Microbial Biomass N	4	21.343***
Microbial Biomass C:N	4	13.56***
Water	4	7.1546***
Glucose	4	3.7322*
Cellulose	4	14.384***
Xylose	4	1.6093
Glucosamine	4	1.8988
Lignin	4	8.7431***
Overall	4	3.6452*

Table A3.2: ANPP and each soil physiochemical property in each microsite with standard error in parentheses. Sampling day was August 2, 2023 for Sampling Day Soil Moisture reference. Bulk density was collected for only two samples in each microsite.

Response Variable	Microsite				
	Between	E_{edge}	Beneath	W_{edge}	Control
ANPP (g/m^2)	535.71 ± 38.57	649.03 ± 32.07	378.15 ± 17.56	555.19 ± 24.49	580.20 ± 52.90
Average Growing Season Soil Moisture (0-15cm)	36.1%	36.7%	28.3%	41.5%	37.2%
Average Sampling Day Soil Moisture (0-15cm)	30.4%	30.2%	27.3%	45.5%	33.8%
Organic Matter (OM)	1.03% ± 0.04	1.22% ± 0.03	1.17% ± 0.03	1.15% ± 0.03	1.10% ± 0.05
Electrical Conductivity (EC) (dS/m)	0.327 ± 0.04	0.288 ± 0.03	0.303 ± 0.03	0.297 ± 0.03	0.370 ± 0.05
Total C (TC)	2.63% ± 0.17	2.90% ± 0.12	3.02% ± 0.12	2.67% ± 0.12	2.85% ± 0.21
Total N (TN)	2.33% ± 0.01	2.45% ± 0.01	2.55% ± 0.01	2.28% ± 0.01	2.40% ± 0.02
pH	7.51 ± 0.10	7.27 ± 0.07	7.37 ± 0.07	7.54 ± 0.07	7.74 ± 0.12
Bulk Density (g/cm^3)	1.071	1.184	1.149	0.929	1.113
Microbial Biomass C (MBC) (μg C g^{-1})	482.72 ± 15.89	637.37 ± 70.97	858.34 ± 49.85	408.76 ± 21.42	889.18 ± 52.10
Microbial Biomass N (MBN) (μg C g^{-1})	76.60 ± 5.89	86.46 ± 4.26	84.59 ± 2.54	62.29 ± 3.50	116.55 ± 2.49
Microbial Biomass C:N	6.37 ± 0.31	7.48 ± 0.43	10.16 ± 0.57	6.59 ± 0.21	7.65 ± 0.57

Table A3.3: Early and late growing season nutrient availability in each microsite. Nutrient accumulation was measured with Plant Root Simulator (PRS®) probes (see Methods). Control values were generated from a single set of probes, while the other microsites are expressed as an average of replicates with standard error. The difference between early and late season nutrient availability is expressed as a positive value if nutrient availability was higher in the early growing season.

Nutrient	Season	Microsite				
		Between	E_{edge}	Beneath	W_{edge}	Control
NO_3-N (μg/10cm^2/burial length)	Early	NA	35.25 ± 7.61	32.64 ± 12.31	33.87 ± 5.17	297.54
	Late	15.79 ± 4.33	20.88 ± 5.52	41.24 ± 19.01	22.44 ± 2.79	39.58 ± 2.46
	Difference	NA	14.37	-8.60	11.43	257.96
Ca (μg/10cm^2/burial length)	Early	NA	3165.43 ± 63.89	1724.63 ± 247.79	3377.92 ± 67.95	3415.90
	Late	2198.10 ± 369.94	2152.45 ± 219.84	1700.67 ± 414.22	2488.92 ± 158.69	2892.31 ± 40.39
	Difference	NA	1012.98	23.96	889	523.59
Mg (μg/10cm^2/burial length)	Early	NA	301.25 ± 5.63	238.06 ± 22.04	306.11 ± 9.13	236.80
	Late	259.81 ± 30.55	232.63 ± 16.35	203.92 ± 25.37	220.53 ± 10.52	251.73 ± 34.06
	Difference	NA	68.62	34.14	85.58	-14.93
K (μg/10cm^2/burial length)	Early	NA	65.41 ± 4.08	247.42 ± 23.72	60.08 ± 4.11	56.80
	Late	169.70 ± 59.33	128.40 ± 20.98	163.85 ± 39.48	62.63 ± 10.85	252.85 ± 143.35
	Difference	NA	-62.99	83.57	-2.55	-196.05
P (μg/10cm^2/burial length)	Early	NA	53.41 ± 5.42	15.87 ± 3.93	56.16 ± 4.85	2.63
	Late	14.20 ± 4.64	19.38 ± 2.82	12.70 ± 4.22	26.07 ± 4.62	8.82 ± 4.08
	Difference	NA	34.03	3.17	30.09	-6.19
Fe (μg/10cm^2/burial length)	Early	NA	40.58 ± 5.78	3.34 ± 0.84	47.85 ± 12.07	11.21
	Late	4.83 ± 2.13	5.93 ± 0.94	3.97 ± 0.83	6.68 ± 0.96	9.82 ± 4.55
	Difference	NA	34.65	-0.63	41.17	1.39
Mn (μg/10cm^2/burial length)	Early	NA	9.99 ± 1.37	1.67 ± 0.37	11.68 ± 1.82	4.01
	Late	1.66 ± 0.66	2.27 ± 0.49	1.04 ± 0.26	2.68 ± 0.77	1.47 ± 0.45
	Difference	NA	7.72	0.63	9	2.54

Cu (μg/10cm^2/burial length)	Early	NA	3.41 ± 0.18	1.26 ± 0.10	3.75 ± 0.18	2.32
	Late	0.53 ± 0.16	0.45 ± 0.13	0.47 ± 0.12	0.50 ± 0.10	1.09 ± 0.46
	Difference	NA	2.96	0.79	3.25	1.23
Zn (μg/10cm^2/burial length)	Early	NA	3.41 ± 0.26	0.91 ± 0.21	3.86 ± 0.32	2.54
	Late	0.75 ± 0.18	1.76 ± 0.35	1.15 ± 0.32	2.06 ± 0.52	3.09 ± 1.90
	Difference	NA	1.65	-0.24	1.80	-0.55
B (μg/10cm^2/burial length)	Early	NA	0.52 ± 0.16	0.24 ± 0.09	0.83 ± 0.35	0.05
	Late	0.24 ± 0.13	0.11 ± 0.03	0.22 ± 0.04	0.14 ± 0.04	0.30 ± 0.16
	Difference	NA	0.41	0.02	0.69	-0.25
S (μg/10cm^2/burial length)	Early	NA	28.21 ± 2.11	17.42 ± 3.93	34.65 ± 3.91	44.68
	Late	8.74 ± 3.93	13.45 ± 1.46	15.16 ± 6.05	17.73 ± 3.20	31.22 ± 20.35
	Difference	NA	14.76	2.26	16.92	13.46
Pb (μg/10cm^2/burial length)	Early	NA	3.82 ± 0.37	0.22 ± 0.08	4.24 ± 0.43	7.22
	Late	0.51 ± 0.32	0.48 ± 0.13	0.55 ± 0.34	0.87 ± 0.23	4.04 ± 2.90
	Difference	NA	3.34	-0.33	3.37	3.18
Al (μg/10cm^2/burial length)	Early	NA	12.93 ± 1.29	7.83 ± 0.59	13.38 ± 1.80	9.05
	Late	7.92 ± 2.05	7.89 ± 0.55	7.62 ± 0.65	8.78 ± 0.57	9.98 ± 2.17
	Difference	NA	5.04	0.21	4.60	-0.93
Cd (μg/10cm^2/burial length)	Early	NA	3.41 ± 0.18	1.26 ± 0.10	3.75 ± 0.18	2.32
	Late	0.53 ± 0.16	0.45 ± 0.13	0.47 ± 0.12	0.50 ± 0.10	1.09 ± 0.46
	Difference	NA	2.96	0.79	3.25	1.23

Table A3.4: ANOVA tests of early growing season nutrient availability using microsite as a predictor. *p<0.05; **p<0.01; ***p<0.001.

Response Variable	Microsite	
	df	F
NO3-N	2	0.025
Ca	2	47.624***
Mg	2	9.0189***
K	2	86.443***
P	2	16.052***
Fe	2	5.9551*
Mn	2	1.774
Cu	2	47.848***
Zn	2	25.44***
B	2	1.2593
S	2	5.8078**
Pb	2	1.5008
Al	2	3.5041*
Cd	2	15.796***

Table A3.5: ANOVA tests of late growing season nutrient availability using microsite as a predictor. *p<0.05; **p<0.01; ***p<0.001.

Response Variable	Microsite	
	df	F
NO_3-N	4	1.0731
Ca	4	1.6584
Mg	4	0.8792
K	4	3.2855*
P	4	2.0455
Fe	4	1.6377
Mn	4	1.0181
Cu	4	1.3705
Zn	4	1.4706
B	4	1.703
S	4	1.518
Pb	4	5.3591**
Al	4	0.811
Cd	4	11.674***

Table A3.6: MicroResp substrate induced respiration rate averages (measured in μg g^{-1} h^{-1} CO_2-C) with standard error. Overall was calculated by subtracting water (i.e., basal respiration) from each, then summing.

Response Variable	Microsite				
	Between	E_{edge}	Beneath	W_{edge}	Control
Water	1.441 ± 0.0687	1.782 ± 0.0757	1.569 ± 0.075	1.573 ± 0.054	1.129 ± 0.092
Glucose	2.551 ± 0.272	4.281 ± 0.521	3.605 ± 0.420	1.967 ± 0.056	3.415 ± 0.494
Cellulose	1.713 ± 0.087	2.428 ± 0.095	1.734 ± 0.098	1.718 ± 0.022	1.366 ± 0.146
Xylose	2.353 ± 0.309	3.147 ± 0.299	2.899 ± 0.336	2.113 ± 0.042	2.466 ± 0.344
Glucosamine	2.540 ± 0.406	3.519 ± 0.379	3.190 ± 0.468	1.771 ± 0.079	3.108 ± 0.811
Lignin	2.101 ± 0.147	2.617 ± 0.102	2.246 ± 0.118	1.594 ± 0.050	1.799 ± 0.246
Overall	4.053 ± 1.022	7.0725 ± 1.221	5.828 ± 1.027	1.297 ± 0.270	6.510 ± 1.53

Table A3.7: ANOVA tests of 16S and ITS diversity analyses using microsite as a predictor. *p<0.05; **p<0.01; ***p<0.001.

Response Variable	Microsite	
	df	F
16S Shannon	4	0.5851
16S Bray-Curtis (PERMANOVA)	4	(pseudo-F) 2.2415***
16S Robust Aitchison (PERMANOVA)	4	(pseudo-F) 1.4601***
ITS Shannon	4	0.7470
ITS Bray-Curtis (PERMANOVA)	4	(pseudo-F) 1.3506***
ITS Robust Aitchison (PERMANOVA)	4	(pseudo-F) 1.2339***